Assessment of the potential and risk of fractionated stereotactic radiosurgery for brain lesions using the Gamma Knife system.

Béatrice Reiner

Submitted in accordance with the requirements for the degree of **Doctor of Philosophy** at the University of Leeds

December, 2018

The candidate confirms that the work submitted is his/her own and that appropriate credit has been given where reference has been made to the work of others.

Chapter two is based on the work “Quantifying the trigger level of the vacuum surveillance system of the Gamma-Knife eXtend™ positioning system and evaluating the potential impact on dose delivery.” published in the “*Journal of Radiosurgery & SBRT.”* in 2016 (Ref [1])

Chapter three is based on the work “Quantifying the effects of positional uncertainties and estimating margins for Gamma-Knife® fractionated radiosurgery of large brain metastases.” Published in the “*Journal of Radiosurgery & SBRT”* in 2017, (Ref [2])

Both publications had the same authors and same contribution per author as is listed below:

Conception and design: [**Beatrice Reiner**]
Data collection: [**Beatrice Reiner**]
Data analysis and interpretation: [**Beatrice Reiner, with review and discussion by David Thwaites, David Buckley, Peter Bownes**]
Manuscript writing: [**Beatrice Reiner**]
Final approval of manuscript: [**Beatrice Reiner, with critical review and comments by David Thwaites, David Buckley**]

Chapter four and **five** will be submitted for publication substantially in the presented form. Authors and contribution per author will be the same (or similar) as for the publications related to chapter two and three.

Acknowledgements

This research was supported by many other people. I would like to thank especially:

Professor David I. Thwaites, PhD; supervisor and mentor

Biomedical Imaging, University of Leeds, Leeds, UK
Institute of Medical Physics, School of Physics, University of Sydney, Camperdown, Australia
For guiding the scientific progress and being open to new solutions.

Professor David L. Buckley, PhD; supervisor and mentor

Biomedical Imaging, University of Leeds, Leeds, UK
For *asking* critical questions and giving supportive and academic advice.

Peter Bownes, MSc, senior clinical scientist

Department of Medical Physics and Engineering, Leeds Cancer Centre, St. James's University Hospital, Leeds, United Kingdom
For specific scientific advice in regard to Gamma Knife and for very critical proof reading.

Simon Smith, Lead radiographer Gamma Knife

Leeds Cancer Centre, St. James's University Hospital, Leeds, United Kingdom
For his great suggestion to use dental models from the dentists department to measure the trigger level of eXtend.

RTS (radiation technical support)

Leeds Cancer Centre, St. James's University Hospital, Leeds, United Kingdom
For their help to create and set up the measurement system for the dental model.

Leeds Gamma Knife Centre run by Nova Healthcare

for supporting this work.

Abstract

Introduction: The Gamma Knife (GK) was originally introduced as a radiotherapy unit for solid brain lesions. The original skull-attached G-frame enabled submillimetre accuracy but allowed only single-fraction treatments, thus limiting to small lesion treatments. To enable fractionated Stereotactic Radiosurgery, the GK Perfexion model (with eXtend) was introduced leading to new questions:

- What is the repositioning system accuracy?
- What effect have positional uncertainties for the target; and for normal tissue (NT) and Organs at risk (OAR)?
- How can positional uncertainties be handled?

Material and Method: eXtend uncertainty was investigated using trigger levels of the vacuum-surveilled patient positioning mouthpiece, measured for ten patients' dental models mounted on a 0.05mm-accuracy computer-controlled positioner. The dosimetric effect of these displacements in a single fraction was evaluated by calculating minimum dose, coverage and conformity-index changes for displacements of 0 to 4mm.The impact of positional displacements for 3 and 5 fraction treatments was evaluated for targets and organs-at-risk (OaR) by calculating total doses with simulated displacements of 0-4mm in combinations of X, Y, and Z directions for nine patients (in total almost 300 sumPlans). All plans were prescribed to the 50% isodose. Effects were calculated in physical dose and in biological effective dose (BED).

Finally, from this a novel approach to minimize effects of displacement was proposed and feasibility-tested for 5-fraction plans. Instead of applying margins to cover potential uncertainties, a correction is applied in the last two fractions only after any observed systematic uncertainty is quantified in the first three fractions. 100 displacement scenarios were tested, comparing for each the dose volume histogram (DVH) and dose profiles and the total dose with and without the correction procedure.

Results: Mean positional uncertainty with a clinical vacuum setting was 0.15mm (SD ±0.05mm, range 0.05-0.29mm) and 0.33° (SD ±0.15°, 0.05°-1.0°).

The most critical parameter in the dose distribution is minimum dose $D_{99\%}$. In the evaluated scenarios $D_{99\%}$ fell by 2% for a displacement of 0.5mm and 16% with 2mm in X or Y direction and >20% in Z direction, dependent on arrangement.

Moving to hypofractionation increases the BED inside the target and reduces it outside, i.e. the dose gradient is increased at the 50% (prescription) isodose.

Displacement in opposing directions is predominantly random, which reduces the dose gradient but does not introduce an underdosage to the target for displacements of up to 2 mm. At the same time the BED to OAR is increased but remains below single fraction dose.

Feasibility testing the proposed correction method showed a significant improvement of the total BED indicating the method's potential.

Discussion: Positional uncertainty is generally low, better than 0.5mm for Perfexion whilst the later GK version, Icon. starts treatment with minimal uncertainties following an initial Cone Beam CT (CBCT). However, for both treatment units, target movement during treatment is possible and may be up to 2mm. The most critical aspect is underdosage of the target. Prescribing the dose to 50% reduces random uncertainty effects and ensures BED is at an optimal value (gradient) to avoid underdosage and protect OAR.

A novel strategy is proposed and feasibility-tested to correct positional uncertainties, showing improved dose distribution in the scenarios tested. However, this test was for static displacements only. GK Icon corrects any positional displacement observed at the initial CBCT, so the correction method would only be needed when the system identifies further movement. For practical clinical use, further investigation is needed.

Table of Contents

List of Abbreviations

4C	an earlier model of Gamma Knife based on collimator helmets.
AAPM TG	American Association of Physicists in Medicine Task Group
ALARA	as low as reasonable achievable
AN	Acoustic Neuroma
AVM	Arteriovenous malformation
BBB	Blood Brain Barrier
BED	Biological Effective Dose
BS	Brainstem
CBCT	Cone Beam CT
CI	Conformity Index, similar to PCI
CNS	Central Nervous System (brain)
CT	Computer Tomography
CTV	Clinical Target Volume
DVH	Dose Volume Histogram
EUD	Equivalent Uniform Dose
fSRT	fractionated Stereotactic Radio Therapy
G-frame	skull attached frame system that allows optimal repositioning of the patient in MR and Gamma Knife
GI	Gradient Index
GK	Gamma Knife
GKP	Gamma Knife Perfexion
GP	GammaPlan
GTV	Gross Target Volume
Gy	Gray, unit of absorbed dose
H&N	Head and Neck
hfSRT	hypo fractionated Stereotactic Radiotherapy
HI	Heterogeneity Index or Homogeneity Index (depends on the context)

HU	Hounsfield Unit
ICRU	International Commission on Radiation Units
IMRT	Intensity Modulated Radiation Therapy
Linac	Linear Accelerator. Flexible treatment unit for radiotherapy
LQ model	Linear Quadratic model (a model to mathematically describe the fractionation effect for short and long term clinical effects)
MLC	Multi Leaf Collimator
MRI	Magnetic Resonance Imaging
NT	Normal Tissue (generally all healthy cells in a body)
NTCP	Normal Tissue Complication Probability
OAR	Organ at Risk
ON	Optic Nerve
PCI	Paddick Conformity Index
PIV	Prescribed Isodose Volume
PTV	Planning Target Volume
QoL	Quality of Life
QUANTEC	Quantitative Analyses of Normal Tissue Effects
RCT	Reposition Check Tool
RPA	recursive partition analysis
RT	Radiation Therapy
RTOG	Radiation Therapy Oncology Group
SABR	Stereotactic ablative radiotherapy
SAD	Source to axis distance (or Source to iso distance)
SBRT	stereotactic Body Radiotherapy
SMX 200	high precision computer controlled milling machine
SRS	Stereotactic Radio Surgery
SSD	Source to skin distance
TCP	Tumour Control Probability
UK	United Kingdom

WBRT	Whole Brain Radio Therapy

List of tables

List of figures

Preface

More than 120 years ago X-rays were observed by W.C. Röntgen, with radioactivity and gamma rays discovered almost at the same time. X-rays and gamma-rays have been used in radiotherapy for cancer treatment from very soon after their discovery.

Three main approaches developed in radiation therapy: Brachytherapy, where sealed sources are placed inside or close to the tumour; systematic radioisotope therapy (nuclear medicine) where radioactive substances are attached to a tracer that brings the radioactive isotope to the relevant metabolism which is predominantly the tumour; and teletherapy which means "from a distance" and means the source is positioned at a distance away from the tumour and radiation beams are directed towards it. Gamma Knife (GK) is a teletherapy technique.

From "source to skin distance" (SSD) to "source to axis distance" (SAD)

With teletherapy, the patient is positioned in the radiation beams from an ionizing radiation source, i.e. for conventional radiotherapy, a high energy x-ray tube, an isotope such as Cobalt 60 (Co60) that is focused in one direction, or the higher MegaVolt energy (MV) x-ray or electron beams of a linear accelerator (linac). Early techniques used open square, or other simply shaped, fields. They also had relatively low dose rates, so to minimise treatment time the distance of the irradiation source to the target was kept as short as possible, but still allowing for some adjustment movements without the risk of collision. To minimize the dose to the skin, an organ highly sensitive to irradiation, (and to other tissues that the beam would pass though before the tumour) and to achieve uniform doses across the target, the dose was delivered with beams from different angles. The treatment unit was set up relative to the patient to a fixed a source to skin distance for each field which made set up simple, but meant that the radiation treatment technologist (RTT) had to enter the room each time the source direction was changed. This is time consuming and increases the risk that the patient moves between fields.

More modern MV linacs were designed to be isocentric, with the machine rotating around a single point that beams from all directions pointed to, the isocentre. The distance from the source to this point on the rotation axis is generally 100 cm which was enough to place the isocentre at the centre of the target and efficiently move the gantry with the source around the target without moving the patient, but still focussing each beam on the target.

From square fields to conformal fields

The field shaping evolved from fixed applicators to variable square or rectangular fields and then conformal fields. The first approach to shaping fields was to use shielding blocks. With patient specific blocks the irradiation field could be formed individually for each patient to shield out areas that required to be spared.

Casting blocks is time consuming and changes to the field are not easily possible. So the next step was to introduce a multi-leaf collimator (MLC). In an MLC, the straight field border is replaced by leaves of a certain width (varying with design) that can be moved individually thus aligning closely to the target outline. Currently, typical standard linacs have MLCs with leaf widths of 0.5 cm as projected to the isocentre distance.

Small field irradiation

Irradiating small fields is difficult. The flexible moving collimators from a linac have a positional tolerance on the order of 1 mm. This is 10% of a small field width of 1 cm. The standard set up accuracy of a rotating gantry-based system can be up to a few millimetres. For small lesions (requiring small fields) this can be too large and requires specific approaches to quality assurance of the machine and the patient treatment delivery. It was not possible until modern linacs and methods became available.

Gamma Knife, a short history

In the 1960s, a Swedish neurosurgeon, Lars Lexell, and two physicists, Kurt Linden and Börje Larsson, developed a dedicated treatment unit to enable high precision treatments of brain lesions. In 1967/68 the first GK was built. The principle was based on isocentric treatment, fixed collimation with several small (on the order of millimetres) diameter field sizes, a coordination system directly attached (screwed) to the skull using the 'G-frame' to minimise set up error, and a couch with only three degrees of freedom on which the G-frame (and hence also the skull) is directly attached. Since the couch can only be moved linearly in X, Y, and Z directions, the accuracy was significantly increased since rotation does not contribute, which can be a major source of uncertainty in other situations.

While a linac had to rotate around the patient, GK used a range of fixed angles, defined by the multi-source positions and fixed collimation system; hence no moving parts and no associated uncertainties. To achieve a steep dose gradient about 200 Co60 sources (201 in the models U, B, C and 4C, and 192 in the model Perfexion) were used.

In the 1980s, CT and MR imaging slowly became more commonly available to public health care centres. With this 3D imaging the diseases treated with GK widened and the targets became more complex. More shots (radiation spot deliveries, which combined make up the total treatment) were used which meant time consuming readjustment of the patient for each shot position. At first the positioning of the patient was done manually (Model U, B and C). With the model 4C an automated positioning system (APS) was introduced, which could enable all shots to be irradiated in one sequence if they had the same collimation requirements and the same plugging (blocking individual beamlets to protect an organ at risk (OAR).

With increasing complexity of the target the number of shots increased. In order to automate the blocking process the GK Perfexion (GKP) model was introduced in 2006. To achieve this, the geometrical source arrangement was modified. The sources were divided in 8 groups placed in sectors each

housing 24 Co60 sources. The physical position of the sources was not on a hemi-sphere anymore but on a conical cylinder. Each sector is attached to a motor that can move that sector's sources to a range of collimation (from 4 to 16 mm diameter shots) or blocked positions. With this arrangement each sector can be individually chosen to be 4, 8, 16 mm or blocked in a single shot, generating so called "composite shots". This reduces the number of times the RTT has to enter the room for a collimation change or for adjustment of plugs and increases the flexibility in conformal planning.

In addition the G-frame system meant that most GK use was for single fraction treatment. However, the GKP allows much easier routine fractionated treatments, using a re-positionable patient immobilisation system based on a vacuum surveilled mouthpiece (eXtend). This enables treatment of larger lesions, but potentially introduces other (repositioning and patient movement) uncertainties. These are the focus of the current work.

A further evolutionary step has appeared during the course of this work, the Icon with a changed re-positioning system and the addition of a Cone Beam CT (CBCT) on-line imaging verification system to help deal with positioning uncertainties and changes and a reflector system that allows an indirect surveillance during treatment.

Physical dose and biological effective dose (BED)

While GK has generally been used to deliver single high fraction doses that destroyed all tumour cells in one session (multi target model), other radiotherapy techniques use lower doses in various fractions. Based on clinical experience and analysis of patient clinical outcome, clinical trials were designed to find the "optimum" dose to minimize damage to individual normal tissues (NT) and OAR while increasing tumour cell damage and thus maximizing the therapeutic range. The conclusion was that the biological effect is not only dependent on physical dose but also on cell type, fractionation, dose rate and other factors. For in-vitro irradiation of cells, it was possible to demonstrate conversion factors (Linear Quadratic or LQ-model) and rules to quantify the biological effective dose (BED) but these do not

necessarily readily translate to in-vivo effects due to the metabolic system in place in living bodies and therefore have to be applied with caution to patients.

Most radiotherapy is external beam using mega-voltage x-rays and mostly given in fractionated treatments. So far, as above, GK has been mainly used for single fraction stereotactic radiosurgery applying a very high dose in one session. The introduction of the Perfexion, and the possibility for more routine fractionated GK treatment, gave rise to the current work, firstly to consider the uncertainties involved in fractionated GK use and also their dosimetric impact for targets and OARs.

In addition, where the prescribed dose is to the 50% isodose, as is common for GK treatment, the dose inside the target is significantly higher than that outside. Hypofractionation with GKP might thus benefit both, inside and outside the target volume, from biological effective dose effects, i.e. the high dose inside the target (multi target effect) and the protection of the NT in the low dose region (LQ region).

Chapter 1:
Introduction and literature review

"Chemotherapy has made substantial progress
in the therapy of systemic cancer,
but the pharmacological efficacy is insufficient
in the treatment of brain metastases."

Lippitz et al 2013 [3].

Improving the treatment of brain metastasis could lead to better survival and Quality of Live for cancer patients.

1.1 Motivation

About 20-40% of cancer patients develop brain metastasis [4]. Approximately 11700 people in the UK have been diagnosed with a brain tumour in 2016. About 65% of those are <65 years old [5].

To treat brain tumours, fractionated whole brain radiotherapy (WBRT) is often applied but provides limited local tumour control and induces side effects such as fatigue or reduced cognitive function which leads to reduced quality of life (QoL [3]).

Stereotactic radiosurgery (SRS) can reduce several of the side effects. New and improved diagnostic technology like PET/CT or high resolution MR imaging can detect much smaller lesions thus reducing the risk of missing small lesions. Due to the low dose in NT re-treatment is possible for both new lesions or recurrence. The GammaKnife (GK) is an efficient and cost effective treatment unit dedicated to SRS of solid brain tumours, that can provide tightly conformal high dose deliveries, thus preserving a high QoL [3].

1.2 Treatment options

1.2.1 The options for cancer treatment in general

Treatment of brain tumours can be with chemotherapy, surgery, or radiation therapy. Often a combination is used. Steroids are often used to ease symptoms from a tumour such as headache.

Chemotherapy is mostly used to treat the primary tumour, such as lung or breast cancer, and disseminated disease. The effectiveness of such chemotherapy on a brain metastasis, for example from a small cell lung cancer (SCLC), is unclear. The blood brain barrier (BBB) makes it difficult for most drugs to penetrate through and reach the brain tumour. However, Steroids are often used to reduce the pressure on the brain caused by cerebral oedema from the metastasis.

If the tumour is accessible **surgery** is an option. Surgery is often combined with WBRT or with stereotactic radio surgery (SRS). Surgery is limited to a single metastasis or a few metastases. Large metastases, multiple

metastases or metastases located next to or infiltrating an OAR cannot be safely removed. In such situations, surgery can reduce the tumour load (total volume of all metastases) combined with whole brain **radiation therapy** for small micro lesions which are not yet visible in the CT or MR scan. Remaining residual tumour, multiple solid lesions, and/or positive resection margins can in addition be treated with an SRS boost. Such a combined approach increases the survival [6-9].

1.2.2 Brain irradiation: WBRT and SRS

Most primary tumours can spread cells to the brain. Some of the most common are lung, breast, colon, kidney or melanoma tumours [5]. While the primary tumour could be controlled with surgery, the location of potentially developing brain metastases was challenging to predict. MR was (and sometimes still is) not always available, and on a CT scan, a tumour is difficult to detect, even when using a contrast agent. Experience from that time showed that, when there were three brain metastases visible, it was very likely that there were many more small ones not yet visible [10]. To be on the safe side, the whole brain was irradiated in order to target all, even the smallest, metastases. This approach worked in terms of tumour control but had side effects in regards to QoL since the whole brain was receiving the prescribed dose, and also the dose was limited by such effects. The patient suffered from fatigue and apathy [6, 9, 11-16]. Before the introduction of CT technology, brain metastases were not visible, and surgery rarely an option. WBRT was the primary treatment method. When CT scanners were introduced, about 50% of the brain metastases were judged as solitary, but later, when MR and became available and T sequences with gadolinium could be used, it turned out that less than 1/3rd of the metastases were solitary [17, 18]. With improving image quality, better resolution, contrast agent use, MR, more widely available etc., brain tumours could be detected at an earlier stage. With few small brain lesions, SRS became an option.

However, even with improved diagnostic imaging, it is not possible to detect all metastases in the first treatment. If the primary tumour is controlled, no further metastases are seeded, but the small ones already sited in the brain

tissue will grow. Therefore, if the patient has all other disease controlled and survives, several metastasis treatment sessions might be necessary. With the development of new technologies such as MLC and intensity modulated radiation therapy (IMRT) on the linac, new approaches for WBRT became possible and were investigated. The idea was that more localised and more conformal treatment, sparing critical brain structures where possible, e.g., the hippocampus, could control metastases but this time without the side effects. Today when high precision is required, and there are only a few metastases , SRS is chosen and when it is clear that there are many metastases and when a high-end linac is available, WBRT with hippocampus sparing and simultaneously integrated boost (SIB) may be chosen. Or a combination with WBRT to a lower dose and a stereotactic boost to the larger lesions.

1.2.3 Treatment of brain lesions

1.2.3.1 Radiation therapy with GK

Radiation therapy can be used for different goals in brain tumour treatment. With WBRT small micro lesions should be prevented from developing to full-size tumours. It should also stop the tumour growth of larger lesions. WBRT is often applied when there is a primary tumour, e.g. lung or breast tumour, which has spread to multiple locations and more than those visible at the time of diagnostic imaging are expected to develop.

Side effects of WBRT are dementia, fatigue, lack of initiative, to name just a few. The approach with GK is different. GK is not capable of WBRT but can only tackle small lesions. Post-surgery RT with GK (or GK alone) aims, therefore to treat all visible lesions. If the control image in a few months shows new lesions, a second round of treatment can be done. This approach often works well. However, if in the second control scan, more lesions are found a decision has to be made. The usual option is WBRT. The problem here is the total dose. When the high dose from the SRS and the WBRT dose are added, the tolerance dose might be exceeded. A compromise in the WBRT dose has to be chosen depending on the dose and size of the previous GK SRS

treatment. However, an alternative option is to treat the new lesions with GK SRS [19, 20].

With the side effects from WBRT and the restriction of GK to small lesions, alternative methods have been explored. It is assumed that the side effects for WBRT are mainly due to the dose to the hippocampus [21-24]. WBRT was developed when there were only "open fields" available. An "open field" is a homogeneous field of a certain size covering the whole brain for irradiation. Everything in the path of the beam gets the prescribed dose. In earlier techniques beam modulation was only minimally possible by using a wedged absorber to induce a gradient in the dose. In about the year 2000 IMRT was introduced, and about ten years later IMRT was widely available. With IMRT it is possible to shape the dose distribution and reduce the dose to the hippocampus. Trials went in this direction in the hope to reduce the side effects of WBRT.

GK went in another direction (see section 1.2.). Large lesions cannot be irradiated with a single fraction but with the G-frame fractionation was not a routine option. Introducing a new model of GK, the Perfexion, allowed the redesign of the head fixation. The frame was replaced by a vacuum surveilled mouthpiece (eXtend) and later (after this work had started) a mask system with a reflector on the patient as a motion detector. With these systems, fractionation is possible.

1.2.4 The treatment units capable of SRS treatment

1.2.4.1 The principle of GammaKnife

The history of the GammaKnife (GK) started around 1950 not with a radiation oncologist but with a neurosurgeon, Lars Leksell, from Stockholm, Sweden. Lars Leksell and a team of physicists led by Borje Larsson developed a treatment unit that was capable to ablate cells with ionizing irradiation [25-27]. As a surgeon, Leksell's aim was to destroy all tumour cells in one session while keeping the dose to the brain and organs at risk (OAR) as small as possible. He introduced the "Gamma Knife" (Gamma=ionizing radiation and Knife=scalpel), a treatment unit containing 201 Co60 sources arranged hemi-

spherically and focused such that their individual beams intersect at one point, the “isocentre”. The objective is to position the centre of the patient’s target volume accurately at that isocentre.

Co60 was chosen for this because the energy of 1.17 and 1.33 MeV is high enough to penetrate through skull and brain tissue and because it's potential for radioactive density (decays per volume) is high enough to make small sources that can be assumed to be point sources. Another important characteristic of Co60 is it’s half-life time of 5.27 years. With the decay of the sources the treatment times become longer. This may be inconvenient and it may have an impact on the biological effect due to different repair mechanism Given that the head is smaller than the body (shoulders, pelvis, etc.), the radius or distance for the sources to the isocentre was designed to be smaller than for a linac thus increasing the dose rate and reducing treatment time.

The system itself had the sources placed in a shielded semi-spherical housing. The shielding door protected the area outside. The sources are considered point sources that irradiate in all directions. Except for a small tube pointing towards the iso centre every other direction was blocked. In order to define a specific beam diameter, a second layer of shielding is available, the so called “helmet”. This is a semi-spherical construct that contains tubes with a specified diameter so that the beam at the iso centre has a defined diameter. The sum of all beams results in a high dose with a near-spherical shape. This single dose distribution is called a “shot”.

For exact positioning at the target in the isocentre the skull of the patient is directly attached (screwed) to a reference frame, the G-frame, which then is attached to the positioning mechanism. This then moves the patients head inside the helmet to be placed more right or left, up or down, further in or out of the helmet. The positioning mechanism that is connected to the helmet is fitted with a high precision adjustment mechanism. The principle of the GK model C is shown in Figure 1.1, the G-frame can be seen in Figure 1.2, the helmet, the collimator tubes, and the positioning mechanism can be seen in Figure 1.3. Once the patient is positioned in the correct place inside the collimator helmet the couch with helmet and patient is moved inside the source housing. After a precalculated time, when the prescribed dose has been

delivered, the couch is moved outside and the position for the next shot is set. The exact workflow id described later.

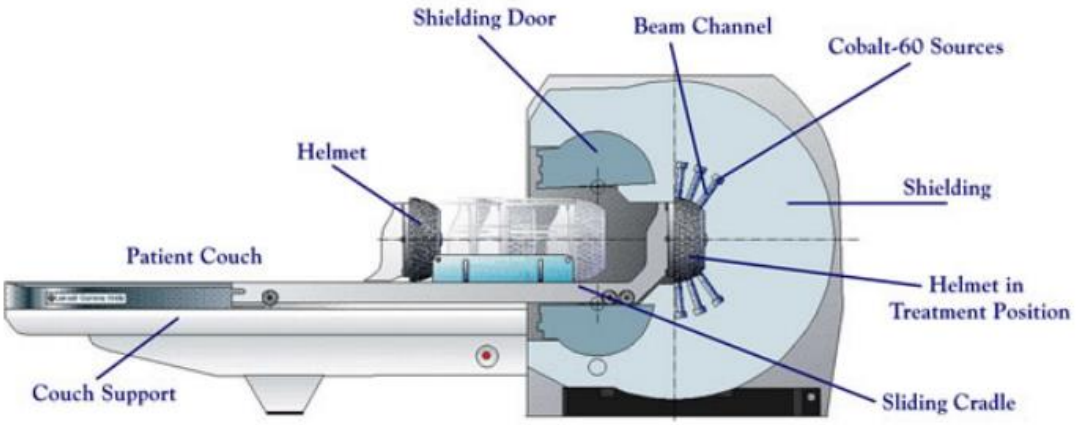

Figure 1.1: *The principle of a traditional GK is shown. A big shielding block houses the Co60 sources. The centre of this block is semi-spherical with an opening towards the couch. The helmet is mounted on the couch together with a connector for the G-frame and a positioning mechanism. For the treatment, the patient is placed in the correct position within the helmet, and then helmet and patient are moved into the treatment position where they remain for a precisely defined time until the prescribed dose for this shot is delivered. (image courtesy of Elekta)*

The connection with the G-frame, the precise (and simple) mechanics for the patient positioning and the static nature of the sources makes the whole system stable and allows for submillimetre accuracy [28-30]. For the small collimators, diameter of 4, 8, 12 and 18 mm are available, enabling even small lesions to be treated with optimal sparing of the surrounding healthy normal tissue (NT).

In 2006, Elekta announced a new GK model named “Perfexion”. This model differs in many ways from the previous models. In addition to the automated couch, which was already installed on the model 4C it has automated source collimation, automated blocking and the option to treat not only with the G-frame but also with a repositioning system that consists of a vacuum surveilled mouth piece and a novel position test tool. More details about the procedure of a GK treatment and the differences of the new GK Perfexion (GKP) system are given in the sections on “workflow” and “the differences in the workflow treating with GKP”.

1.2.4.2 Adapting linacs for SRS

Early linacs had simple jaws to irradiate square and rectangular fields. Field conformity was achieved with blocks. This was good for large volumes (larger than 4x4cm^2) but too big for small brain lesions, especially if they were close to critical OARs like the brainstem or the chiasm. For SRS, small fields were required. The first systems for SRS on linacs were based on add-on systems using small circular collimating 'cones' and head frames or dedicated masks [31-33] e.g. Gill-Thomas-Cosman (GTC Frame) or BrainLab system [31-36]. The BrainLab system, for example, consisted of cone collimators with various circular diameters that could be attached to the linac with a special adapter. Whenever the linac was used for stereotactic treatment the adapter was mounted and a Quality Assurance (QA) procedure was performed to make sure it was adjusted correctly. A special mechanical system allowed the fine-tuning of the adapter so that the collimation tubes were aiming perfectly towards the isocentre. For this QA check, the Winston-Lutz-test was developed. With this test, a radiographic film is irradiated to measure the isocentre accuracy of the gantry-, collimator-, and couch-rotation. In all cases, an elongated, small irradiation field is rotated and the centre line per field drawn. The intersection area indicates the isocentre accuracy. The other part of the Brainlab system was the immobilization device. Two options were available: A minimally invasive frame very similar to the G-frame of GK and a special designed mask system for fractionated treatment. This mask has a reinforced part exactly under the nose and at the forehead, meant to minimize the head rotation. Furthermore, on the side of the mask, there are spacers. If the mask becomes loose or unbearably tight a spacer can be removed or added and the mask re-fitted again. This should be with an investigation of why the mask has become loose. Often it is an effect of the behaviour of thermal plastic but it might also be a change in patient anatomy. With this dedicated system, accuracy of one to two millimetres is achievable [34, 36-39].

This presented the challenge of accuracy. SRS is treated with no margin or a very small margin. The accuracy of the whole procedure on a linac should therefore be within 2 mm or better. This includes imaging (resolution,

distortion), reproducibility of the set up between CT scanner and linac or frame-based SRS with a reliable docking system for the frame in the CT scanner and on the linac, couch position in X, Y and Z direction and couch rotation. Set up, preparation and QA were very time consuming and required highly trained teams for mounting and adjusting the add on micro-MLC systems, and five, six or nine field plans were still no match for the dose gradient of GK. Another option on linacs was non-conformal arc therapy. This results in a steep dose gradient but loses conformity for irregularly shaped lesions. Around the year 2000 dedicated micro MLCs were introduced with thinner, (e.g. 3 mm) leaves that allowed conformal fields [40, 41].

The next step in linac SRS was combining MLC and IMRT. At first there were dedicated linacs with small field sizes and high-resolution MLC's. Today SRS is on "dedicated standard linacs" (high end) which have MLCs with a leaf width of 2.5mm in the centre and a positional accuracy of submillimeter for gantry, collimator and couch rotation, without the patient. This is close to and maybe even reaching the accuracy of GK using a G-frame [42]. With arc technology (developing towards VMAT) conformal fields were replaced by conformal arcs thus distributing the entrance dose over a larger volume coming closer to GK dose distribution.

1.2.4.3 Other types of treatment units: Tomotherapy and Cyberknife

Linac and GK are the oldest treatment units used for SRS. Starting from about the 1990s other systems have emerged, based on variations and novel designs of the traditional linac. They play more a niche role but for the sake of completeness the most important ones are briefly described here.

One such device is the **Tomotherapy** which was invented in the early 1990s at the University of Wisconsin–Madison by Mackie and Reckwerdt [43-45]. Tomotherapy is built like a CT scanner, but with a short 6MV linac instead of a kV tube and delivering treatment dose instead of measuring the transmission dose for imaging. n a way, it is equivalent to an inverse, single detector row, CT scanner using MV X-rays and delivering dose in a continuous helical manner via novel MLCs to provide flexible tailored dose distributions. It is

particularly useful to treat complex target distributions or indications where a long field size is required.

Another device from about 1991 is the **Cyberknife**. The system was proposed and realized by Adler [46-48], a Stanford University Professor of neurosurgery and radiation oncology, and with Peter and Russell Schonberg of the Schonberg Research Corporation. Here the linac tube is mounted on a robotic arm. The original intention was to irradiate brain tumours, but due to its ability to move in all directions since it is a robotic arm, it is often used to irradiate moving targets in lung and liver.

1.2.5 Why GK?

Originally, the accuracy and possibility to treat small lesions provided by the GK was unrivalled by linacs. Today, however, linacs can have a similar accuracy and have small MLC leaves that allow good conformity [49-51]. However, a linac dedicated to stereotactic RT, is one of the high end expensive models. It also requires additional costs like a bigger treatment room, much more expensive room shielding, expensive therapy planning system (TPS). Comparing plans from a linac with that of GK is difficult because the two treatment techniques are fundamentally different. A linac can shape the field contour according to the target from every angle. The aim is to achieve a homogeneous dose distribution. This is important when large volumes are irradiated that contain an area with mixed tumour cells infiltrating NT. The homogeneity protects the NT (therapeutic window). On the other hand, GK methods prescribe the dose for most malignant tumours to around 50% because the cell type inside the target is considered to contain exclusively tumour cells. In this situation, a higher dose inside the tumour is an advantage. Such comparisons show that a high-end linac is close to GK treatment in many cases.

Even though the linac is not quite as accurate as GK it can deliver good quality SRS of the brain [52, 53]. Linac-based SRS might be more cost-effective than a dedicated GK machine where the number of patients for brain SRS is limited and the linac can be used to develop and deliver SRS to other body areas e.g.

lung, liver, spinal cord too. These new techniques, Stereotactic Body Radiation Therapy (SBRT), or Stereotactic Ablative Radiation Therapy (SABR) have been used mainly for lung, bone and liver tumours [54-60]. For these techniques, a highly focused beam is applied to treat a small volume with a very high dose. As for SRS in the brain, accuracy is very important to reduce the dose to the surrounding tissue, especially since the lesion is either in the lung or near the spinal cord, etc.. To achieve a steep dose gradient, the gantry moves in an arc around the patient. In order to spread the dose further such arcs are planned and delivered with various couch angles which limits the potential arc angles due to collision avoidance.

GK on the other side is dedicated to brain SRS and is relatively easy to use, is comparatively low maintenance, and is cost-efficient, where the patient numbers are sufficient [61].

1.3 Workflow of a GK treatment (traditional GK prior to Perfexion)

The G-frame is directly attached to the skull bone. It has to remain firmly attached from MR scanning for planning until the end of the treatment. Fractionated treatment requires a minimum of six hours between fractions to allow for the repair of NT to take place. A day would be better. Thus a three fraction treatment would mean a planning MR in the morning, first fraction at noon ar afternoon, second fraction afternoon or next morning and the last fraction the next day or ideally the second next day. This means the patient has to sleep with the frame on. This is not only uncomfortable for the patient but also involves the risk of the frame slipping during the night. A feasibility study by simonova et al. [62] showed fractionation with GK and G-frame is possible. However, during the author's own experience at the University Hospital in Zurich (Switzerland) one out of a total of three patients lost the frame overnight. Therefore, even though fractionation would potentially reduce side effects, it is difficult to apply it on a routine basis with the G-Frame system. Therefore the new GK model Perfexion and the relocatable system eXtend was introduced.

The following part shows the workflow of a treatment and explains the challenges and science of each step.

1.3.1 Preparation and fitting the G-frame

The original intention of GK was to treat a patient in a single fraction with a high, ablative dose. The resulting workflow is described below.

The patient arrives early in the morning in the GK centre. The patient was informed about everything on the previous consultation, so he or she is mentally prepared for the next step. Using local anaesthetic, the G-frame is attached to the skull bone (Figure 1.2).

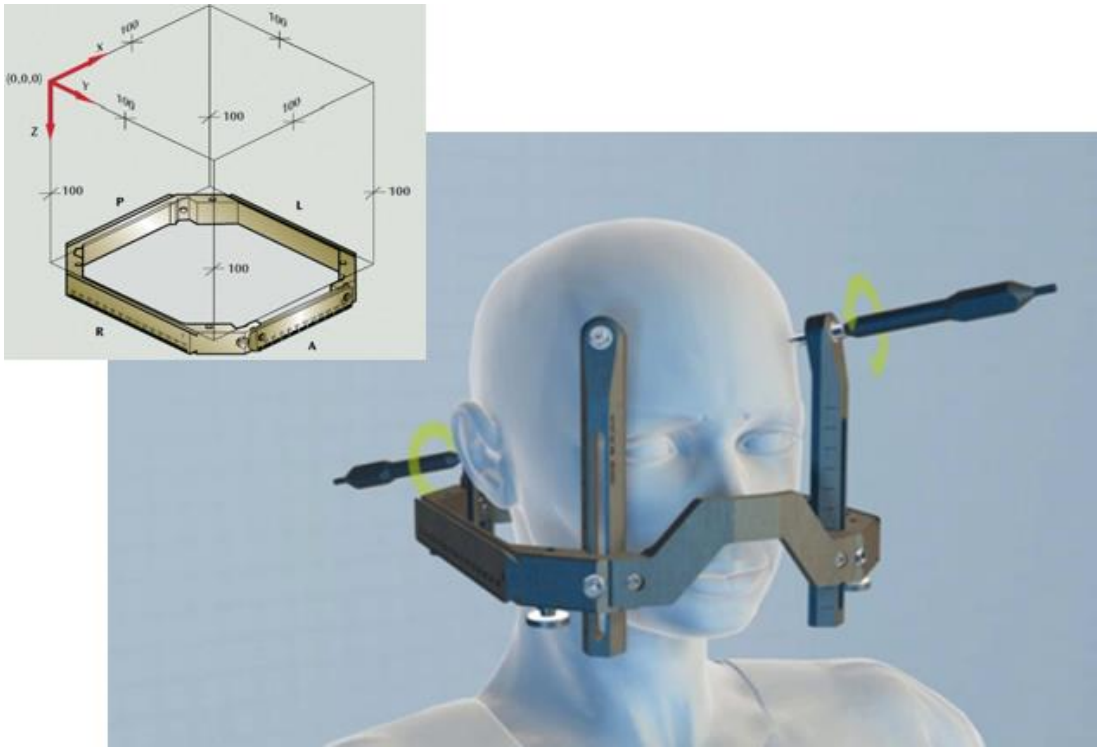

***Figure 1.2**: Top left shows the coordinate system used by GK. The base frame (squared structure) is the original structure. The main image shows how the frame is attached to the skull bone. This frame base is from a newer model and which was modified to spare the mouth. During the preparation of the patient for treatment, the G-frame is attached to the skull using screws. Four posts are attached to the actual frame. The length of the posts is chosen to allow the screws to be placed on a safe and solid place on the skull. Screws are always tightened in opposing pairs. (image courtesy to Elekta)*

With the frame firmly attached to the skull, the patient is taken to the MR scanner. Here the localizer is attached to the frame base, and a planning MR scan is performed. The localizer is a box with a "Z" like marking on either side so the exact orientation and position of the frame, and therefore of the head, within the GK coordinate system can be determined.

The direct connection between frame and skull bone eliminates most sources of uncertainty. Potential reasons for positional deviations could be flex in the posts or the frame fixation screws not properly tightened. The overall accuracy of the G-frame is in the range of submillimetre [29, 30].

1.3.2 Acquiring the planning MR image

For accurate treatment, the position of the tumour and target within the GK coordinate system has to be identified correctly. MR scanning is generally used. The detailed functioning of an MR system is beyond the scope of this work. However, one characteristic of an MR system is essential to understand: distortion of the acquired image! For an MR scan, an object, here a patient, is placed into a magnetic field. Any object brought into a magnetic field disturbs and distorts the field, such that, the resulting image does not directly reflect the geometry of the actual image. The distortion depends on the parameter setting of the MR unit (T1-, T2-weighted, relaxation time, etc.) and on the type of object entered in the field. For diagnostic radiology, a distortion of a few millimetre is generally not a problem. However for radiation therapy treatment purposes geometric accuracy is critical. For GK treatment, displacing a shot for a small target by this amount could mean to miss a significant part of it. If the materials and shapes of the object that is placed into the magnetic field are known, a correction can be applied for the reconstruction algorithm. Since the head is close to spherical, this is taken into account. In addition to that, scanning parameters can be selected that result in a more robust image. So it is important to optimize the MR scan for minimal distortion. Often there are dedicated sequences that are also checked in regular QA procedures.

1.3.3 Planning with GKP

Now, with the planning MR image available, the planning can take place based on this. The frame must stay attached to the patient during this time. In the

meantime, a dosimetrist imports the image data to the TPS and defines the localizer in order to define coordinate system. This is by identifying the dots from the localizer in the transversal slices. The TPS expects these in a clearly defined relationship to each other, which provides an internal QA. If the dots are within a predefined tolerance of the expected position, the planning can proceed. If the discrepancy is too big, the data set may not be accepted for planning. One reason for this may be that the patient's head differs too much from the assumed model used to correct the distortion of the magnetic field. In this situation, a CT scan can be performed, where contrast and image quality are less, but almost no distortion is present. In this situation, the CT scan and MR scan are matched on the TPS with the best matching accuracy in the target region and the CT scan is used for the positional definition of the shot placements. The clinician then uses the MR scan to delineate the target and possible OARs near the target.

1.3.3.1 Prescribe to an isodose level

In order to deliver the dose, several shots are placed inside the target where their combination is planned to covered the whole target volume with the prescribed dose. Due to the overlap of the shots, the dose inside the target is inhomogeneous. Since the target consists of tumour cells only, this is an advantage as long as all cells receive a certain minimum dose. The dose is therefore usually prescribed to 'about' the 50% isodose, where "about" is used for two reasons. Firstly, in order to treat the tumour a minimum dose has to be achieved. To allow a tight fit of the isodose to the target, a small part of it may be below that prescribed dose. This also covers uncertainties due to the finite pixel size and dose calculation resolution grid. Covering every voxel in the target would result in a technical margin of half a voxel size since the target line just passes through the voxel and does not include the box-shaped voxel meaning NT or OAR is irradiated. The amount of under-dosage allowed is smaller, e.g. 1%, for a malignant tumour and larger, about 2-5 %, for a benign tumour. A critical aspect is the location of the under dosage. If there is a small "tail" in the tumour growth that has been identified as tumour cells, the clinician should make sure that it is not that part that is underdosed. The under dosage should smooth out the surface and should not be in a critical part of the target. The second reason relates to nearby OAR. If a tumour is close to or even invading an OAR a decision has to be made whether the coverage of the target has to be compromised near the OAR to keep the dose to the OAR below a critical level or if the OAR (or an area of it) may be sacrificed. This might be

possible, for example, for an essential but not life-critical organ such as the optic nerve. Such a decision has to be discussed with the patient and is usually only made if the function is already very poor or non-existent.

Planning for GK treatment involves shot placement. Prescribing to the 50% means that for every change in the plan, i.e. adding a new shot or moving a shot, the dose maximum has to be re-calculated and then the new 50% defined. Therefore, even small changes can result in significant changes in shot times and therfore in isodose in different places. For that reason, if a plan is almost perfect, but the coverage is too low (or for benign tumours too high), the prescribed isodose may be adjusted. Lowering or increasing the prescribed isodose increases or reduces the prescribed dose volume respectively,

There are other options for prescribing the dose. A variation could be used for very small or near perfect spherical targets up to 20 mm in diameter. By changing the prescribed isodose level the diameter of the shot can be varied and adjusted to fit the target. The other usual variation is for the treatment of the trigeminal nerve. Since the aim for trigeminal treatment is not to stop tumour growth but to block the transmission of facial sensation and pain, no volume needs to be treated, only a single, small point in the centre of the nerve. So for the trigeminal the prescribed dose is to the 100%, the dose maximum.

1.3.3.2 Protecting OAR

To achieve a steep dose gradient there are 201 beams pointing from all directions towards the isocentre and the target. This steep dose gradient should protect OAR's. However, in some situations the beam might pass through the eye (aging, cataract) or the target is just very close to the optic nerve or the BS. In such a situation it is possible to block these individual beams by replacing the collimator insert with a plug that stops the beam in that direction.

1.3.3.3 Plan evaluation with quality indices PCI and GI

Often several plans for the same target are created. Due to the steep dose gradient, it is difficult to decide based on the dose distribution which plan is the best.

In order to evaluate different plans for the same target objective standard parameters are used. To put a number to the plan, quality indices have been

introduced. For GK planning, the Paddick Conformity Index (PCI) and Gradient Index (GI) are most commonly used [63-66]. The PCI is an indication of how well the dose is covering the target without excessively spilling over to NT. When Paddick suggested the new “proposed” conformity index there were two other indices used. One was the PITV ratio from Shaw et al. (1993) [67]. For this, the prescribed isodose volume (PIV) is divided by the target volume (TV). The problem with this index is that it results in a value of “one” (perfect plan) whenever the PIV is equal to the TV, regardless of the actual location of the dose. In theory, the PITV could have a value of one, indicating a perfect plan, even when the dose distribution completely misses the target. It would not cover any potential underdosage of the target. In 1998 Knöös et al. [68] proposed another conformity index dividing the target volume receiving the prescribed isodose (TV∩PIV) by the target volume. This method covers any underdosage of the target but fails to indicate excessive dose outside the TV.

So in 2000, Paddick et al. [63] proposed another conformity index that covers both excessive dose outside the target in NT and underdosage of the target. Firstly, excessive dose to NT is picked up by calculating the ratio of the TV covered by the prescribed isodose divided by the PIV. This factor is always smaller or equal to one. Then to indicate potential underdosage of the TV, the ratio between TV covered by the prescribed isodose to TV (i.e. that should receive the prescribed isodose) is calculated. Again, this value is always less or equal to one. Multiplying the two ratios gives the Paddick Conformity Index (PCI). A small PCI indicates either an underdosage of the target or a large volume of NT irradiated with the prescribed dose, but cannot distinguish between the two. This is important because for a malignant tumour, underdosage is more problematic than irradiating some extra volume. Benign targets, on the other hand, are treated to lower doses not risking severe damage to the NT. In addition to PCI, the minimum dose and coverage are usually also reported.

PCI gives information about the prescribed dose. It says nothing about the low dose outside the TV. In theory, the whole brain could be irradiated with a dose of only 1% below the prescribed dose, and the PCI would not indicate that. In 2006 Paddick and Lippitz [69] suggested a “gradient index (GI)” that

would indicate the steepness of the dose gradient in order to protect the normal tissue outside the target. The only aim is to reduce the dose to NT outside the TV as quickly as possible. For this reason, the GI is the ratio between the volume of half the prescribed isodose and the volume of the prescribed isodose.
It may be noted that all these conformity indices are unitless numbers, being ratios of volumes.

These indices are useful to compare plans for the same patient but have little or for some even inverse significance in indicating clinical outcome [70-72]. Clinically, small tumours have a better prognosis than large tumours. In order to evaluate a plan, a higher PCI and a higher GI indicate better plans. This is true if several plans for the same target are evaluated and compared against each other, but the achievable values depend on the target size. For a large volume, it is much easier to achieve a PCI of 0.95 than for a small one. This is because displacements are in one dimension and on the order of a millimetre, whereas a volume is amplified by the power of three. For example, if a target with 10 mm diameter and one with 30 mm both have a plan that has about 1mm extra tissue irradiated to ensure coverage, then for the small volume, this is a volume of 173 mm^3 NT or OAR irradiated and for the large volume an additional 1461 mm^3 NT or OAR irradiated. The PCI is 0.75 for the small volume and 0.91, much better, for the large volume. This is because the coverage should be within a certain distance in millimetres (power of one), but the PCI is calculated from volumes (power of 3). For that reason, PCI should only be used to compare various plans for the same target, and achievable goals should be adjusted to tumour size.

1.3.3.4 Prescribed dose

The dose prescribed depends on various parameters. Most important is the target cell type.

- *Malignant tumours* are preferably irradiated with a minimum of 20 Gy[73, 74]. The aim is to stop cell proliferation and destroy the tumour cells. Malign tumours grow rapidly and destroy surrounding tissue in a

short time. The primary may also seed and create new tumours elsewhere. For that reason, SRS is often combined with WBRT [7], but an alternative can be repeated SRS.

- *Benign tumours* grow slowly and do not seed. The aim is to stop tumour growth for the long term. This can be done with 12-16 Gy. The lower dose protects NT. Examples are meningioma [75-80] or Acoustic Neuroma [81-83].

There are also other indications for GK treatment, for which different prescribed doses are chosen. These are listed briefly below, but are not discussed in detail:

- *Trigeminal nerve*: 80Gy (70-90Gy depending on institute guidelines [84, 85]) placed over the skull bone and close to the BS so that the BS receives less than 20% - 50%, depending on institute [86]. Others limit it to a specific dose like “no more than 20 mm^3 receive 15Gy” or “no more than 10 mm^3 receives 12Gy and only 1 mm^3 receives 15Gy” [87]. (Note: This range in the literature concerning BS tolerances may highlight an important point. One reason for the range may be a factor that is not published. In this case it could be a different policy in contouring the BS or different parameter of the MR imaging or window/level setting during the contouring. It is advisable to ask an author about local policy that might influence such variation before applying a higher tolerance level.)
- *Arteriovenous malformation (AVM)* is a disorder in blood vessels in the brain. Untreated the bulk of vessels can burst, and the patient can die. The prescribed dose selected is 25Gy for small AVM’s <2.5 cm but the dose is reduced to 16 to 20 Gy, depending on the target size [88-90]. A special technique is sometimes used for large volumes, treating in two or three stages. This means only half the volume is treated during a session. After a 3 to 6 month gap, the second part is treated. This is to reduce the dose to the brain or OAR and allowing recovery of the NT.
- A newer treatment area is for *psychiatric conditions*, such as obsessive-compulsive disorder. Patients who are resistant to pharmacological and psychiatric treatments can be treated with a radiosurgical capsulotomy where two 4-mm isocentre targets at the midputaminal

point of the anterior limb of the capsule with a maximum dose of 120Gy [91]. This is not part of this work and is listed only for the sake of completeness and a potential future field of treatment.

Another factor taken into account in prescribed dose considerations is toxicity. This might give dose limitations and will depend on the size of the lesion and therefore the volume and dose that NT and OAR are receiving. Large lesions touch on more NT than small lesions. In addition the dose gradient is reduced with increasing target size. Therefore larger targets are often prescribed with lower doses than small targets.

1.3.4 Treatment of the patient

Once the plan is accepted and approved the patient is taken for treatment. The patient is positioned on the GK couch where the first collimator is mounted, and the frame connected to the positioning system. Until GK model C the positioning of every shot was set manually with a ruler for each axis. When the position for the first shot is set, the couch with helmet and patient moves inside the associated planned time. When another shot size is required the helmet has to be changed and the patient positioned accordingly. This is repeated until all shots are irradiated. The model 4C has a robotic couch. So all shots with a specific collimator can be irradiated in one sequence. The patient is only retrieved from the GK when the collimator has to be changed. For OAR protection the relevant collimator tubes had to be replaced by plugs.

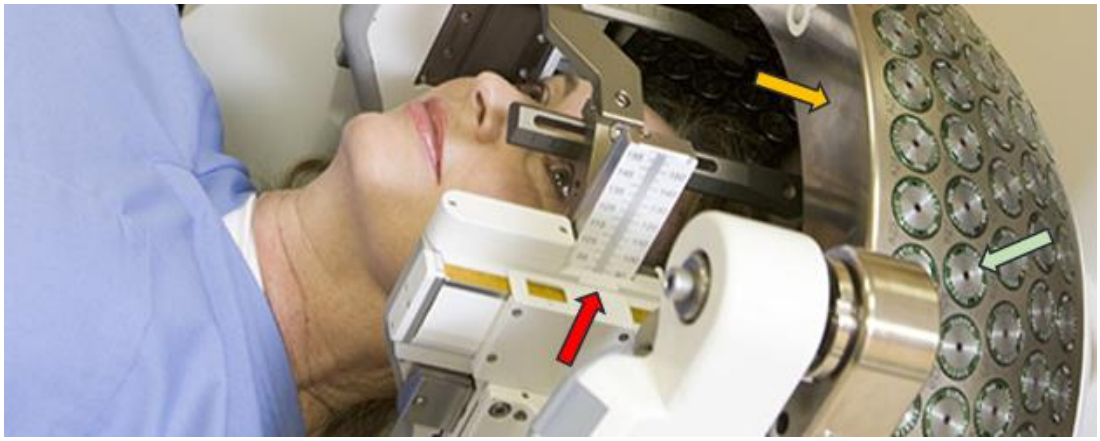

Figure 1.3: *Patient prepared in a GK with a helmet system. Each shot position was manually adjusted until with the GK model 4C the robotic couch was added. The* ***red arrow*** *shows the ruler used for exact positioning. The* ***yellow arrow*** *points to the collimation helmet. Before the Perfexion model, the helmet had to be changed when the shot diameter was changed. The light* ***green arrow*** *points to a collimation insert. For OAR protection the Insert could be manually replaced by a plug that would block the beam for the respective Co60 source.*

1.4 The GK modifications that allow automation and fractionation

The high dose required for single fraction treatment limits the treatable lesions in size and proximity to organs at risk (OAR). Although fractionated treatment with GammaKnife was tested early [62], to consider overcoming those limitations, the skull attached frame makes it difficult. The new GK model Perfexion (GKP) had a larger head space (Figure 1.5, top right) that allowed to introduce a new, non-invasive fixation system, the eXtend. The key component was a vacuum assisted and surveilled mouthpiece. The function of the mouthpiece can be seen in Figure 1.4 bottom and in Figure 1.5. This non-invasive positioning system allowed repositioning but introduced new uncertainties.

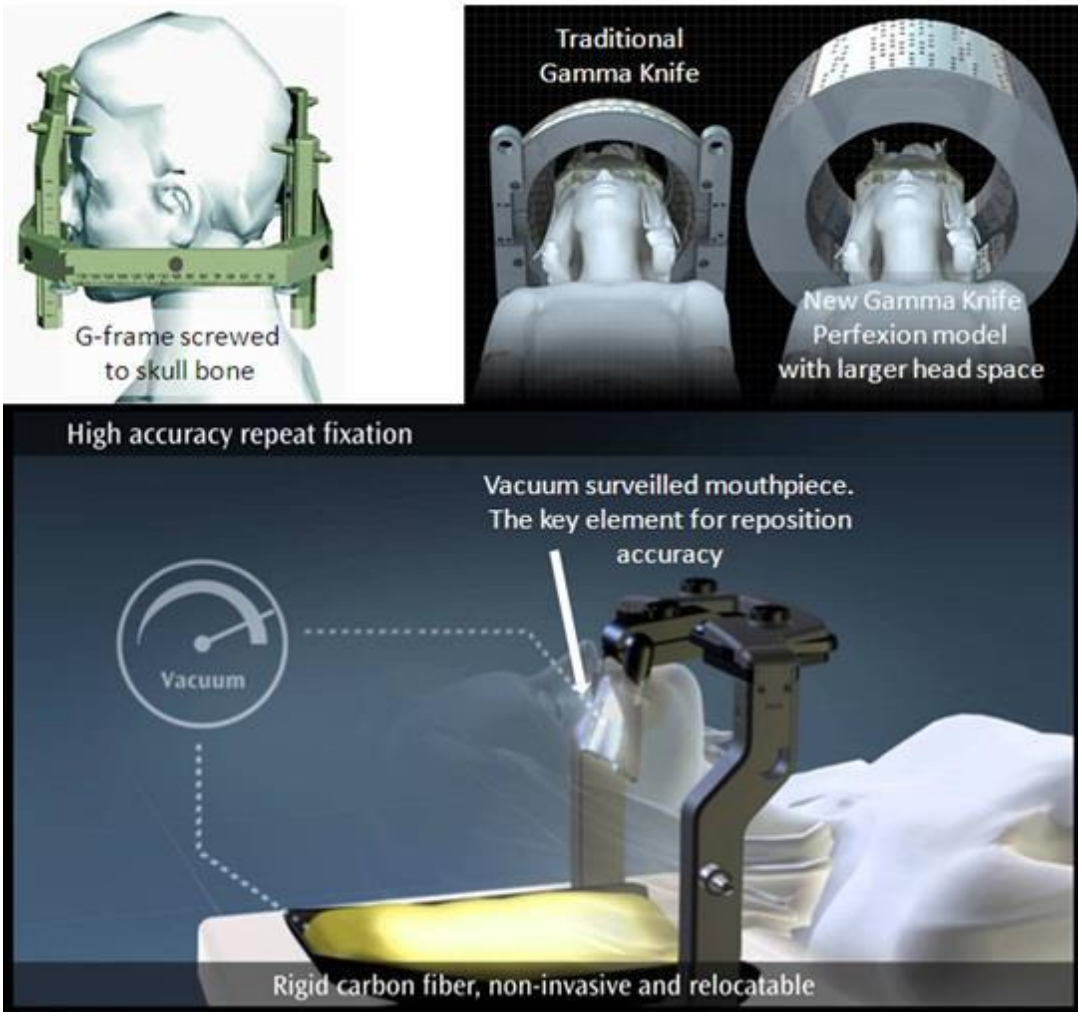

Figure 1.4: *Top left: G-Frame for Gamma Knife treatment. A localiation frame is directly screwed to the patients' skull. Top right: the Perfection model was completely redesigned. Among other major improvements the headspace was increased (right). Bottom: For eXtend, the key fixation point was moved from the four screws at the skull to the vacuum surveilled mouthpiece. (Images courtesy to Elekta)*

Figure 1.5 shows the new model GammaKnife Perfexion with a modified arrangement of 192 motor driven sources. This arrangement produces a steep dose gradient leading to the best possible conformity [92]. In the Perfexion model, the Co60 sources are no longer placed in a semi-spherical arrangement with equal distances to the isocentre but on a conical collimator block made of tungsten. The collimator is rigidly attached to the shielding block and contains four possible source positions: 16 mm, 4 mm, blocked, and 8 mm (Figure 1.5). This arrangement of the collimators was chosen to minimise unwanted irradiation. The blocked position is between the smaller two collimators so the source can be moved directly to the 4mm or to the 8

mm collimator. When the 16 mm collimator is chosen, the source has to travel over the 4 mm collimator. This passing over the 4 mm collimator adds a very small dose to the intended dose of the 16 mm shot. The so called “transit dose” was measured to be 0.035 Gy by Bhatnagar et al 2009 [93]. The linear design of the collimator allows to move the sources automatically with eight motors each moving 24 sources in a sector.

Figure 1.5*: The GK Perfexion, that was introduced in 2006, had a fundamental change in design of the source housing and the collimator system. The tungsten collimator array is fixed and directly attached to the shielding block that houses the Co60 sources. Rather than being spherically arranged, the geometry of the Perfexion is conical. This allows linear movement of the sources between collimators.*

With the collimator moved closer to the Co60 housing and shielding the new GK model Perfexion (GKP) had a larger headspace (Figure 1.4, top right) that allowed introducing a new, non-invasive fixation system, the eXtend. The key component was a vacuum assisted and surveilled mouthpiece. The function of the mouthpiece and the attachment to the frame can be seen in Figure 1.6. This non-invasive positioning system allowed repositioning.

1.5 Workflow for fractionated SRS with Perfexion and eXtend

For fractionated SRS the patient has to

attend several times for treatment. The different steps are:

- moulding the mouth piece
- planning MRI scan
- outline the target and create the plan
- first treatment fraction
- further treatment fractions

1.5.1 Moulding the mouthpiece

The patient arrives in the centre to prepare the mouthpiece. This can be done in any examination room. The patient sits in a chair (not in RT position) while a dentist or trained staff member prepares the mould. The procedure is similar to that a dentist uses when making a mould. The suitable U-shaped form (small, middle, or large) is selected and a two-component-paste mixed. The mixed paste is filled into the U-form and the spacer adjusted. The spacer is a small plastic disk with a pin in the centre. The pin is fitted through a hole in the form so that during treatment, the vacuum tube can be connected. Important is that the disc is completely enclosed in the mould paste so that a sealed cavity is formed once the mould is hardened and the spacer removed.

1.5.2 Finding the position for the mouthpiece and the frame

The same day or another, the planning MR is done. For this, the mould is loosely attached to the front piece of the frame. The patient is then positioned on the couch with the head on a patient specific cushion and the mould attached to the upper palate to fit tight. The front piece of the frame is then fit to the frame base and clamped tight. For the set-up, the mouthpiece can be moved slightly to fit tight in the mouth of the patient while the patient is in a comfortable position. When this is the case, the tightening screws are tightened and from then on never loosened until the treatment of the last fraction is finished. Figure 1.6 shows the frame and the mouthpiece in preparation and for treatment.

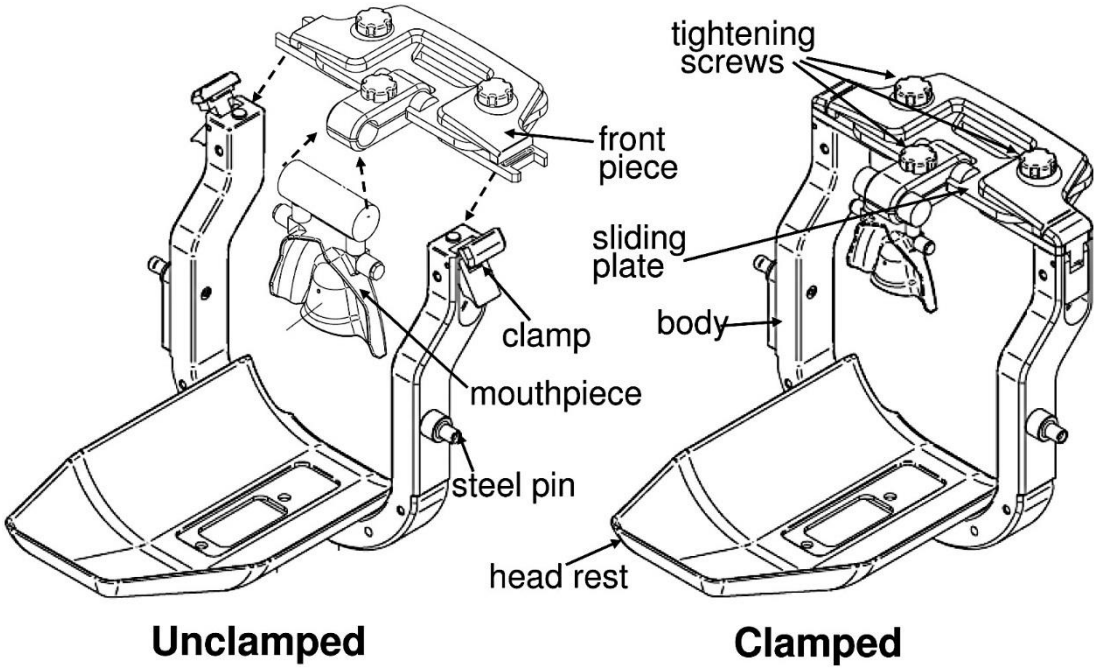

***Figure 1.6**: The frame with the front piece to which the mouthpiece is attached is shown. Left the loose frame before set up, Right: the frame with tightened screws which remain tightened and clamped down until the last fraction is completed.*

1.5.3 Planning MR and reference values

The GKP, at the time of this work, had no CBCT system available for positional verification prior to the treatment session. An indirect positional verification was therefore introduced with the Reposition Check Tool (RCT) The planning MR is then taken in this position. The sequence after frame fitting is:

- Sit up and rest again
- Then take reference measurements and verify after another sit up.
- Then MR scan
- Planning, to calculate the composite shots required for delivery.
- Treatment, including verification
- Trigger level of vacuum is considered and what happens when the vacuum is lost (and treatment pauses)

The RCT consists of a reference box and a probe that measures the distance between various reference points to the skull. The box is see-through and contains several holes on the top, on the left and right side and the front. The

box is attached to the frame in the same way as the localizer, thus allowing to verify the patient's head position in relation to the mouthpiece and frame (Figure 1.7 head and localizer). The holes in the box guide the probe in a defined direction towards the patients head. The probe has a spring-loaded top which is pushed back when it hits a surface. The digital display indicates the distance between the box and the head (Figure 1.8). On each side, at least one measurement should be made, but several and taking the average is recommended. From these measurements, a 3D displacement vector is calculated. (Formula 1.1).

$$V = \sqrt{\left(\frac{\bar{X}_{rigth}+\bar{X}_{left}}{2}\right)^2 + \bar{Y}^2 + \bar{Z}^2} \quad \text{Formula 1.1}$$

With

V	total displacement
$\bar{X}_{rigth}$	average of the displacements measured on the right side
$\bar{X}_{left}$	average of the displacements measured on the left side
$\bar{Y}$	average of the displacements measured on top side
$\bar{Z}$	average of the displacements measured on frontal side

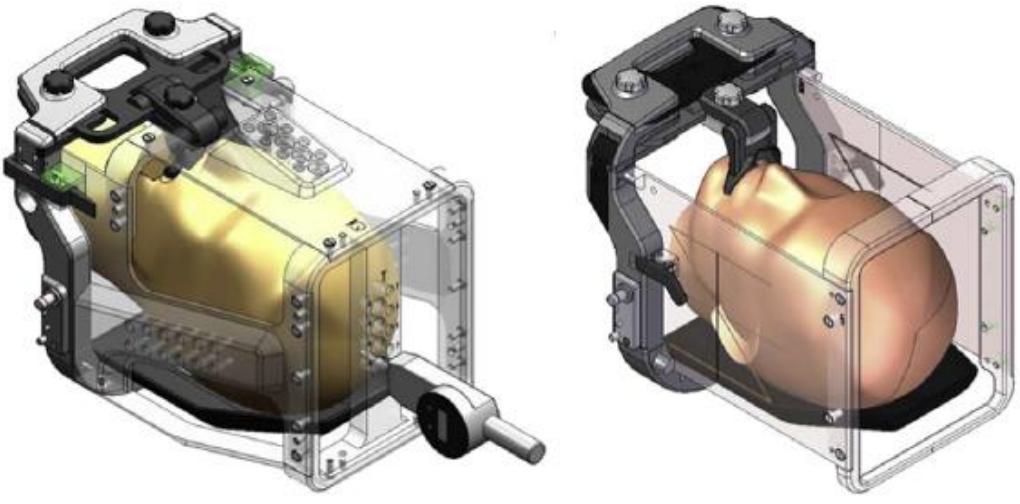

Figure 1.7: *Left: the eXtend system with the RTC box is shown. The distance from reference points (holes with identifications) are measured. A reference measurement is taken during the Planning MR session. Before and after each treatment the values are re-measured andcompared with the reference values. When the differences are within a specified limit the treatment can proceed. Right: the frame with the localizer ready for the planning MR. (images are from Rushin et al. 2009, [94])*

Figure 1.7 from Ruschin et al. [94] shows on the left side the repositioning tool consisting of the box with the reference holes and the spring-loaded gauge (top of the frame box) and on the right side the localizer with the Z shaped reference structure to define the coordinate system. Checking that the head is in the same place for treatment, each fraction ensures the correct position in relation to the MR planning scan. Because the RTC box is attached to the frame box it is independent from the mouthpiece attached to the front piece. If the screws would loosen and the patient position would change this would be detected.

Figure 1.8: *The gauge with the designed measurement start-position and a part which is slightly thicker than the measurement probe. This thicker part is used to guide the probe into the defined direction without swiveling. There is a long and a short probe since they have a limited measurement range. The indication is the difference to the calibrated zero position. The calibration takes place in the QA phantom (not imaged). (image from Sayer et al 2011, [95])*

1.5.4 Setting the vacuum

Before the patient can undergo the MR scan or the treatment, the vacuum level has to be set. The value that can be set is in relation to the normal air pressure. So a set value of 30% is 30% reduced air pressure inside the cavity. The value can be chosen and set by the user. The recommendation is to set the value between 30% and 35%. A value too low would not support the patient, and a value too high would be uncomfortable.

1.5.5 Planning with composite shots

Once the planning MR is imported to GammaPlan (GP) the clinician can outline the target and the planning can be started. The new design of the GKP has not only a motorised collimator system, but the sectors can have different collimator diameters at the same time. This enables forming the individual shots and techniques that can be used to better protect OAR. Some examples for shot forming are given in Figure 1.9 from Lindquist and Paddick's "The Leksell Gamma Knife Perfexion and Comparisons with its Predecessors" in 2007 [96].

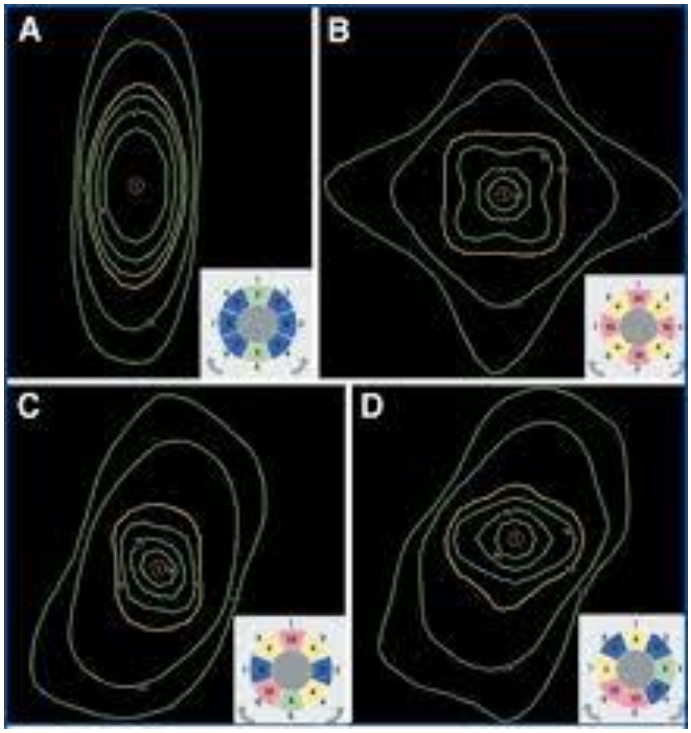

Figure 1.9: *Some examples for shot forming are presented. Example A, with all but two opposing shots blocked, may be used to achieve an extremely steep dose gradient on the sides. This goes at the expenses of loss of dose gradient in the other direction and an increased treatment time because fewer sources are used for the dose delivery. (Image from Lindquist and Paddick, 2007, [96])*

1.5.6 Treatment with vacuum surveillance

Once the plan is ready and approved, an appointment with the patient can be made for the treatment.

On the treatment day the patient is prepared, the mouthpiece with the front piece of the frame is fitted to the upper palate, the patient is carefully positioned on the couch and helped to find the optimum position in their custom made head rest. When the patient is comfortable in the right position the front piece is clamped down tightly to the frame. The vacuum is set to the value used for the MR scan and the RCT box is attached to the frame. With the probe the same reference positions are measured as were for the MR scan and the values entered in the Gamma Knife system. The GK system calculates then from the differences a total displacement vector (magnitude but without direction). If this value is larger than 1 mm the patient is taken out of the frame and then re-positioned, and the measurement repeated. When

the displacement vector is below 1 mm the treatment can start.

The vacuum functions as support for the patient and as surveillance to detect patient movement. If the patient moves, an air leak will appear and the vacuum level drops. When a leak is detected a flag is raised and the treatment paused. The definition of a leak that initiates a pause in the treatment is a drop of the vacuum by 10% of the initial set level. If this is the case, the patient is removed from the frame, and repositioned. As soon as the new measurements are better than 1 mm the treatment can continue where it had stopped.

1.6 What to consider for fractionation

1.6.1 Introducing fractionation introduces uncertainties: Accuracy and how to measure it

High positional accuracy is required to place the gradient exactly on the border between target and NT. Before this, with the previous GK models which were intended to work like a knife destroying the tumour in a single session, this is achieved by a direct, rigid, screwed connection between the skull bone (containing the target) and the G-frame (Figure 1.4, top left). The G-frame is then connected to the Gamma Knife coordinate system. This direct connection between imaging and treatment unit coordinate system is unique to Gamma Knife and eliminates the positioning error present in other treatment units such as Linac or CyberKnife. The system achieves submillimetre accuracy [29].

However, for the re-positioning system on the Perfexion, additional potential positional uncertainties in the set up can be introduced. These may be due to displacement or shift in X, Y, or Z direction. The X and Y direction would be a lateral shift, respectively in ventrodorsal direction within the mouthpiece. In these two directions, the mouthpiece should give excellent support. The third direction is the Z direction craniocaudal. The Z-direction is the direction in which the mouthpiece is attached, and certainly a direction the patient can

move. In addition to a linear displacement inside the planes, rotation is also a possibility.

Set-up uncertainties of eXtend and the reliability of the RCT have been evaluated by Ruschin et al (2009) [94]. They mounted the system to an Elekta Linac equipped with a CBCT. In linac therapy, a planning CT is performed to acquire the anatomy and to do the planning. The advantages of a CT scan over MR images is that the anatomy is not distorted and the Hounsfield units (HU), a measure of linear attenuation of the photon beam for radiodensities in relation to water, can be used for accurate dose calculation. A CBCT works with a larger field and has more scatter, which reduces the image quality. Furthermore, the construction is more sensitive to flex than a CT scanner [97]. However, a CBCT is small and can be mounted on the linac and therefore be calibrated to the same isocentre as the linac. CBCT for positional verification is standard in linac radiotherapy. At the time Ruschin's work was carried out, GK did not have a CBCT, so this linac-based method was an excellent way to verify the RCT. With this setting, Ruschin et al. treated intracranial tumours with a conventional fractionation scheme. Position accuracy was verified with a CBCT scan. The CBCT deviation was compared to the 3D deviation vector as measured with the RCT from eXtend. The 3D vector as displayed on Gamma Knife is the distance from the original planning position to the actual treatment position but does not include the direction. Considering only RCT deviations of ≤1.0mm (suggested action level by Elekta) the mean deviation measured with the CBCT was 1.3mm with the largest contribution in superior-inferior direction. The largest mean rotation was 0.6° in pitch. The mean intra-fraction motion (pre and post treatment) was <0.4mm. However, this was the difference between pre and post treatment. In one case the post treatment 3D vector was 3.9mm. They assumed that " … the patient attempted to turn his or her head when the therapist entered the room … " [94]. This is a likely explanation for the large displacement. However, it leaves the question open: at which point would the vacuum surveillance system have paused the treatment? The conclusion of this study was that the system provides excellent immobilisation and the RCT is a reasonable surrogate for bony structure. However, this paper does not address the question of what level of intra-fraction movement the treatment would be paused at.

In another study Ma et al (2013) [92] evaluated the full chain (or end to end) accuracy simulating the whole treatment process starting from imaging, including image registration, planning, mounting the mouthpiece in treatment position and irradiation, thus including all potential errors and deviations in a treatment routine except for the patient introduced errors such as inducing torsion or flex in the mouthpiece adaptor or not fitting perfectly to the mouthpiece. For this measurement, the Winston–Lutz-test [98] was adapted for use with GKP. As a reference point, metal wire was put through the hole for the vacuum surveillance connection (Figure 1.10). The tip of the wire was aligned with the film which was placed in the mouthpiece. A CT scan with 1.5mm slice thickness was made for planning. A single shot was planned at the centre of the wire tip. The plan was transferred to the treatment unit and the dose delivered. The film was then evaluated with an in-house programme (**Error! Reference source not found.**). The method allows a full chain test u sing CT imaging. They found a 3D mean deviation of 0.69mm (SD 0.73mm). However, their experimental design is limited to measure the centre point of the mouthpiece only; the origin of a potential rotation. Ma et al [92] mention that the only way to measure rotation is with on-board-imaging at the GKP which was not then available.

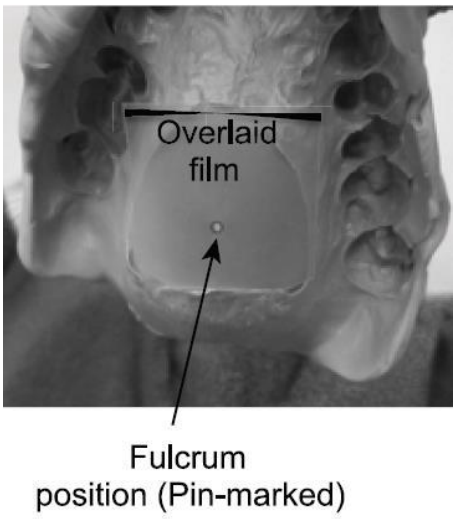

Figure 1.10: *Arrangement of film on a patient mouthpiece with the wire as marker as reference point to verify the irradiation position. (image from publication Ma et al [92])*

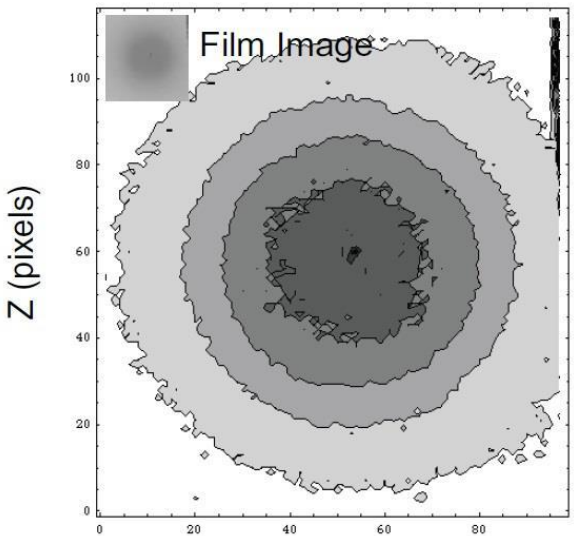

Figure 1.11: *Isodoses on scanned film for evaluation of reference point. (image from publication Ma et al [92])*

The difficulty to measure set-up uncertainty independently may be shown from the study by Sayer et al (2010) [95]. The group reported on handling of fractionated radiotherapy (RT) with eXtend. Their only criteria regarding accuracy was the 3D vector measured by the RCT. No attempt was made to evaluate the sensitivity or correctness of those measurements.

To date, (to the best of the author's knowledge) no publication has reported on the trigger level of the vacuum surveillance system which defines the intra-fraction accuracy and to a significant part the set up accuracy. Ruschin et al (2010) [99] measured initial set up uncertainties on a linac where rotation in pitch can also be induced by table sag, Ma et al (2013) [92] measured the whole chain accuracy including imaging and other uncertainties which are not eXtend specific and Sayer et al (2010) [95] and the author's own measurements [100] showed the procedure can be performed within RCT tolerance but no independent verification of the positioning was done because no direct set up verification is available.

Research question 1:

What is the intra-fraction tolerance from the vacuum surveillance system of eXtend? Special consideration is given to the question at which level the treatment is paused by the vacuum surveillance system.

1.6.2 What effect does positional uncertainty have on the dose distribution of a GK plan prescribed to the 50% isodose?

So far, the philosophy of GK treatment was always that the uncertainty in positioning with the skull attached G-frame is so small (submillimetre) that it can be neglected [27, 30]. And the little uncertainty remaining was a simple displacement or shift when treated as a single fraction. Now GK treatment may be fractionated. The uncertainty will be bigger and with several fractions the effect of a dose shift is only one option in the case that all fractions are displaced in the same direction. With displacement in different directions for different fractions the total dose will look different. Effects of displacement have been intensively studied in conventional conformal (fractionated external beam) radiation therapy [101-104].

The result was that systematic effects should be avoided with QA. This means for example that for a patient treated on the same linac every day and if the linac has a displacement of the couch of 2mm to the right (hanging couch top, miscalibration …) then the patient will receive the dose 2mm displaced. The treatment will be every day with the same displacement in the same direction until the couch is re-calibrated. Such a systematic displacement can be avoided if the couch is checked more frequently, and re-calibration is performed at a smaller threshold level. Other inter-fraction uncertainties are anatomical, e.g. bladder filling, rectum filling or change in weight or tumour size. Bladder and rectum filling can be influenced by a strict diet and treatment schedule (treatment at the same time every day).

However, for a brain treatment diet and treatment schedule time are less important. More relevant could be some behavioural habits of the patient. For

example, if the patient is used to watch the RTT when they leave the room or if the patient relaxes a small systematic movement may occur. Such habits may lead to head rotation in the same direction each treatment. Such possibilities are minimized with the immobilization aid but cannot be eliminated completely.

For random effects, in contrast, the dose is not displaced but drops near the edges [103, 105]. Since conventional conformal radiation treatment targets a mixed cell target volume the aim is to achieve a homogeneous dose distribution at a dose level in the therapeutic window (high enough to destroy tumour cells but low enough to spare the NT) any displacement leads to an underdose in the target area that is missed out. This missing dose cannot be compensated for in the next treatment because the area gets just the “exact” dose with a dose maximum of ideally less than 107% [106, 107]. Any random displacement results therefore in a sum of “prescribed dose” and “less than the prescribed dose” and is therefore in total always lower than the prescribed dose. Because this displacement is random, it is potentially smeared in all directions. Whilst for a systematic displacement the dose is correct on one side but too low on the other side, for a random displacement it drops on all sides (but not as low as for systematic displacement because sometimes the dose is randomly correct).

The situation for GK is completely different. The prescribed dose is usually around 50%. This means the dose gradient at the target circumference is steeper and a displacement may have a dose drop but also a significant dose increase. Another difference is the fraction size. While conventional external beam fractionation uses a high number of fractions in the range of 20 to over 40, of conventionally around 2 Gy each, GK is intended to use schemes with three, five or seven fractions and with higher hypo-fractionated dose. For a large number of fractions, the dose distribution is averaged out. However, for small numbers of fractions some specific scenarios are more likely. This could be “all three or five fractions are displaced in the same direction”, “in a similar direction” or “ with some fractions incompletely different/opposing directions to others”. The potential for averaging out is much less. Due to these differences

the effect of displacement uncertainties needs to be evaluated specifically for the hypofractionation situations used in GK treatments.

In order to evaluate the changes in the total dose, standard parameters are used in treatment planning to report the quality of the plans. There are in general two systems. One is based on ICRU (International Commission on Radiation Units) recommendations [106-109] for treatment techniques aiming for a homogeneous dose distribution, such as in most external beam radiotherapy, and it requires reporting of target coverage, hotspot and underdosed volume. The other, used for and based on GK irradiations, where the prescribed dose is usually around the 50% isodose, reports the quality of the plan as given by the Paddick Conformity Index (PCI) and Gradient Index (GI) or similar parameters [63-66].

These indices are useful to compare plans for the same patient but have little or even inverse significance in indicating clinical outcome [70-72]. However, PCI and GI are most commonly used in GK SRS. Plan evaluation produced in this project will therefore be reported using both types of reporting, ICRU style and SRS standards. An international working group has developed a standardization for SRS reporting [110, 111] taking both philosophies into consideration and considering clinical relevance.

Research question 2:

what effect does positional uncertainty for GK have in a three or five fraction setting?

1.6.3 Relation between fractionation size, dose reporting and biological effect.

The biological effect of a delivered physical dose depends on factors like tissue type, total dose, dose per fraction and others. For example a total dose of 30Gy delivered in ten fractions to the whole brain is considered to be

safe and often used as a standard treatment [112] whereas Korytko et al. 2006 [113] found a significant increase in necrotic tissue for a volume of $10cm^3$, irradiated with 12Gy in a single fraction

The reason for this difference is the cell mechanisms to repair some damage when embedded in a living organism. When the dose is above a certain level, the damage is too complex to repair. This is the case with a single high dose. The actual level of “too high” depends on the cell type, the function this cell fulfils in the body, and whether it is possible that other cells take over the function or not. One criterion for the tolerance dose is the cell dividing time. As a rule of thumb, the more frequently a cell goes into mitosis, the more sensitive to short term damage. The tissues in this category include, for example, mucosa or bowel wall. Tissue that undergoes mitosis rarely, such as the brain is far less sensitive. However, another aspect in radiation damage is the effect damaged tissue has. If a part of the lung is damaged, other parts can take over the function. The loss of some lung tissue reduces the overall capacity but the function as such remains. This is called a parallel organ .

In contrast to this is a so-called serial organ where the function of a damaged volume cannot be substituted by other parts. An example of a serial organ is the spinal cord, which is a tube-like structure that carries messages between the brain and the rest of the body. If a part of this tube is damaged, no signal can pass through, and the whole function is lost.

The brain stem, as one main OAR in this work, is between the two. The brain stem is an organ that performs many vital functions such as breathing or sleeping. If a part of it is damaged, its role cannot be taken by another part of the brain stem. Hence any damage can cause a specific function to malfunction or cease to function at all.

Tumour type cells are different from healthy type cells in the way that they divide continuously without regulation mechanism and without a functioning mechanism that could send them into apoptosis. This lack of regulation mechanism is the reason why a tumour grows fast, and one reason why a tumour is more sensitive than the surrounding healthy tissue. Tumour cells undergo mitosis more often, where a cell is more vulnerable. For that reason, irradiation does more damage to tumour cells than to healthy tissue. Another effect that can protect healthy tissue is the repair mechanism. Because a

tumour grows fast and unorganized the vessel system as a supply chain is not as well defined as in healthy tissue. This allows NT to repair some damage more efficiently than a tumour cell. This repair mechanism is the reason why fractionation reduces side effects. Moreover, it is the reason why physical dose cannot just be summed up to estimate the biological effect of cell damage. For this reason, the “Biological Effective Dose” (BED) was introduced. Note: since repair mechanism strongly depend on the cell type each cell type has a different BED for the same physical dose. To compare the different fractionation schemes dose conversion models have been developed. The most commonly clinically used one is the Linear-Quadratic model (LQ-model) [114-116] that converts physical dose to BED based on the theory that normal tissue can repair sublethal damage between fractions better than tumour cells. The model parameters are derived from conventionally fractionated RT data [114, 115, 117, 118].

The multi-target theory became one of the crucial concepts for understanding radiobiology other than the LQ model. For higher doses, the multi-target single-hit model is more applicable. The model assumes that a cell has several targets that would inactivate it with a single hit [119, 120]. The research for this model was done on bacteria and viruses and showed that the survival of the organism decreased exponentially with increased dose [121-123].

For hypo-fractionated radiotherapy the situation is not fully known but is likely to be a transition from one model to the other or a mix between them. Whether or not the LQ model is appropriate is a controversial issue [124-130]. Park et al (2008) [131] tried to close the gap by combining the two models mathematically, ensuring a seamless transition between the two. However, in order to find reliable parameters for these models, clinical data are required.

The data published by Emami et al 1991 [118] are based on irradiating the volumes with a uniform dose with a conformal technique and a fraction dose of 2Gy to the target. Modern RT techniques like image guided radiotherapy (IGRT), intensity modulated radiotherapy (IMRT) or SRS can replace the uniform dose by a dose distribution adapted to any available knowledge on the tumour cell density, a voxel based approach. In order to compare different

plans, concepts like BED [132-134] where different dose/fraction schemes are compared by recalculating the physical dose into a standard dose/fraction scheme with the same biological effect, or another “Equivalent Uniform Dose” (EUD) [135, 136] where a dose distribution over parts of an OAR is reported as the homogeneous dose to the whole organ that would result in the same clinical effects.

The on-going QUANTEC (“Quantitative Analyses of Normal Tissue in the Clinic”) project was recently initiated [116, 137, 138] aiming to add knowledge about the clinical effect of such new techniques. In order to start the project a number of literature reviews have been published about the existing data available.

Lawrence et al 2010 [139] summarized the available data for brain irradiation and Mayo et al 2010 [140] made a similar literature review for brainstem toxicity. Both found that most data available is about fractionated treatment schemes. Few publications were available for single fraction treatment and even then the problem was that patient numbers were low, generally no randomization was involved and the reported results were not standardized and therefore were not comparable.

Today, in 2019, the treatment on a linac has considerably changed. As mentioned, the original data were collected for treatments of homogeneous field and most of the time for 2Gy or near it and delivered from distinct directions. The result was a dose distribution where the target had a homogeneous dose distribution and the surrounding healthy tissue hat either part of the dose or no dose at all. The aim was to keep large OAR volumes outside any fields and keep the dose zero (except for the scatter dose). So the Emami table [118] refers to dose limits with 1/3rd of an organ irradiated, 2/3rd or the whole organ irradiated. Today arc therapy is becoming more and more the standard technique. In arc therapy, the Gantry rotates around the patient and delivers continuously dose to the target. Even though the dose-rate is varied and kept low while the beam travels over the OAR during the rotation the result is still that a larger volume of the OAR is irradiated. It is a long-standing question: "What is better: a lot to a little or a little to a lot?" [141]. The techniques have moved from the first to the second. The Emami data

were collected in a time when dose was delivered was as a homogeneous fields. When data were ready to use the technique advanced to “SIB” “simultaneously, integrated boost”, and QUANTEC are both from the time when 2Gy was standard, and OAR was avoided if possible. So QUANTEC faces a new challenge. How to deal with inhomogeneities? Despite the new challenges, QUANTEC is widely used as a reference, and new data are compared with the database [142-144].

For the evaluation used in the current work, the approach of Park et al to define a combined conversion curve for both, dose level in the LQ range and dose level in the high dose region is adapted. For this theoretical evaluation the BED to the OAR at the target circumference was kept constant and the total BED for a range of fractionation schemes was compared to evaluate which would result in the best OAR protection; and for two schemes the effect of displacement was evaluated. Dose evaluation was done by comparing Dose Volume Histograms (DVH) and profiles. The DVH was used to investigate the potential underdose of the target to the initial fractionated plan, and a potential increase of the OAR to the initial fractionated plan and the single-fraction SRS plan.

DVH does not contain any spatial information. Therefore, profiles are used to evaluate the distance from a critical isodose due to displacement from that of the original plan and from the single fraction plan.

Research question 3:

What effect has fractionation on BED to the OAR and is the dose to the OAR increasing with displacement?

1.6.4 In the special situation of GK, can margins be replaced by a correction strategy?

Lesions in the brainstem are particularly difficult to manage. Yen et al (2011) [145] evaluated the effect on the BS in a series of 85 arteriovenous malformation (AVMs) in or adjacent to the brainstem treated with GK SRS. AVM is a benign disease where the patient has a long life expectancy but may die at any time due to sudden bleeding in the brain. The dose to the AVM target is similar to that of a malign metastasis, at about 25 Gy for AVM's <2 cm in diameter and 16 Gy for large AVM's >3 cm in diameter [88-90]. The long life expectancy allows a long follow up on the one hand and on the other, any side effects are long lasting and therefore should be avoided even more than for malignant targets. Despite the high radiation-induced changes, nine patients with neurological deficits and one large cyst, the authors considered GK SRS a reasonable method to treat AVMs in or near the BS. Toxicity with brainstem metastasis is lower, partly because of the shorter survival and partly due to different tissue mechanics with AVM treatment aiming only to obliterate the vessels with effect in a few weeks or month. Any brain tissue between the vessels is not identified as a target but cannot be avoided. In contrast to this, treatment of metastasis aims to destroy all cells within the target.

Jung et al (2013) [146] evaluated the outcome of 32 consecutive patients treated for brainstem metastasis. Seventeen of those received prior WBRT. Median target volume was 0.73 cm^3, median age was 50 years, and median margin dose was 13 Gy. They found a statistically significant survival benefit based on the Radiation Therapy Oncology Group (RTOG) recursive partition analysis (RPA) class, especially early stages RPA class 1 with a median survival of 19.2 months and concluded that brainstem metastasis should be considered for SRS.

In conventional external beam fractionated radiotherapy, margins are added to the actual tumour (Gross Target Volume GTV) to compensate for sub-clinical microscopic malignant disease to get the Clinical Target Volume (CTV) and a margin to cover positional uncertainties which results in the final Planning Target Volume (PTV) [106, 107]. Adding all these margins results in a larger volume of NT to be irradiated. For small lesions, a margin would add

relatively more NT volume to be irradiated. However, for GK fractionated treatments there is a possibility that it might not be necessary to add physical margins. Results found from the work on research question three showed that the errors in dose associated with opposing displacements are cancelled out. It might be possible to use this effect to apply a correction strategy instead of a margin. The problem is the low number of fractions. Each displacement might be due to random or systematic error. The option of a correction strategy is therefore evaluated with a series of simulations with random and systematic displacements.

Research question 4:
Do OAR still benefit from fractionation even if there is a margin required? Can the need for margins be influenced by different planning strategies, for example with the use of a correction strategy?

1.7 Aims and Objectives

In order to treat brain lesions with hypo-fractionated treatments using the GammaKnife Perfexion, set-up uncertainties should be minimal. In order to avoid recurrence, adequate dose coverage of the target has to be guaranteed while at the same time the BED to any OAR should not be significantly increased. The aims and objectives of this work are summarised together in the research questions discussed above:

1.7.1 Research Questions:

Research question 1:

What is the intra-fraction tolerance from the vacuum surveillance system of eXtend? Special consideration is given to the question at which level the treatment is paused by the vacuum surveillance system.

Research question 2:

what effect does positional uncertainty for GK have in a three or five fraction setting?

Research question 3:

What effect has fractionation on BED to the OAR and is the dose to the OAR increasing with displacement?

Research question 4:
Do OAR still benefit from fractionation even if there is a margin required? Can the need or margins be influenced by different planning strategies, for example with the use of a correction strategy?

The overall aim is to study these effects to provide information that can inform and optimise clinical strategies and decisions for the application of fractionated GK treatments for brain lesions.

Chapter 2:
Accuracy of the eXtend system

The work in this chapter was published as [1]: "**Quantifying the trigger level of the vacuum surveillance system of the Gamma-Knife eXtend™ positioning system and evaluating the potential impact on dose delivery**" in the journal of *Radiosurgery and SBRT*, 2016, Vol. 4.1, pp. 31-42

2.1 Introduction

To treat brain tumours, fractionated whole brain radiotherapy (WBRT) is often applied but provides limited local tumour control and induces side effects like fatigue or reduced cognitive function which leads to reduced quality of life (QoL) [3]. Stereotactic radiosurgery (SRS) can reduce several of these side effects by focusing the dose on the target and sparing normal brain tissue [13, 147]. Gamma Knife (Elekta Instruments, AB, Sweden) (GK) is an efficient and cost effective treatment unit dedicated to SRS of solid brain tumours [61, 148]. For the clinical success of intra-cranial SRS, high positional accuracy is required to place the dose gradient exactly on the border between target and normal tissue (NT). This was originally achieved by a direct, rigid connection between the skull bone and the G-frame where the G-frame is screwed directly to the skull bone. The G-frame is then connected and aligned to the GK coordinate system. This direct connection between imaging and treatment unit coordinate system is unique to GK and eliminates the positioning error present in other treatment units, thus achieving submillimetre accuracy [29, 149].

A high dose per fraction limits the treatable lesion size (<3 cm in diameter) and proximity to organs at risk (OAR) [150-152]. This can be overcome by fractionating the treatment [15, 36, 151, 153, 154]. Fractionation or hypo-fractionation results in a lower dose per fraction and allows the NT in the gradient region to repair sub-lethal injury between the fractions thus reducing toxicity [46, 131, 155-157].

There is no universally agreed definition of exactly what SRS is. The international Gamma Knife society has recently published a standardization report [111] which suggests regarding the treatment unit as “a system for stereotactic guidance of radiation output with submillimetre accuracy”. Fractionated radiosurgery is expected to achieve that specification (with an arbitrary limitation of five fractions).

The spacious design of the Leksell Gamma Knife Perfexion™ (GKP) (Elekta Instruments, AB, Sweden) model led to the introduction of a new non-invasive repositioning system known as eXtend™ (Elekta Instruments, AB, Sweden). This is based on a head rest with an individually formed vacuum cushion and a vacuum assisted mouthpiece. As a positional verification during the treatment, the vacuum level of the mouthpiece is continuously monitored and the treatment interrupted as soon as a movement induced drop of the vacuum is detected.

The key part of this vacuum surveillance is a spacer that is placed on top of the mouthpiece towards the upper palate to create a cavity. While the mouthpiece is in close contact with the upper palate the cavity is sealed and a vacuum can be established. Any movement of the patient would create a gap and the vacuum would be lost. A good mould fits tightly and allows setting a vacuum level indication of 50 to 60% (deviation relative to ambient atmospheric pressure). However, for patient comfort in clinical practice, it is recommended to set the level between 30 and 40%.

The vacuum surveillance software of the patient control unit constantly monitors the vacuum level and pauses the treatment as soon as the vacuum drops by 10% of the initially set level. Any movement or displacement until this trigger level is reached causes a deviation of the delivered dose from the calculated one.

Uncertainties of the initial patient setup associated with the use of eXtend™ have been assessed by Ruschin et al [99] as described previously. One finding was that the largest mean deviation of 1.3 mm was in the superior-

inferior direction. This is the direction in which the mouthpiece is fitted each day and likely the direction with the least support.

Ma et al [92], also as described previously, tested the whole chain accuracy (or 'end to end' testing, i.e. including a combination of all defined contributing factors) of eXtend™ on GKP. This was a test including imaging, image registration, planning and delivering the dose but excluded the patient. The test was basically to evaluate pure mechanical accuracy without human effects. Even so, they found a mean systematic deviation of 0.69 mm (0.73 mm SD).

Schlesinger et al [158] reported a series of ten patients undergoing fractionated treatment by GKP. In one case, the treatment was paused by the vacuum surveillance system. After re-set up the treatment was continued without further problems. However, they mention the importance of "further work to characterize the sensitivity of the vacuum monitoring system to detect patient motion."

To date, to the authors' knowledge, there has been no report on the trigger level of the vacuum surveillance system which defines the intra-fraction accuracy. This work investigated the trigger level and characteristics of the vacuum surveillance system of eXtend™ and what effect a displacement would have on the dose distribution in the target.

2.2 Material and methods

2.2.1 Dental model, mouthpiece moulding and fixation

For accurate measurements on the order of 0.1 mm, clearly defined surfaces and reference points are required. Such a surface should be flat, have a reference point, and should be hard enough so that pressure would not influence the result. If trying to measure on a patient, teeth would be the only accessible hard surface, but teeth are neither flat, nor do they have a reference point, nor are they accessible. Accessible surfaces would be nose, lips and possibly top of the scalp. All are less than ideal for accurate measurement.

The mould itself has hard surfaces, but not flat. However, it might be possible to create a reference point by drilling a small reference hole.

However, to measure the distance between patient and mould, which is attached to the frame of the GKP, two surfaces are required.

Another problem is movement. In order to measure at which point the vacuum level is broken, the mould and patient would have to be moved away from each other in small accurate increments on the order of 0.1 mm, the accuracy that is required. The two options would be:

- The patient is fixed, and the mould is moved
- The mould is fixed, and the patient is moved.

The patient is fixed: The problem here is that the patient actually can move one or two millimetres despite being fixed in the mask. An option might be the G-Frame, but the procedure to attach the G-frame just for measurement is not realistic (and not ethical). The second problem would still be to move the mould in 0.1 mm increments in relation to the patient, which would require a complex and difficult method to be designed.

The mould is fixed: A design where the mould would be fixed is easier. It could just be mounted on the frame but then the patient would have to be moved in 0.1 mm increments. As above, the only feasible way would be with the G-frame and that is not practical or realistic.

For these two reasons, no surface to measure the distance and no fixation for the patient that limits movement to 0.1 mm or less, means another solution is required, based on a simulated ‘patient’.

Of interest is the distance the upper palate moves away from the mould until the trigger level of the surveillance system is reached. Therefore a model needs to represent only the teeth and upper palate. Such models were available from the dentistry department. On one side, the model is of the real patient while on the opposite, rear, side there is a flat and hard surface from which accurate measurements are possible. Thus dental models have been used for the measurements. Twenty moulds from dental plaster models of the upper human jaw were produced applying the procedure described by

Ruschin et al [99]. The dental models were a random selection representing a range of dental conditions and geometric shape. The solid flat surfaces on the model allowed the definition of a reproducible reference point for the measurements. Examples are shown in Figure 2.1.

Figure 2.1: *Four examples of the dental models used to evaluate the trigger level of extend. The model represent a variation of dental condition from “”excellent” (all teeth in good condition) to “poor” (few teeth left). The flat surface of the models provides a solid, plain surface for exact measurements.*

To fit the mouthpiece to the patient in clinical practice the mould has to be slipped over the teeth in an upward movement and wiggled into snug fit with the teeth and the upper palate. This represents a shift in the Z-direction (superior/inferior) and a rotation around the X- and Y- axes. These movements are the most likely ones to happen during treatment and are those quantified in this work (**Error! Reference source not found.**). If the mould w ould be loose and allow movement, the vacuum could not be established and treatment prevented at all. However, there might be a very small movement possible if the dental mould can be slightly compressed.

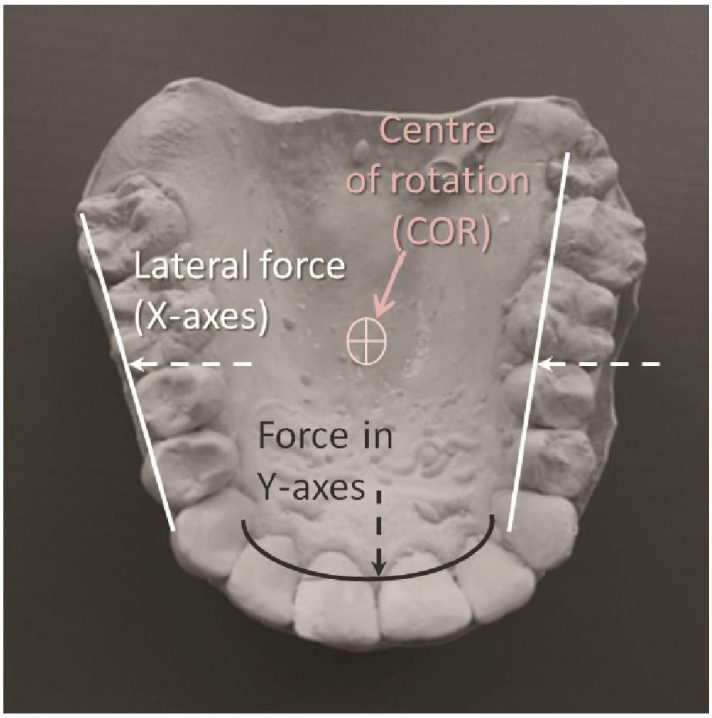

Figure 2.2: *The image shows one of the moulds. The fitting procedure is that the mould is moved in inferior direction (Z-direction) towards the upper palate and then wiggled slightly around X and Y axis (involving movement in the Z direction) to achieve a perfect fit. Movement in lateral (X-axis) and ventro/dorsal (Y-axis) directions are minimized due to the large contact area (with and black lines). A movement in those directions is only possible when the mould is loose or by compressing the mould material. Compressing the material is negligible, and when the mould is loose, no vacuum can be established.*

2.2.2 Translational measurements

To measure translational movement the mouthpiece was fitted to a holder with a pole and then mounted with a collet on a computer numerically controlled (CNC) machine (SM2000 milling machine) with positional accuracy of 0.01 mm. The dental model was fixed on the CNC table. For best alignment the mouthpiece was formed in the measurement position (**Error! Reference s ource not found.**). As a surrogate for the mucosa, Vaseline gel was applied to the surface of the dental model.

Dental model and mouthpiece were put together in close contact. Then the vacuum level was set and the collet from the CNC machine tightened. This position was set to zero. The mouthpiece was then moved away from the dental model in steps of 0.05 mm and the vacuum level was recorded at each position until it had dropped to zero indication which equals atmospheric

pressure. The position where the vacuum level had dropped by 10% of the original setting was recorded as the trigger distance. This was repeated for each mould 30 times at different vacuum levels (10 times at 30% vacuum level, 15 times at 35% the recommended vacuum level and 5 times at 40% vacuum level). Where a higher (non-clinical) vacuum level was achievable, measurements between 45% and 70% were added. The measurements have always been performed in groups of five to get information about the reproducibility. After five measurements, the vacuum level was changed. Measurements were performed in the order of 35% vacuum level, 30%, 35%, 40%, 30% and then again 35% vacuum level. This way, in addition, to test the reproducibility, it was also possible to check if the same results are measured when the vacuum level is re-set afresh.

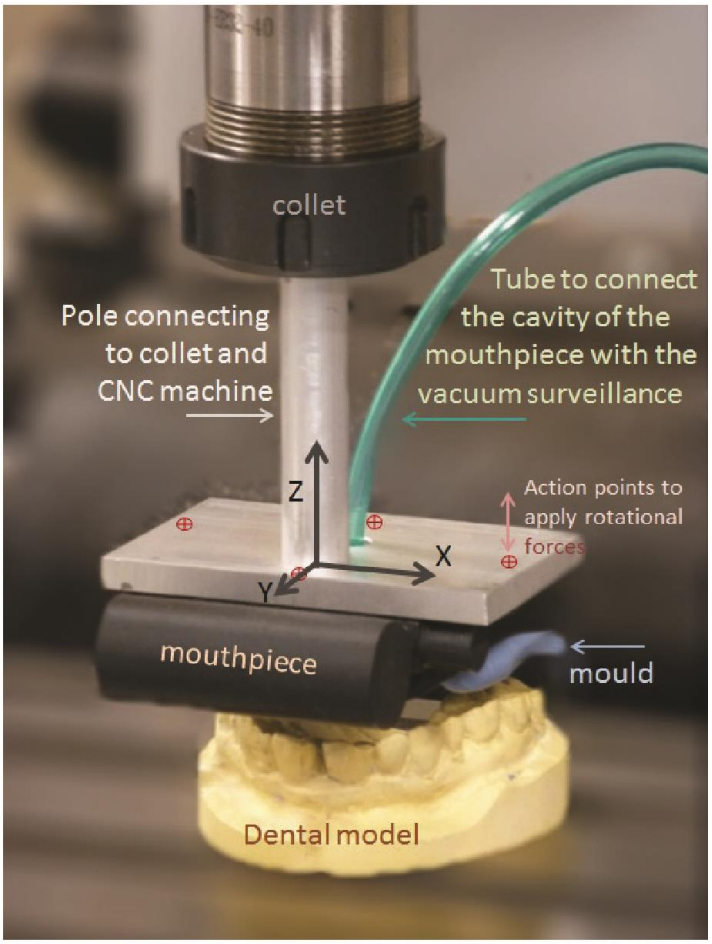

Figure 2.3: *the eXtend™ mouthpiece with a pole attached was fitted to the collet of the computer numerically controlled (CNC) machine for precise positioning.*

2.2.3 Rotation measurement

To measure rotation, the dental model was fixed to a base plate with the mouthpiece and dental model in close contact then the vacuum level was set to the initial level. A digital inclinometer (Fisco Solatronic, Model EN17, resolution 0.1°) was placed on the flat surface of the mouth-piece and the indication set to zero. As for the translational measurements, five measurements each were performed for vacuum levels in a consecutive series of 35%, 30%, 35%, 40% and 35%. The value of 35%, as the recommended clinical level, was measured in between the other levels to confirm reproducibility.

Head rotation around X- and Y-axes may cause a significant change in target position. A head rotation would cause pressure on one side and tension on the opposite side of the mouthpiece. The more tension is applied, the more this resembles the situation of a simple shift that can break the vacuum. If the pressure is dominating the patient is moving towards the mouthpiece and thus keeping the vacuum seal tight. Applying pressure simulated the worst-case scenario. Therefore, a rotation was induced by applying pressure at the periphery of the mouthpiece. Action points were right, left, front and at the back of the mouthpiece (marked as circled crosses in Figure 2.3). The pressure was applied in the superior and inferior directions. When the vacuum level was set, pressure at each action point was continuously increased and the rotation measured with a digital inclinometer (Fisco Solatronic, Model EN17, resolution 0.1°). The rotation at which the vacuum level had reached the trigger level, a drop by 10%, was then recorded.

2.2.4 Target selection

Very small lesions were excluded from this investigation because small lesions are no problem for single-fraction treatment. Any displacement on a small lesion would mean a miss of a large proportion of the volume, and adding a margin would increase the NT volume significantly. So the G-Frame, with its

high accuracy, is best for small lesions. The aim of fractionated SRS is to treat larger lesions of more than 3 cm in diameter (roughly 10 cm^3 in volume) or medium-sized targets near OAR. The targets selected for this simulation were from real patients previously treated with single-fraction SRS Plans for ten metastatic lesions with a size between 7.7 cm^3 and 19.3 cm^3 were selected for dosimetric simulation of displacements. Location varied across the brain including three lesions adjacent to the skull bone and two near an OAR (optic nerve and chiasm). Detailed characteristics are given in Table 2.1. All patients had been previously treated in a single fraction using the G-frame screwed to the skull for imaging and treatment. This plan was used for recalculation of the dose distribution with a displacement induced.

Table 2.1. *Characteristics of ten targets treated with single fraction used for calculating the dosimetric effects of hypothetical displacements due to rotation*

Characteristic	Mean	Range
Tumour volume (cm3)	12.8	7.7 – 19.3
Distance to centre of rotation (mm)	105.3	55.7 – 147.8
Prescribed dose (Gy)	17.4	16 - 18
Prescription Isodose (%)	48.7	45 - 51
Minimum dose (Dose to 99% of volume, D (99%))	17.08	15.6 - 18
Coverage (%)	98.6	97 - 99
Total number of shots	23.1	16 - 32
Paddick conformity index (PCI)	0.873	0.765 – 0.918

2.2.5 Potential displacement due to rotation for target, chiasm and optic nerve

For a given patient, the potential displacement of the target due to rotation depends on its position relative to the centre of rotation (COR, the centre of

the mouthpiece at the hard palate). Ma et al [92] had the point defined at the connection of the vacuum tube to the mouthpiece. In this work it was defined at two centimetres dorsal from the dentures on the level of the hard palate in the central sagittal slice of the MR image. Figure 2.2 shows the estimated point. In reality there is no single COR for each rotation but it is close to the pressure point along the teeth. The patient cannot move into the mouth piece but will rotate “out of the mouthpiece” with the COR on the inside of the rotation radius. It could be one time on the right, another time on the left side or could be the front teeth or the back. The centre of the palate was taken as an estimate and average of all options.

Rotation influences the target position in two ways: a target rotation and a translational displacement. In this work, the target rotation was ignored because of the near spherical shape of the selected targets. The spherical shape of metastases is favored due to the location where metastases develop. Usually, there is no solid barrier in the proximity, so the cancer cell expands in all directions and forms often a sphere-like volume. An AV in contrast, is more pear-like shaped with the spike squeezing through the skull bone or a meningioma that grows along the meninges and has flat extensions.

However, one pixel at a distance of 2.5 cm from the tumour centre would be displaced by 0.8 mm from a two-degree rotation. This would mean if a cube would be rotated by two degrees, only the corner pixels would be compromised. All lesions selected are spherical like and are therefore much less compromised.

The potential displacement was evaluated from the distance between the COR to the centre of the target (centre of gravity) for the mean and maximal rotation around X and Y axes, respectively measured in the previous experiment. The displacement was calculated for each axis individually as in Figure 2.4 and equations 1 to 3 for rotation around the Y axis. The same analysis was made for the chiasm and ON.

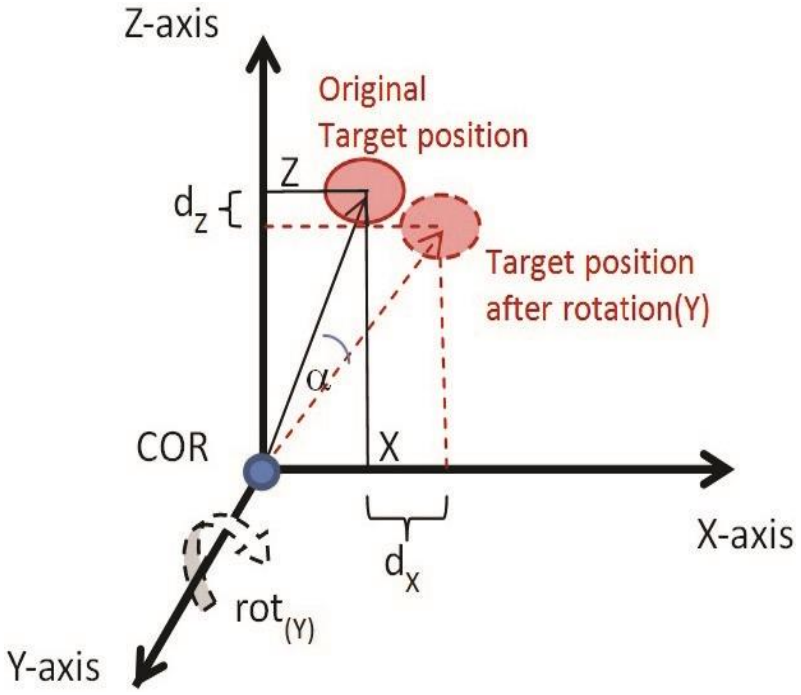

Figure 2.4: *Graphic visualisation of the effect of rotation on the target. A rotation around the Y axis causes a displacement of a target in the X and Z directions. The magnitude of such a displacement depends on the rotation angle and the distance in the Z direction between target and COR for the magnitude of the displacement in the X direction and the distance in the X direction for the displacement in the Z direction.*

$d_X \approx Z * TAN(a_{(Y)})$ (1)

$d_Y \approx 0$ (2)

$d_Z \approx X * TAN(a_{(Y)})$ (3)

d_X: displacement in X direction (d_Y and d_Z accordingly)
Z= distance in Z direction between COR and target
(Y accordingly)
$a_{(Y)}$= rotation around Y axis

2.2.6 Keeping shot time constant

Recalculation of the effect of a displacement requires the plan to be calculated with the actually irradiated shot times, i.e. the times from the original plan. GammaPlan Software® (Elekta Instruments, AB, Sweden) automatically adjusts treatment time for all shots to achieve the prescribed dose in relation to the actual maximum dose. A shift of the shots may change the path length and therefore the dose to the modified point. The shot time is automatically "corrected" for this change. This time modification by GammaPlan was reversed to the original planned time by modifying the prescribed dose and where necessary the individual shot weight. This method allowed us to keep the total treatment time variation ≤0.5% and the individual shot time variation ≤1.0%

2.2.7 Re-calculating dose distribution after displacement

For the original treatment plan the effect of a potential uncertainty was simulated by shifting the shots in all three axes in positive and negative directions for 18 positions in steps of 0.1 mm up to 0.4 mm and then in steps of 0.2 mm up to 1 mm plus shifts of 1.5 and 2 mm. The shift was performed for one axis at a time. The small step size at the centre was chosen because small displacements are more likely than large ones and it is more important to see the detailed behaviour of displacements. A maximum realistic displacement was considered to be 1 mm. To cover potential outliers displacements of 1.5 and 2 mm have been added to verify that the trend (of the curve) would be continued.

2.2.8 Plan evaluation

For plan comparisons three parameters were considered: minimal dose to the target $D_{(99\%)}$, percent target coverage and Paddick Conformity Index (PCI) [63] as a commonly used quality index in GK radiosurgery.

The values of the original plan were set to 100% to normalize the values. Parameters calculated from the shifted plans are given in relation to the original plan.

2.3 Results

2.3.1 Accuracy of the vacuum surveillance

2.3.1.1 Translational measurements: Shift until trigger level is reached

With the vacuum level set in the clinical range between 30% and 40% the mean shift was 0.15 mm (SD ±0.05 mm, range 0.05-0.29 mm) until the vacuum level dropped by 10% of the initially set value. When the vacuum level was set to a non-clinical level of ≥45% the shift until trigger distance was 0.22 mm (SD ±0.09 mm, range 0.09-0.43 mm).

2.3.1.2 Rotation measurements: Rotation until trigger level is reached

For the clinically used vacuum level between 30% and 40%, the mean rotation was 0.33° (SD ±0.15º, range 0.05º – 1.0º) until the vacuum level dropped by 10% of the initially set value. Analysis in respect of the direction of the applied force showed twice as large a rotation for an inferior force (pressing the teeth on one side into the mouthpiece) than for a force in the superior direction (a patient 'pulling out' of the mouthpiece) from one side; being a mean rotation 0.42º (SD ±0.16º, range 0.05º -1.00º) and a mean rotation 0.21º (SD ±0.09º, range 0.05º - 0.60º), respectively. A possible explanation for this difference is that pulling on one side means the teeth move away from the mould and the vacuum seal breaks. Applying pressure means the teeth are pressed into the mould and deforming it slightly. However, pressing the teeth into the mould means the vacuum seal is tightened until the deformation is so severe that it creates a leak.

No dependence on the point of action, right (0.31°, SD ±0.19º), left (0.32º, SD ±0.17º), front (0.33º, SD ±0.19º) or back (0.35º, SD ±0.24º), of the rotational force was observed.

For both, translation and rotation, the results were very reproducible. However, it appears that better moulds where a high maximum vacuum level

could be set (better quality mould and/or dental condition) have a higher tendency to have an occasional larger displacement than those with lower maximum vacuum level even when the vacuum level is set to the same value for the measurement.

2.3.1.3 Resulting displacement due to rotation

The mean distance from the COR to the target was 112 mm (SD ±27.9 mm, range 59.7 mm – 147.8 mm), from the COR to the chiasm was 68 mm (SD ±7.1 mm, range 57.2 mm – 75.4 mm) and from the COR to the optic nerve was 57 mm (SD ±5.2 mm, range 48.8 mm – 68.1 mm). These distances result in a potential displacement for the mean rotation of 0.33° of 0.64 mm, 0.39 mm and 0.33 mm, respectively. For the largest rotation measured, 1.0°, a target displacement of up to 2.56 mm total vector might be possible, for chiasm 1.32 mm and for optic nerve 1.11 mm respectively. Individual results for target and chiasm are shown for mean displacement and one standard deviation in Figure 2.5.

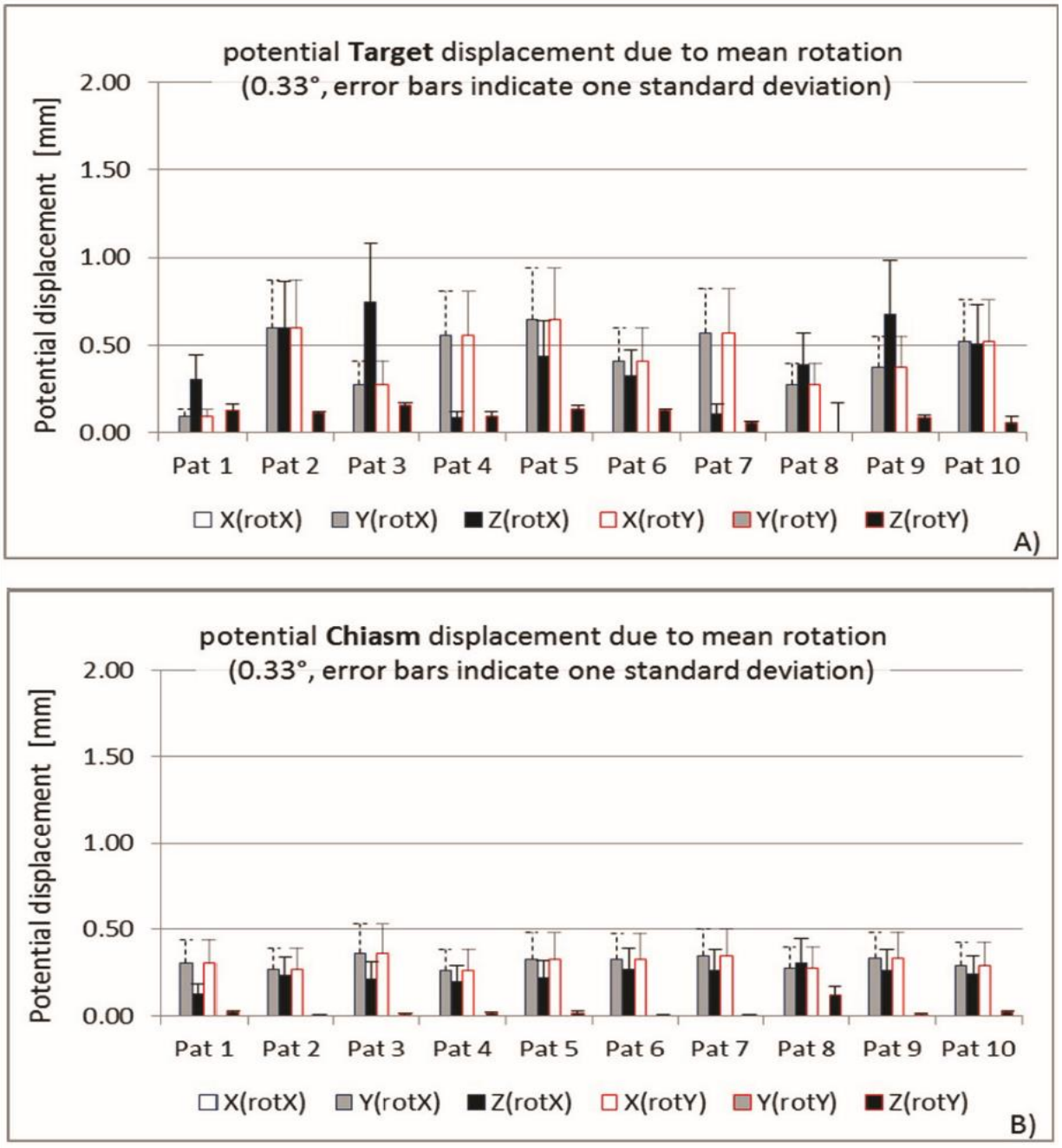

Figure 2.5: *Displacement of the target (A)) and chiasm (B)) for ten patients in the different directions due to mean rotation (0.33°) and one standard deviation added (0.48°) as line.*

2.3.2 Impact of position uncertainty on dose distribution

The main criteria for plan acceptance for brain metastasis are minimum dose $D_{(99\%)}$, coverage and PCI. Figure 2.6 presents the recalculated values as a function of the displacement as a percentage from their original plan values.

All three parameters show little change in the first 0.5 mm shift. With increasing displacement the curves become steeper and indicate compromises in the plan quality. In all three curves an asymmetry between the right and the left side of the +Z direction can be seen. This is due to the OAR protection in two plans. In these two plans, the target was adjacent to the BS. The dose distribution was therefore planned to minimize the dose to the BS. The prescribed dose was very tightly positioned, and in places, a minimal underdosage in the target was accepted while the opposite side encompassed the target with 0.5 to 1 mm margin. Therefore a displacement away from the BS results in an underdosage even for small displacements. The difference to a plan without special attention to a steep dose fall of on one side is within one standard deviation.

The asymmetry for the displacement in Z direction is more systematic due to the shot profile. While the beamlets are aiming from all directions around the head (transversal) towards the target, the directions in up and downwards are limited. There are no beamlets from lower angles coming towards the target because those beamlets would go through the mouth and the eyes. All beamlets are inclined upwards and incoming from above. This results in a shift of D_{max} towards the cranial direction and affects the steepness of the dose gradient, with a steeper gradient on the cranial side than on the caudal side. The effect is visible in the coverage and the PCI change. This is also still just inside one SD.

The minimum dose $D_{(99\%)}$ in the target changes by less than 2.5% for the first 0.5 mm shift and then starts to drop rapidly with 7.5% reduction for 1mm displacement. While there is no significant difference between X and Y axes, the Z axis shows a steeper drop after about 0.75 mm shift. The standard deviation increases with distance (1 SD indicated in Figure 2.6 A)).

Coverage in **Error! Reference source not found.** B), represented as p ercentages of the original parameter taken from the reference plan, shows less change and drops only by 0.5%. In comparison to the minimum dose $D_{(99\%)}$ the coverage in Z direction changes in a similar way as for a shift in X or Y axis on the left side (inferior shift). On the right side coverage drops less for a shift

in +Z direction (superior) than for X or Y shift. This is due to OAR protection in two plans.

PCI changes behave similarly for shifts in all three axes (Figure 2.6 C)). Differences in the +Z direction are again due to the OAR protection in two plans as seen in minimum dose $D_{(99\%)}$ and coverage changes.

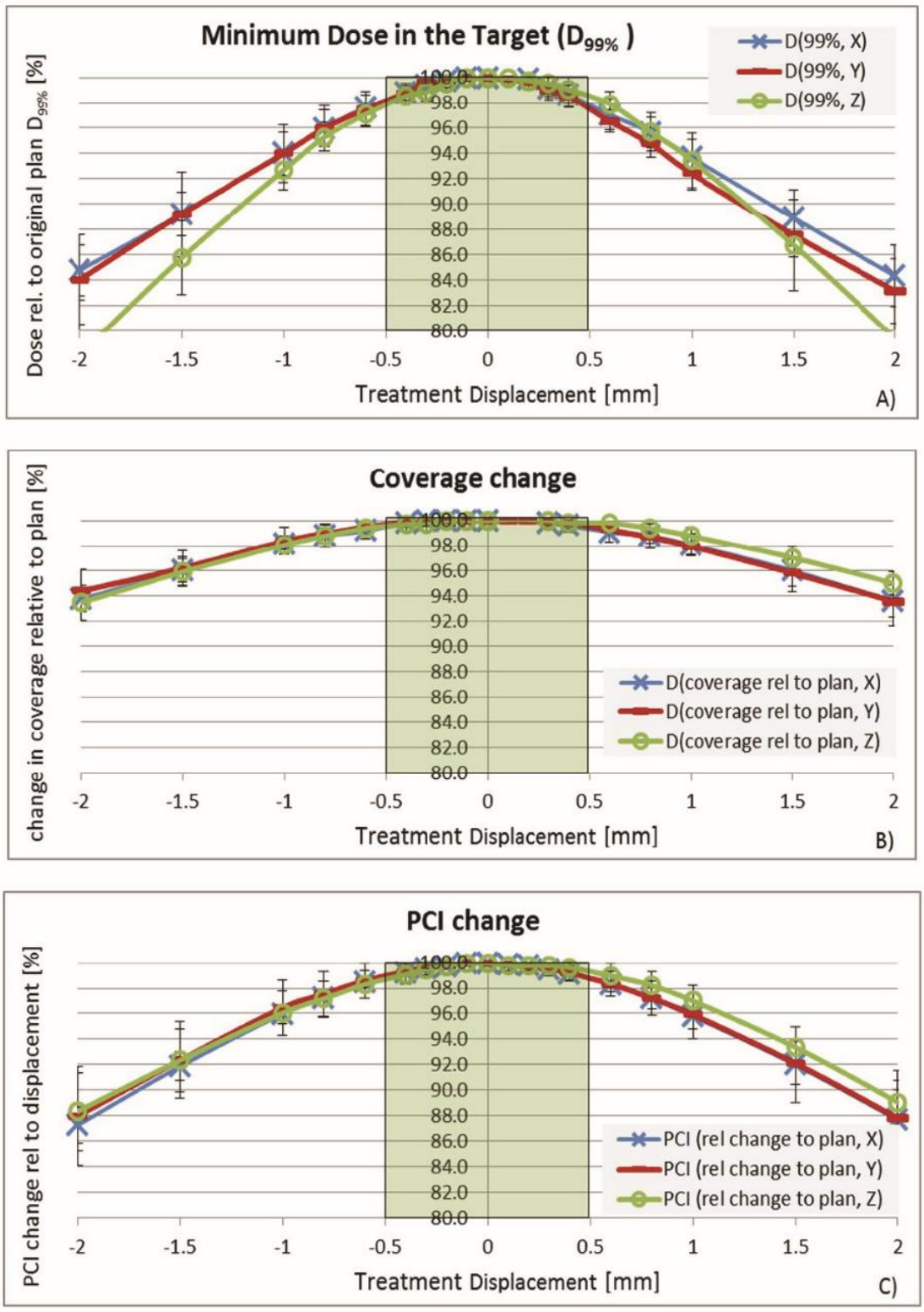

Figure 2.6: *Effect of displacement on typical plan evaluation indexes. A) Minimum dose drops faster for Z direction (superior/inferior) shifts than for those in X or Y directions (right/left and ventro/dorsal respectively). This is due to the steeper dose gradient in the Z-direction. Figure B) (coverage change) and C) (PCI) show no axis specific variation. The asymmetry seen in the +Z axis is due to a compromise in two plans in order to keep the dose to an OAR below a certain tolerance level. The shift towards the OAR improved the plan quality parameters which do not take the OAR risk into account. All values are normalised to the original plan parameters. Error bars indicate one standard deviation.*

2.4 Discussion:

2.4.1 Accuracy of the vacuum surveillance

The use of dental models provides solid and flat surfaces that allows the measurement of not only a static set up but to quantify the submillimetre changes with both shift and rotation that can lead to a treatment interruption. It was possible to evaluate different situations such as simulating a patient "pulling out" of the mouthpiece or to "settling in" to a more comfortable position (rotation with one sided pressure in inferior direction). Assuming that in most cases the patient moves with distinct, sudden motion the treatment surveillance is very sensitive and would pause the treatment before any deviation in irradiation could take place. If the patient gradually moves into a slightly different position then rotation is the most critical aspect which usually results in submillimetre displacement of the target but might cause up to 2.56 mm displacement in one of the selected test cases.

A vacuum can only be established if a tight fit is achieved between patient and mould. Ideally, the positional relation is identical as it was during mould forming. In real life this will never be exactly the case. Assuming the trigger level is activated as soon as the vacuum breaks would mean that any position of the patient where a vacuum can be set has to be within the range between "ideal and perfect" set up and "just before trigger level activation". Several authors [92, 95, 99] evaluated the set up and intrafraction accuracy of eXtend. If this assumption is correct the setup displacement measured in those studies should be within the intrafraction range evaluated in this work.

The RCT system from eXtend™ measures the distance from a predefined reference point to the surface of the head. No discrimination between shift and rotation is available nor is a displacement due to rotation linked to the target position. For this reason, Ruschin et al [99] mounted the eXtend™ system on a linac and evaluated the difference between RCT indicated displacement and CBCT measured displacement from the CT localiser box to the anatomy. They evaluated twelve patients treated for a total of 333

fractions. For RCT deviations of <1.0 mm per axis they reported a total vector mean deviation of 1.0 mm measured with the RCT compared to 1.3 mm measured with CBCT. Ruschin et al [99] deliberately chose the most distal measuring points. This is probably the most sensitive indication of displacement in case of a rotation. The biggest displacements were measured in connection with a rotation. This is in agreement with the work reported here, that rotation leads to the largest displacement for distal targets. The mean displacement of 1.3 mm they found was slightly larger than that found in this work's experiment with just below 1 mm due to rotation. However, no information is given about target location. Furthermore their results included whole chain uncertainties such as imaging, fusion error or CBCT tolerances, in addition to set up uncertainties whereas the results in this work are exclusively the potential difference between patient and mouthpiece. The aim of the work of Ruschin et al. was to establish that the RCT is a reliable tool, and the set up with the mouthpiece is reproducible. Also, the vacuum system can be set to assist the patient for positioning , so the actual vacuum function to pause the treatment would not work on a linac. This work was aiming to find out at which point the treatment pause would be.

The uncertainties for the whole chain accuracy excluding the mouthpiece patient interface was measured by Ma et al [92] using the centre point of the mouthpiece as reference for an adapted Winston-Lutz-Test [98]. The measured uncertainty included errors from imaging resolution, target definition and mechanical uncertainties of the frame and holder when mounted on GKP. Patient dependent uncertainties were not included. They reported a mean deviation of 0.55 mm, 0.78 mm and 0.72 mm for X, Y and Z axes. Adding these full chain uncertainties of the system to the measurements from this work from the experiment evaluating the intrafraction uncertainties between the mouthpiece gives patient results in good agreement with Ruschin's results.

Sayer et al [95] reported a good reproducibility of the setup with eXtend™ while treating four patents with three to four fractions each. All setups were within <1.0 mm radial deviation ranging from 0.33 mm to 0.84 mm mean value. From the same institute, Schlesinger et al [158] reported in more detail on ten patients undergoing fractionated treatment. They compared measurements

pre and post irradiation to estimate a potential intrafraction uncertainty and found a mean radial displacement (vector) of 0.64 mm and a mean intrafraction displacement of 0.47 mm. Both experiments are based on RCT measurements only and include potential measurement errors from soft tissue effects (e.g. muscle flex on the side when the bite pressure changes, hair at the top) and do not give direct information about the actual target position. Their work shows that a tighter tolerance than 1.0 mm is generally achievable. However, they too mention the importance to choose the RCT measurement points in a way that a displacement due to rotation can be recognised.

2.4.2 Strategies to deal with displacement uncertainties due to shift and rotation?

To be sure the delivered dose is covering the target, margins can be applied. A commonly used method is proposed from van Herk et al [103]. He simulated random set up uncertainties and internal motion of prostate treatment for 36 fractions and derived a formula from those data for a margin to achieve the desired tumour coverage. However, with SRS only four or five fractions are treated. A true randomisation that would blur the dose distribution is therefore not possible. So questions remain as to how to add margins, what size and should margins be evenly applied in all directions? Ma et al [159] demonstrated that even small margins increase the volume of irradiated NT significantly. Therefore it is important to minimize margins.

Particularly interesting for Gamma Knife treatments are lesions near the optic nerve, chiasm and brainstem. Several authors reported good results when treating tumours near the optic nerve, chiasm or orbital targets both, in tumour control and in preserving the OAR [155, 160-163]. Ganz et al [155] even found an improvement of the visual function for cases where the optic nerve was considered damaged by the tumour and not specially protected. To minimize margins in these areas is in particular important. The results of this work revealed that the main factor for a displacement is a rotation. Therefore targets closer to the COR (mouthpiece) have a smaller potential for displacement due to rotation than distal targets. Figure 2.7 demonstrates the

difference in displacement between chiasm and a distal lesion for the same rotation and therefore the same RCT values.

The change in coverage and minimum dose $D_{(99\%)}$ is small for 0.5 mm displacement as demonstrated in Figure 2.6. This is likely due to the slightly larger volume of the treatment dose volume compared to the target. So targets near the chiasm or ON might not need a margin at all.

However, peripheral targets may require 2 mm and more positional uncertainties. This could reduce the minimum dose $D_{(99\%)}$ to 80%. To minimize the margin the potential displacement direction due to the target position could be taken into account. For example patient 3 in Figure 2.5 A) has a target dorsal in close proximity to the skull. Potential displacement in X and Y direction is less than 0.5 mm but might be more than 1.0 mm in Z direction. Minimizing margins in X and Y direction might spare NT. For patient 7 on the other hand, the margin might be minimized in the Z direction.

It may be noted that image resolution in Z direction (cranio/caudal) is typically 1.5 mm which is the resolution for target outlining in this direction. Furthermore, inter-observer variation may vary in many cases by more than the just one millimetre. The magnitude of the set up uncertainties or intrafractionation movement is about within the range of target delineation accuracy.

Due to the proximity to the mouthpiece, being the COR, lesions near the optic nerve, chiasm and brainstem may be very suitable for fractionation with eXtend™. Several authors reported good results when treating tumours near the optic nerve, chiasm or orbital targets [155, 160-163].

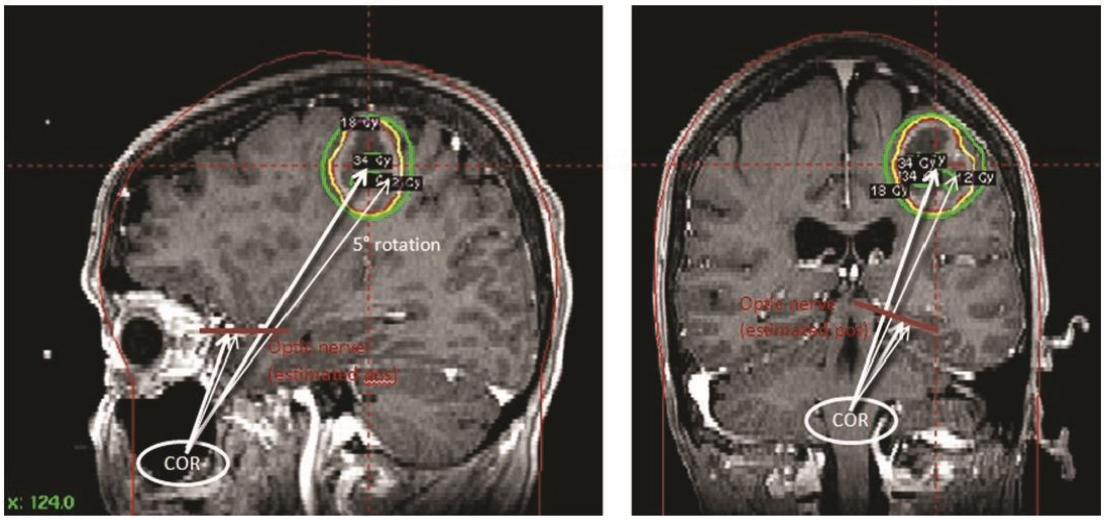

Figure 2.7: *Example of the effect of a rotation visualized in a patient image. The effect of rotation depends on the target location in respect to distance and direction to the mouthpiece as the COR. With rotation only possible around X- and Y- axes the target displacement is ventro/dorsal for a lesion above the COR and sup/inf for a lesion in the back of the head. (Note: the COR is defined in the central saggital slice. The images shown here are off centre. The COR in these images is an estimated projection from the true COR.)*

2.4.3 Availability of CBCT on Gamma Knife

While this work was being completed, Elekta launched the Icon model, which adds a CBCT and a High Definition Motion Manager (HDMM) system to the GKP, intended for use with thermoplastic masks and customised made head cushions. This CBCT replaces the RCT verification system. Some authors have demonstrated in the past that patient movement during long treatments can be in millimetre range [164-166]. With the Icon HDMM system patient position is continuously verified to an accuracy of 0.15 mm with a reflector point on the nose tip of the patient. On the treatment console a tolerance level depending on target and proximity to OAR can be set. As soon as the detected position exceeds this tolerance the treatment is paused until the patient position is again within tolerance.

Thermoplastic masks have been used for SRS for a long time. The accuracy of a such a mask is typically around 3.0 – 3.7 mm ± 2 mm [36-38, 167]. For dedicated SRS treatment, critical points are strengthened or supported (BrainLab mask or GTC system [35, 36]) and with image guidance, mean

accuracies are achieved in the range of 1-2mm. The mask system from Icon is aided by a CBCT for initial set up accuracy and the HDMM.

In a pre-clinical setting Chung et al. [39] evaluated the accuracy of the HDMM using a mechanically controlled device to position the reflector in various known positions. The mask and HDMM system were used on a linac for four patients, treating 28 fractions in total where the HDMM measurement was verified to pre and post CBCT. The agreement for the pre-set position was 0.1 mm under good conditions, with one difference between CBCT and HDMM of 0.5 mm. The intrafraction motion was up to 3.6 mm, in agreement with previous experience of other thermoplastic mask systems. In their study, no detailed information about direction or rotation is given. As seen in previous work of the same group [99] and in the measurements in this work, rotation is most critical for a potential displacement. A single point cannot detect a rotation. In a mask system the COR might more likely be expected to be at the centre of the head, so the reflector at the nose may overestimate the displacement. On the other hand, a rotation around the nose tip might produce an undetected displacement which could potentially be up to several millimetres. Thus pre and post CBCT seem advisable, but can only document a potential displacement during RT not discriminating when the displacement has occurred.

Using the mask is probably more comfortable for the patient but may increase the uncertainty to potentially several millimetres. This can be compensated by gating the treatment. A threshold can be set in the HDMM system so that dose delivery is paused while the position of the reflector is exceeding the set tolerance. The level of the required threshold might be estimated from the measurements presented in Figure 2.6 always bearing in mind that a single point cannot detect a rotation and therefore target location should be considered too.

The Icon may also impact on imaging uncertainties. MRI, as used for input to GK planning has recognised distortion issues. Special sequences have been developed to minimize this. With a CBCT on the treatment unit a new workflow might be considered, using the diagnostic MR images and matching the target to a distortion free CT scan. Wangeried at al [168] have compared this

workflow with the usual one using the distortion optimized MR. They found a mean difference in the resulting isocentre of 0.47 mm. This comparison was simulated and it is unclear which workflow is more accurate in practice.

2.4.4 Limitations of the current study

This study was performed on dental models. The results are in good agreement with the literature. However, in particular the simulation of the upper/hard palate as a rigid structure has to be considered with care. Real patients might have some upper palate changes between fractions such as swelling. Whether this would make the system more sensitive (different anatomy, more likely to produce a leak) or less sensitive (more soft tissue, better fit with the mould) remains to be investigated.

Furthermore, the movements tested were each applied individually, a shift or a rotation in one specific direction. In a clinical situation it is likely that multiple movements will occur simultaneously. Again, whether this would increase or decrease the intrafraction trigger distance remains to be investigated.

In Figure 2.6 the curves on the right side are slightly biased due to the plan modification to protect an OAR in two plans. Keeping the dose tight towards the OAR (ON / chiasm) results in a compromise in coverage which is undone when the plan is “moved” towards the OAR. With a shift towards the OAR, the coverage is increased and the parameters seem to indicate a better plan. The effect on the OAR would need a separate investigation.

The measurements show the potential uncertainties and demonstrate the significant effect of rotation. As has been mentioned by other authors [92, 99, 158], there is no direct link between target position as evaluated in this work and the RCT values. A rotation would result in a specific RCT deviation but the target displacement is depending on the target position, with the highest displacement in peripheral lesions.

The recalculation of the dose distribution with displacement assumes that the treatment is interrupted by a sudden and distinct movement and any positional displacement is mainly due to set up error. This is a likely scenario. However,

it is also possible that the patient gradually changes its position and the displacement of the different shots varies leading to a “blurred” dose distribution.

2.5 Conclusion

The vacuum surveillance system on the eXtend system for the GKP is sensitive and reproducible. For lesions close to the COR (mouthpiece, top of hard palate), e.g. near the optic nerve, chiasm or brainstem, the trigger level reliably prevents mistreatment within submillimetre accuracy. Potential movement of the chiasm was <0.6 mm for a rotation of 0.48° (mean rotation observed, plus 1SD).

Lesions which are further away might experience deviations up to one millimetre as a result of a mean rotation, which would reduce the minimum dose to 94% of the original value. A 2 mm deviation is in rare situations possible and would reduce the minimum dose to 80% if it were a deviation in the Z direction. Often the potential displacement is dominant in one direction, dependent on the lesion position, so this direction might be given special attention when considering the addition of margins.

Chapter 3:
Effect of positional uncertainties on dose to the target volume

The work of this chapter was published as [2]: "**Quantifying the effects of positional uncertainties and estimating margins for Gamma-Knife® fractionated radiosurgery of large brain metastases.**" in the journal of *Radiosurgery and SBRT*, Vol. 4.4, 2017, pp. 275-287

3.1 Introduction

3.1.1 From single fraction to fractionated SRS

Stereotactic radiosurgery (SRS) is an effective treatment option for brain metastases. It can reduce toxicity associated with whole brain irradiation [3, 13, 147]. The high single dose is very effective for local control but can cause radiation injury for larger volumes [169, 170]. Treatment dose is therefore reduced for large volumes, which may be one of the main reasons for the lower local control of large brain metastases compared to small ones [148]. Biological effects allow repair of some cell damage after each irradiation. The effectiveness of this repair depends on the tissue type and is usually better for normal tissue (NT) than for cancer cells [154, 171]. Therefore there have been moves towards (hypo-) fractionated SRS to increase the effective dose and reduce toxicity [46, 139, 157] for these larger volume cases.

For the traditional single fraction GK SRS the G-frame is used. This rigid frame fixed to the skull provides a direct link between imaging and treatment unit thus achieving a sub-millimetre accuracy [29] but due to its invasive nature it is not ideal for fractionated treatment.

3.1.2 GK systems suitable for fractionated SRS

In 2006 the GK model Perfexion™ (Elekta Instruments AB, Stockholm, Sweden) was introduced. The completely new design has a conical housing for the 192 cobalt sources and three different flexibly-selected integrated collimator sizes. Thus the older-design collimator 'helmets' are no longer required. The extra space now available has been used to introduce re-locatable non-invasive fixation systems that allow repositioning a patient on different days for fractionated treatment.

The original repositioning system for the Perfexion™ was eXtend™. It is based on a vacuum surveilled mouthpiece and vacuum cushion. Accurate position is verified with the repositioning check tool (RCT) that measures the distance from various specified points to the surface of the head. Intra-fraction movements during treatment are detected with the vacuum surveillance system at the mouthpiece and will pause the irradiation. The positional accuracy of eXtend™ has been evaluated while it was mounted on a linear accelerator (linac) [99], in a clinical setting [95] and in a whole chain test up to the centre point of the mouthpiece [92]. The trigger level of the vacuum surveillance was evaluated based on phantom measurements [1]. Displacements were found to be usually within 1 mm but larger displacements of 2 mm and more are possible.

In 2015 the Icon™ repositioning system was introduced. It uses a mask, a custom formed cushion, cone beam CT (CBCT) to verify the initial set-up position and a tracking system. the "high definition motion manager" (HDMM), which tracks a marker placed on the tip of the patient's nose. The mask system itself has been tested in a clinical setting on a linac using CBCT pre and post treatment. Intra-fraction displacements of up to 3 mm were found [39]. The HDMM system allows setting a threshold level at which the treatment is paused if the patient moves. The tracking accuracy of the marker is 0.15 mm [39].

Positional uncertainties in the order of millimetres require special attention, which could be to define a margin, or in the case of the Icon™ to select the optimal threshold level on the HDMM.

3.1.3 Analysing uncertainties

In order to make an informed decision regarding margin or threshold the behaviour of the total dose depending on the positional error per fraction should be understood.

In conventional conformal radiation therapy applied with 20 or more fractions, positional errors are separated into systematic errors and random errors. The systematic error results in a mismatch of target and dose distribution. Systematic error (shift), caused for example by a miss-calibration of the imaging device would result in a displacement in the same direction and magnitude for each treatment. The result would be a “shift” of the dose distribution. A systematic error can be minimised by quality assurance of the system and appropriate procedures. The remaining random error (spread) is unpredictable in direction and magnitude. It is for example caused by play in table positioning or a mask that is not tight enough. Random error or spread blurs the edges of the dose distribution and reduces the dose to the target. A margin can be calculated and added to the clinical target volume (CTV) to define the planning target volume (PTV) and ensure coverage despite positional uncertainties [116, 117].

Hypo-fractionated SRS uses far fewer fractions, typically between three and five. A representative random dose distribution is therefore not reached. Any random error with a single fraction appears as a shift of the planned dose distribution, i.e. is effectively systematic in terms of the dose distribution for this particular patient. If the cause of the error is systematic it would be in the same direction each time whereas if the cause is random it could have been in any direction. Two fractions are a combination of spread (distance between the same shots in the two fractions) and shift (displacement of the centre of gravity of the shots). Hypo-fractionated treatments are usually dominated by one or the other effect.

In this work the impact of positional error on the dose distribution was investigated, choosing a systematic approach. The worst case scenarios for

random error (spread) and systematic error (shift, calculated in a previous work [1]) were used to define the largest deviations from the ideal dose distribution. Based on the results a formula was introduced to estimate the required margin for each simulated set-up scenario. A novel strategy to handle uncertainties is suggested that reduces NT irradiation compared to using fixed margins alone.

3.2 Material and methods

3.2.1 Evaluating the effect of set up uncertainties on total dose for large metastases

3.2.1.1 Simulated displacement

According to the standardization report from Torrens et al. [111], a hypofractionation is considered as SRS if the fraction number is between two and five. So five fraction treatments were chosen for simulation as the maximum fractionation scheme that is still considered SRS. Three fractions were also selected to give a comparison with treatments with a smaller number of fractions. In a single fraction, any displacement is a shift (systematic in effect) independent of its cause, whether random or systematic. With two fractions, the displacements can be a combination of shift and spread (random in effect). This is comparable to a plan with two shots, so no additional significant insight can be gained from two fraction scenarios. Three and five fractions are commonly used schemes with on-going discussion as to which might be better. With three fractions, there is less opportunity to have displacements, while with five fractions, random displacements might have less impact because they would average over the five fractions. Thus three and five fraction schemes were chosen to be analysed.

Since random error would not create a representative average for three or five fractions a “worst case scenario” with maximal displacement in different directions has been evaluated. Three and five fraction plans were simulated with displacements in a specific different direction for each fraction. For practical reasons, the directions allowed were X, Y, and Z. For the three

fraction plans the simulated displacement directions were ±X (spread) and +Z direction ($3F_{\pm XZ}$). The five fraction plans represent an extreme spread scenario. The displacements were symmetric in ±X and ±Y directions and a shift element in +Z direction ($5F_{\pm X\pm YZ}$). The displacement in the Z-direction was chosen because this seemed to be the most likely direction for a systematic error. This is the direction in which the patient has to move to reach the treatment position.

In order to add a situation between shift and spread, a second three fraction displacement is calculated with a displacement in +X (lateral), +Y (ventro/dorsal), and +Z (cranio/caudal) direction ($3F_{XYZ}$). In this setting, shift is the main effect with a minor spread contribution. No such "intermediate" situation was chosen for the five fraction plan because the simulation task would have been significantly greater, and the result would be similar to that of the three fraction plan without producing significant additional information. All plans have been calculated for displacements of 0.0 mm, 0.5 mm, 1.0 mm, 2.0 mm, 3.0 mm and 4.0 mm to cover and go beyond normally expected values. Figure 3.1**Error! Reference source not found.** shows the different directions of the simulated set-up uncertainties.

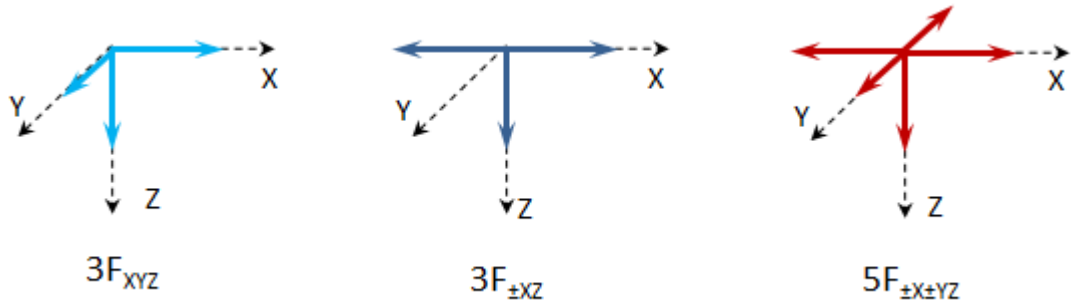

Figure 3.1: *The simulated displacements for each fraction are shown. The magnitude of displacement is simulated to be the same for each fraction of a course. For example if the displacement is 2 mm for the $3F_{XYZ}$ plan then the first fraction is displaced 2 mm in X direction, the second fraction 2 mm in Y direction and the third fraction is displaced 2 mm in Z direction.*

3.2.1.2 Target selection

For this simulation five targets with a large single brain metastasis (median 12.18 cm^3; range 10.72 – 19.31 cm^3) at various locations have been selected. Four lesions had no organ at risk nearby, one lesion was close to the optic nerve and more attention was given during planning to create a steep dose fall off towards it.

The dose was prescribed to a nominal 50% (range 45-50%) of the maximum dose, following our usual local clinical practice. In this work the difference between calculated dose and irradiated total dose including set-up uncertainties was evaluated. Therefore the original dose was set to 100% with each fraction contributing 33% and 20% of the total dose (distribution) for three and five fractions, respectively.

3.2.1.3 Creating a sumPlan for multiple fractions

All targets have previously been planned on GammaPlan Software® (GP, Version 10.2.0) and treated in a single fraction. These plans were used to simulate a fractionated treatment by multiplying the plan according to the simulated fraction number. At this point, no displacement had been introduced. Correct positions and beam weighting (shot time) were verified.

In a second step the displacement was added to each “fraction” i.e. the group of shots representing the fraction. Each fraction of the treatment plan had the same magnitude of displacement but was simulated to be in a different direction. The sumPlan was created by summing up the dose of each fraction incorporating the positional information.

3.2.1.4 How to keep shot time constant with GammaPlan®

For these simulations, every displaced shot time has to be the same as the originally planned one. However in GP, there is only the dose, the prescribed dose, and the shot weight defined. It is not possible to define the shot time and observe what the resulting dose would be. The total dose is defined, the shot is placed, and then the weighting can be modified.

GP normalizes the dose distribution based on the maximum dose D_{max}. Each added shot modifies the dose distribution and D_{max}.

When two fractions without positional error are calculated then the plan has an identical shot at the same place for each “fraction”. The resulting change

is simply that D_{max} is doubled. Since the total dose too is doubled, the individual shot times do not change.

However, simulating a displacement means that the shots are moved by up to 4 mm. This changes the dose distribution, and with it, the value of D_{max} considerably.

If this would be the only influence, then the weighting of all shots of a fraction would simply have to be changed by an identical factor. Unfortunately, this is not the case. With any displacement the path length of the shot from the entrance point to the shot centre and the shot time changes. Moreover, because each shot is in a different place, the change in path length is different for each. For the normalization, the dose in the shot centre is used for relative weighting, meaning that for each displaced shot the shot time is changed individually. Changing the weight of a single shot changes the dose distribution and therefore D_{max} and all other shots.

In summary, changing the positions of the shots to simulate a positional error modifies the plan and therefore the position and value of D_{max}. This results in a renormalisation and thus in a change to all shot times. Then the individual shot weights and times also change linked to the path length issue. This effect has to be reversed. The time cannot be directly set in GP. Instead time corrections have to be made by changing the shot weight. This might change D_{max} and thus change the normalisation. An iterative process was used to set the correct time for each shot:

1. The isodose level to which the dose was prescribed was modified until the total treatment time matched the total treatment time of the original plan.
2. Due to the different path length the shots from one “fraction” might now be different than in the original plan. This can be corrected by modifying the shot weight first as a bulk function, then fine tuning the individual shots until an accuracy of <0.5% was achieved.

3. Modifying the shot weight changes the contribution of each shot to the normalisation point. The maximum dose might have changed and therefore changed the overall treatment time.
4. The procedure was repeated until all individual shot times were within the limits below.

With this method the total time was corrected to <0.1% deviation from the original plan time. The individual shot time was in general <0.5% deviation, but up to 1% deviation was accepted for short shot times.

3.2.1.5 Parameters evaluated from the simulation:

In relation to the target the following parameters were recorded:

- Minimum dose as the lowest 1% ($D_{min1\%}$) in the dose volume histogram (DVH) of the target volume (TV) (≈0.5% of the TV) normalised to the original plan.
- Coverage in percent of the TV receiving the prescribed dose
- Maximum dose (D_{max}) normalised to the original plan

Volumes evaluated:

- Prescribed isodose volume in the matrix (PIV)
- Volume of the 50% of prescribed dose (PIV_{50})

Two quality indices are commonly used for stereotactic radiosurgery:

- Paddick conformity index [63] (PCI) relating to target coverage and normal tissue sparing
- Gradient index (GI) [69] as a measure of the dose gradient and normal tissue irradiation.

Both indices are size dependent but are useful for comparison of plan variations.

3.2.2 Estimating the required margin

From the results of the simulation a margin was calculated such that there was adequate target coverage with the imposed displacements.

Metastatic volumes are approximately spherical and are ideally covered with the reference dose in a close match. For the estimation of the required margin, the volumes TV and PIV are assumed spherical and similar in size and position. Displacements of the individual fractions change the shape and position of the PIV. This leaves part of the TV underdosed. Assuming that a shift element is involved, the underdosed part of the TV is always located on one side. To cover all (100%) of the TV a margin (m) of the size of the shift (s) of the PIV would have to be added to the CTV to create the PTV.

The parameters available from GP for this calculation are: TV, PIV and the intersecting volume (PIV∩TV), as in Figure 3.2. The intersecting volume PIV∩TV is the volume where the target receives the prescribed dose and is approximately the sum of the two spherical caps, TV_{cap} plus PIV_{cap}. The volume of a sphere cap is calculated with the formula $V_{cap} = \frac{1}{3}\pi h^2(3r - h)$. Assuming the two volumes TV and PIV are approximately identical then the volume of the cap can be evaluated by dividing PIV∩TV by two. With iteration the height (h) of the cap was evaluated and then the shift (s) of PIV is calculated with the formula: s=2(r-h): The minimal margin (m) to cover the whole TV is equal to the shift. Figure 3.2 illustrates this. This theoretical margin was calculated for each plan.

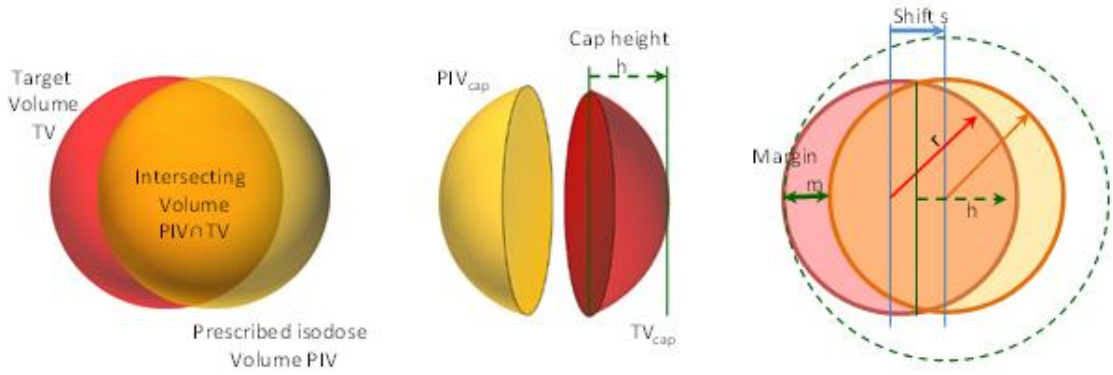

Figure 3.2: *Positional uncertainty changes shape and position of the PIV. Splitting the intersection volume PIV∩TV into two cap volumes, the cap height h and from there the shift s can be calculated. The required margin m is at least equal to the shift s.*

3.3 Results

3.3.1 Effect of set-up uncertainties on total dose

3.3.1.1 Coronal images of total dose

Figure 3.3 shows the dose distribution of the sumPlan in a coronal slice for one patient. The effect goes from systematic error (shift) in the top line to “random error” (spread) in the bottom line. With a shift, the PIV is unchanged in shape but displaced, leaving a sector on one side of the TV underdosed and another sector of NT on the opposite side irradiated.

Spread ($5F_{\pm X \pm YZ}$) is shown in the last line. Here the position appears unchanged except for a small caudal displacement due to one fraction displaced in the Z direction. The shape of PIV appears to be wider in X and Y directions and compressed in the Z direction (no opposing displacement). The high dose volume of 24 Gy is smaller than in the original plan.

Lines two and three are a combination of the two effects. In line two, shift is the dominant effect with some spread ($3F_{XYZ}$) and in line three spread is the dominant effect with some shift ($3F_{\pm XZ}$).

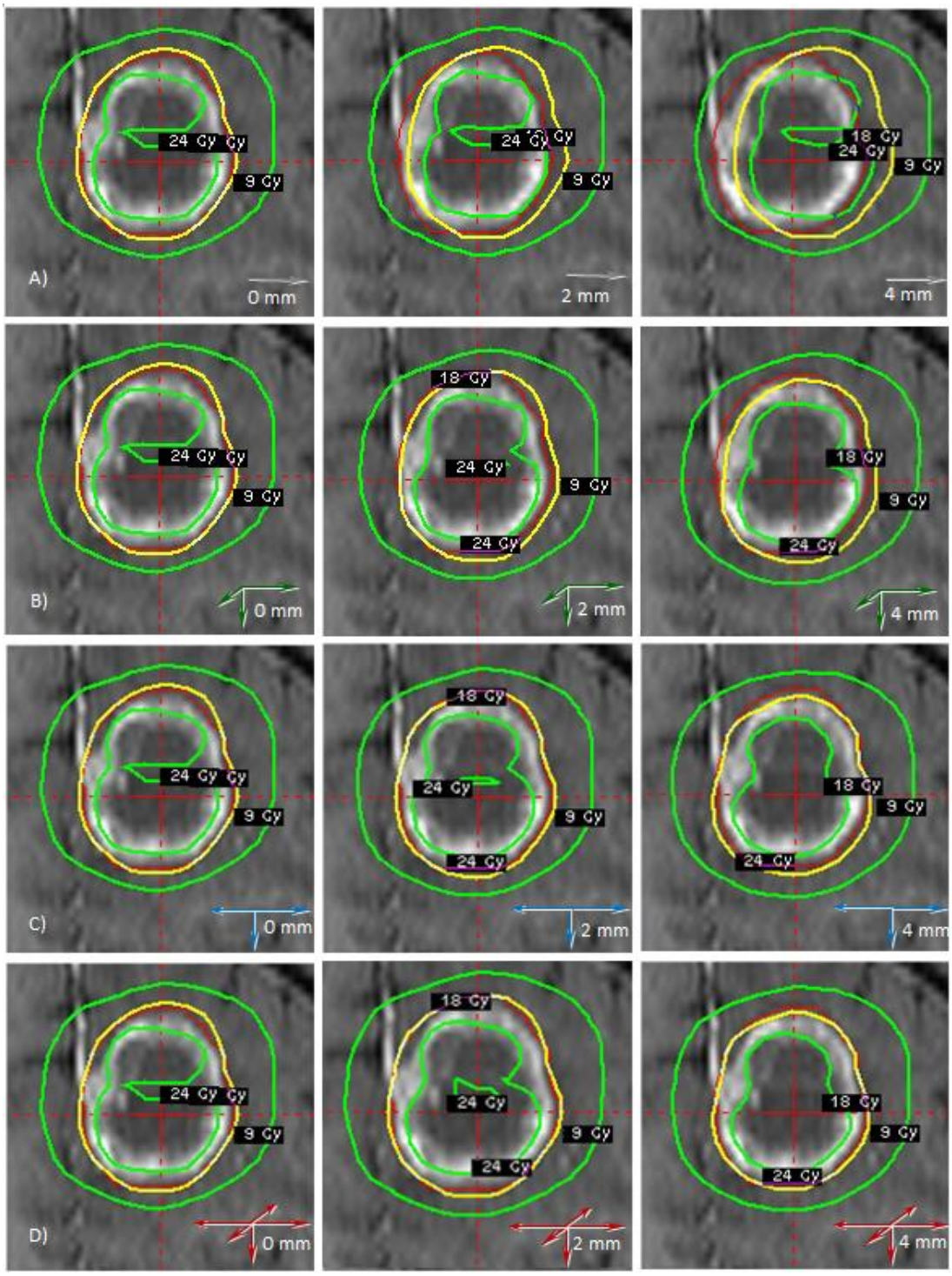

Figure 3.3: Isodose lines shown for the simulation of various fractionated plans. From top to bottom: row A): systematic error or shift, B): three fraction plan $3F_{XYZ}$ with shift dominating combined with some random error or spread, C): $3F_{\pm XZ}$ with increased random error (spread) and reduced systematic error (shift in z direction) and last D): $5F_{\pm X\pm YZ}$ with dominant random error or spread. Systematic error (A) displaces PIV but does not change its shape, whereas a spread (D) for the five fraction plan leaves PIV almost unchanged but reduces the high dose volume (24 Gy) and increases the low dose volume (9 Gy).

3.3.1.2 Behaviour of minimum dose $D_{min1\%}$ coverage and maximum dose D_{max}

Minimum dose and coverage drop with increasing displacement (Figure 3.4). Any shift element of the total error increases the dose drop while a spread reduces the effect. For a displacement of two millimetres $D_{min1\%}$ (Figure 3.4 A) is reduced by 16.7%, 9.0%, 4.4% and 0.9% for a plan with systematic error (shift), a plan with dominant shift and some spread ($3F_{XYZ}$), with dominant spread and some shift ($3F_{\pm XZ}$) and with spread ($5F_{\pm X\pm YZ}$) respectively. Coverage (Figure 3.4 B) is reduced from the original mean of 98.4% to 90.8%, 95.6%, 97.8% and 97.8% respectively for the same 2 mm displacement.

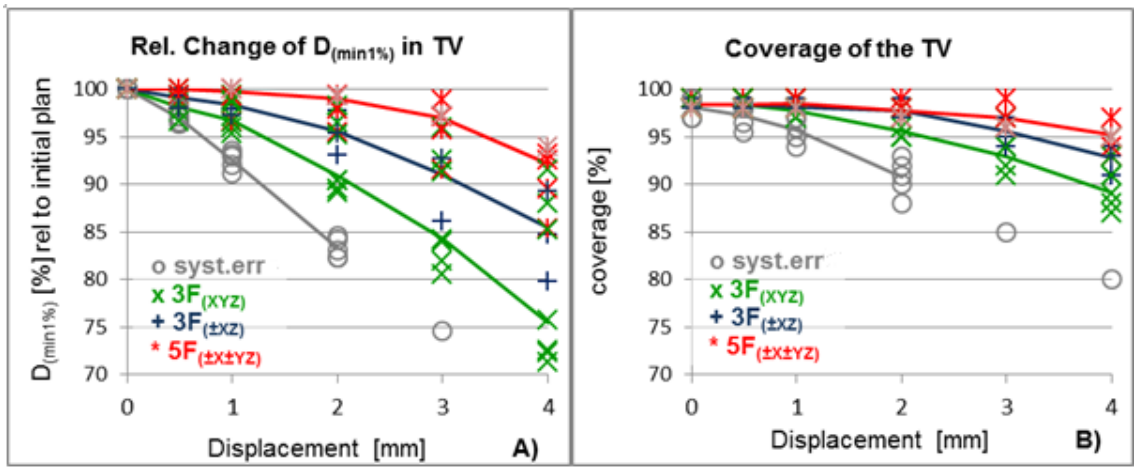

Figure 3.4: *Behaviour of $D_{min1\%}$ and coverage for systematic error and selected fractionation simulations. While $D_{min1\%}$ and coverage drop quicker with a systematic error because the distance to the reference dose is increased within the steep dose gradient whereas coverage does quantify the underdosed volume but not the dose level. (Note: values for syst.err are taken from previous work [1]. Lines represent mean value of the patients.)*

$D_{min1\%}$ is more affected than coverage because any shift element in the total error moves the dose distribution to one side increasing the distance of the underdosed part of the target to the reference dose along the steep dose gradient.

With displaced fractions the dose maximum D_{max} is in a different place for each treatment. Therefore, D_{max} of the sumPlan is smaller than planned D_{max}. The effect is strongest for the five fraction simulation. For the different simulations at 2 mm displacement, the mean value of D_{max} is 100.3%, 95.7%, 95.5% and

94.1% for a shift, $3F_{XYZ}$, $3F_{\pm XZ}$ and $5F_{\pm X\pm YZ}$ respectively. For a displacement of 4 mm the corresponding values are 100.4%, 89.9%, 89.3% and 87.6%.

3.3.1.3 Effect of displacement on PIV and PIV_{50}

For a systematic error or shift the volume receiving the reference dose PIV and the volume receiving 50% of the reference dose PIV_{50} remain almost unchanged because the shape of the isodose lines is only influenced minimally by a slight change in attenuation on the pathway but not by rearranging the shots in relation to each other. With a random error, where the fractions are irradiated with displacement in relation to each other, the borders are blurred thus reducing PIV (Figure 3.5 A)) and enlarging PIV_{50} (Figure 3.5 B)).

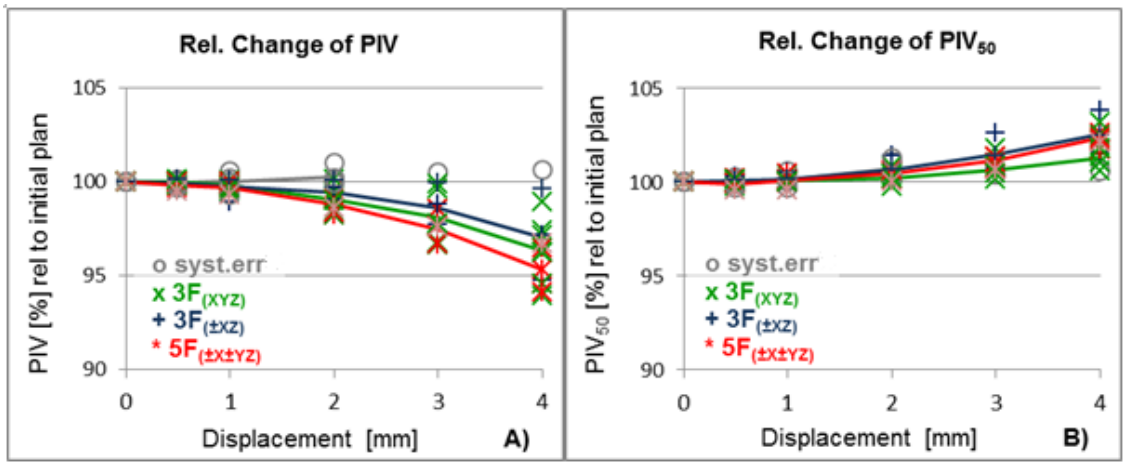

Figure 3.5: *PIV and PIV_{50} are predominantly affected by the relation of the shots/fraction position to each other. Positional error reduces the high dose volume and increases the low dose volume for the total dose. (Note: values for syst.err are taken from previous work [1]. Lines represent mean value of the patients.)*

3.3.1.4 Plan evaluation parameters, PCI and GI

The quality index PCI decreases with shift (syst.err and $3F_{(XYZ)}$) because an essential part of the PCI is the actual coverage of the target and with a systematic error the dose distribution is moved away from the target. When the displacement is random (spread) and in different, near opposing directions, the PCI changes only slightly for spread ($3F_{\pm XZ}$ and $5F_{\pm X\pm YZ}$) (Figure

3.6 A). Note: The highest PCI value of 0.895, as compared to 0.892 in the original plans, is with a displacement of 2 mm.

Contrary to PCI, GI, the ratio of the volume of half the prescribed dose divided by the volume of the prescribed dose, varies with spread. However, all plans remain within the commonly used tolerance value for GI of less than 3.0 [63, 69, 71, 110, 111] (Figure 3.6 B)).

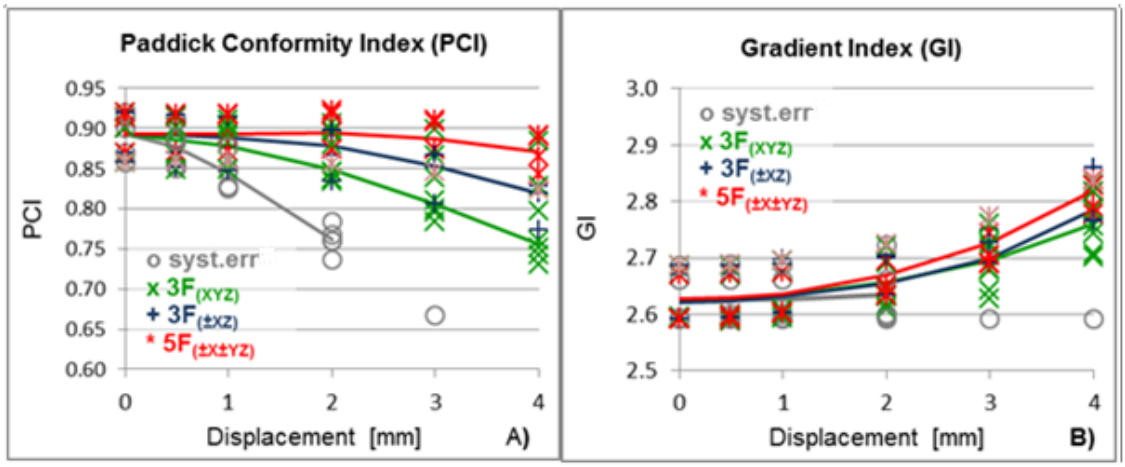

Figure 3.6: *Quality indices for GK SRS are PCI and GI. The PCI depends mainly on relative position to the target and is therefore sensitive to systematic error or shift (A). GI is a function of random error (spread) (B). (Note: values for syst.err are taken from previous work [1]. Lines represent mean value of the patients)*

3.3.2 Margin required to cover target for selected scenarios

The required margin for a shift is of the same magnitude as the shift itself for values of between 1 and 4 mm. The required margin becomes smaller with increasing spread and reduced shift and it levels off below 0.7 mm. Figure 3.7 shows the details.

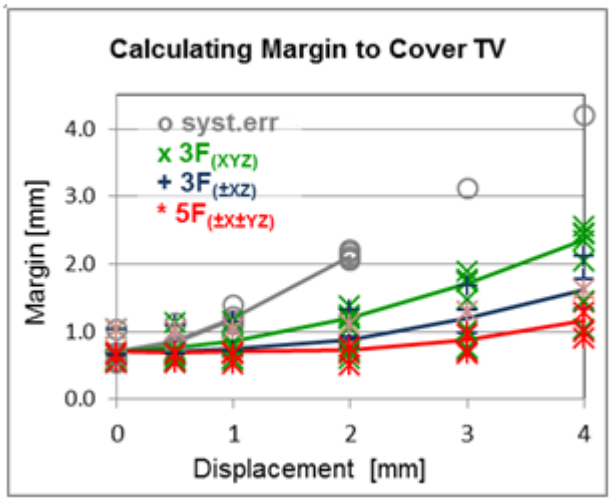

Figure 3.7: *a potential margin required to cover 100% of the target is smaller for plans with little systematic displacement component even if the individual displacements are as large as 4 mm. (lines represent mean value of the margin of the five patients evaluated in this analysis)*

3.4 Discussion

Overall survival of cancer patients has increased in recent years due to new and better treatment options. In this situation brain metastases can severely reduce quality of life (QoL) for the patients. SRS can improve local control with minimal toxicity. However, for large metastases the problem is the toxicity due to the irradiation of NT proximal to the TV. Fractionation allows the total dose to be increased but introduces positional uncertainties. Biologically Effective Dose (BED) effects favour NT over some tumour cell types for the same dose thus increasing the therapeutic window [139, 140, 172]. Unfortunately, if a margin is added to the TV the NT inside this margin would get a higher than prescribed dose if the dose is prescribed to 50%. It is therefore essential to minimise the initial NT included in the PTV. Good knowledge of the effects of uncertainties can help to choose the optimal strategy to reduce the required margin.

In this work the effect of different displacement patterns on the total dose distribution for fractionated SRS with GK was analysed. A systematic

approach was used to find the most critical parameters and suggest strategies to minimize uncertainty effects.

3.4.1 SumPlan and the estimated margin

The effect of a shift or systematic error has been evaluated in the earlier work for a displacement of up to 2 mm [1]. Some of those results are included here for comparison. Furthermore, for one patient the isodose lines of the sumPlan are shown in the coronal slice. For this patient the sumPlan for a displacement up to 4 mm was added.

The estimated margins plotted in Figure 3.7 match the visual impression of the isodose lines in Figure 3.3. The plan with the systematic error (grey circles) requires the same margin as the displacement whereas the $5F_{\pm X \pm YZ}$ and even the $3F_{\pm XZ}$ fractionation scheme where random error dominates need only small margins such as 0.7 and 1.2 mm for $5F_{\pm X \pm YZ}$ and 0.9 and 1.6 mm for $3F_{\pm XZ}$ for 2 and 4 mm displacements.

A margin of 0.7 mm is calculated for the original plan yet the reference isodose line of 18 Gy in Figure 3.3 A) (with 0 mm shift) seems to match the target volume (red) with almost no margin. The reason for this discrepancy is the assumption for the margin calculation that the underdosed area is entirely on one side. This is the case as soon as a systematic error (shift) is involved but not in the initial state of the original plan where underdosed areas are distributed in small patches all over the surface of the TV. In this situation without shift of PIV the required margin is half the size. Since neither the TV nor the PIV are perfectly spherical the two volumes are slightly different. In fact, the PIV (yellow line in Figure 3.3 would have a margin of 0.4 mm towards TV if both volumes were perfectly spherical. This is the magnitude of margin that occurs in normal planning in the attempt to cover 99% of a large target.

3.4.2 Robustness for higher fraction schemes a consequence of prescribing to the 50% isodose line

For plans with spread (random uncertainty) as the dominant effect the coverage and $D_{min1\%}$ in the TV change by 0.6% and 0.9% respectively for the $5F_{\pm X\pm YZ}$ plan with 2 mm displacement. For the symmetric $3F_{\pm XZ}$ simulation where two fractions were displaced in opposing directions the reduction was 0.6% for coverage and 4.4% for $D_{min1\%}$.

Why is there so little change in coverage and $D_{min1\%}$ for GK treatments? The secret lies in the dose homogeneity within the target. In **Error! Reference s ource not found.** the principle is visualised. The profiles of three single beamlets from a 16 mm shot of the GK collimator are plotted in the planned position and with +2 mm and -2 mm displacement. Then the sum of all three profiles was calculated and normalised (red line). While a 2 mm shift to one side increases the dose at the reference point by about 40% to 90% the dose is reduced when shifted to the opposite side by almost the same amount. Such an error would reduce the integral dose inside the TV (blue area) and increase the integral dose outside the TV (red area). At the centre of the profile (50% level) the two effects cancel out and the total dose of the sumPlan remains unchanged at the 50% level. For comparison, at the 70% isodose line the volume treated with the prescribed dose would be smaller (**Error! R eference source not found.**, blue triangle at the 70% isodose line) while the volume would increase for a prescribed dose to the 30% isodose line (Figure 3.8**Error! Reference source not found.**, red triangle). The main effect of up to ±2 mm displacement (dependent on the steepness and distance between the 10% and 90% isodose line) in exactly opposing directions is a reduction of the dose gradient but would not change the position of the 50% isodose line. In clinical practice, random displacements may not be in exactly opposing directions, but still prescribing at the 50% level would give more robustness than other levels.

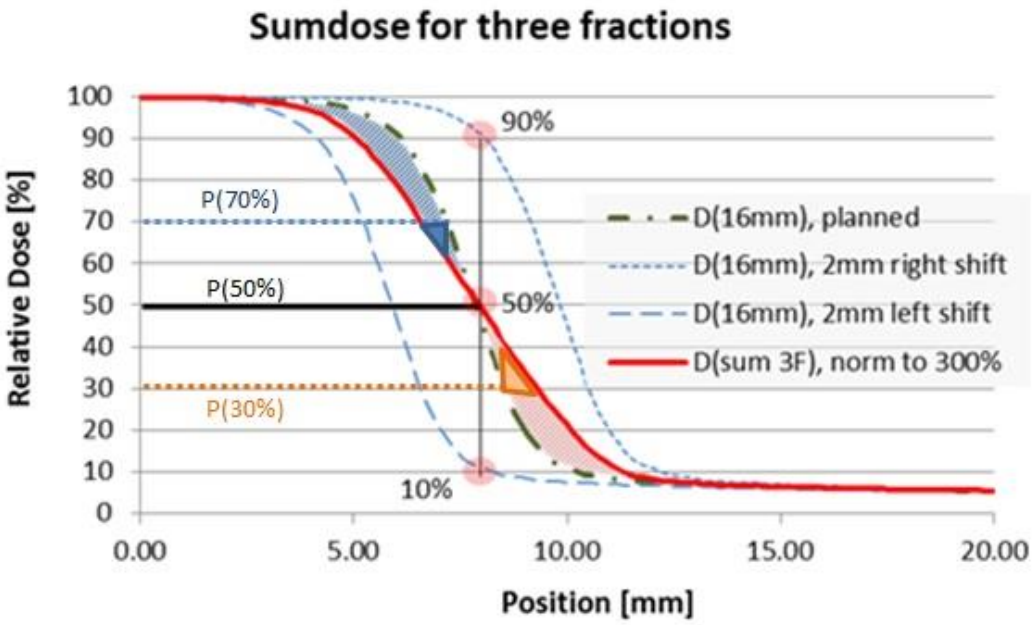

Figure 3.8: *The graph shows the effect of displacement for a single 16 mm shot. The normalized profile (red) is the sum of three profiles from a treatment with one 16 mm shot in place and the other two displaced by +2 and -2 mm. The dose on the 50% dose level remains almost unchanged but the gradient becomes less steep. Choosing a prescribed dose of 70% results in an underdosage (blue triangle) while a prescribed dose of 30% results in an overdosage (red triangle).*

3.4.3 Alternative handling of set-up uncertainties for GK: margins on demand

3.4.3.1 Why margins are more critical in GK SRS than in linac SRS

Linac based RT, including linac based SRS, aims for a homogeneous dose distribution in the target. Any set-up uncertainties reduce the volume of the treatment dose because the prescribed isodose level is typically 80% or higher. Margins are introduced to prevent underdosage but quickly increase the volume of irradiated NT [101, 151, 173`].

GK treatment has often been prescribed close to the 50% isodose, although other prescription levels are also used. Dose inhomogeneity is accepted, in practice a high dose inside the target is favoured for single fraction GK SRS because any hot spot is within the solid tumour. If a margin is added, normal tissue is included in the treated volume that receives a dose between prescribed dose and the maximum dose. An option to reduce the dose to NT is to choose a higher prescribed isodose. However, this requires more small

shots and therefore increases the treatment time and the additional NT irradiated would still get a higher dose then the prescribed dose. Minimizing margins is therefore even more important than for linac RT.

3.4.3.2 Estimating the potential maximum uncertainty with the GK Icon

With Icon™ a CBCT is performed pre-treatment. Then a virtual six degrees of freedom correction is performed by adapting the planned shot positions to correct for translation and rotation. So every treatment starts with no measurable positional displacement. During treatment the HDMM system verifies this position continuously by tracking a single point and stops treatment if the deviation exceeds the predefined threshold, usually 1 mm. However, the positional accuracy of thermoplastic masks is generally in the range of 3-3.7mm [36-38, 167]. Chung et al (2014) [39] evaluated the Icon™ mask and HDMM system in a pre-clinical setting on a linac, ie using the CBCT, geometries and correction approaches of a linac system. They evaluated the intrafraction motion for four patients treating 28 fractions. After setting up the patient a pre-treatment CBCT was performed and any uncertainty corrected as done on the Icon. Post treatment a second CBCT was performed. The mean deviation between pre and post treatment was 0.49 mm (CBCT) and 0.51 mm (HDMM). However, this does not mean that the displacement was in the same direction since the HDMM value has no direction. In theory, but also unlikely, the two mean values could be up to 1.0 mm apart from each other.

The maximum displacement measured in Chung et al's series was up to 3.6 mm intrafraction displacement using CBCT. The maximum difference between CBCT and HDMM of the reflector position mounted on the nose tip was 0.55 mm (3.71 mm measured with CBCT compared to 3.16 mm measured with the reflector). The reason for the difference between CBCT and reflector position post treatment is not clear. One explanation might be a rotation of the head induced during treatment. A linac CBCT matches to the anatomy of the patient. A rotation might induce a different displacement of the target than of the marker on the nose tip. This problem, that the marker displacement might

not precisely represent the target displacement, is the reason that only the magnitude of the marker displacement is given and not the individual coordinates. A 1.0 mm threshold as tolerance for the HDMM plus up to 0.55 mm discrepancy between CBCT and reflector would result in a worst-case (direct addition) potential displacement of 1.55 mm of the nose tip as a total intrafraction uncertainty. Murphy et al [165, 166] found a drift pattern for intrafraction motion which reached 2 mm in 20% of the cases and 1.0 mm in 80% of the cases in their studies. So in order to ensure that the whole target is covered with the correct dose a margin of at least 1.55 mm would be required.

3.4.3.3 Not every displacement pattern requires an action

Margins increase the irradiated volume of NT and not all patients have a significant intrafraction movement at all. The HDMM system displays the magnitude of the intrafraction movement (of the nose tip) but not the direction. If the patient moves one millimetre each treatment but in a different direction no margin might be required, whereas one millimetre systematically in the same direction plus a potential rotation causing an additional uncertainty might require a correction. For patients who move during treatment more than, for example, 0.5 mm depending on the distance to critical structures, a post CBCT could provide this directional information. Rather than adding a margin to cover such uncertainties a corrective shift could be applied.

3.4.3.4 A potential novel approach to deal with positional uncertainties for GK

The work above begins to suggest a possible novel approach to handle the impact of intrafraction positional uncertainties for fractionated GK treatments. GK SRS is planned in a different way than linac SRS. For the GK, the effect of two opposing displacements has been shown to not result in a reduction of the prescribed dose but only in a reduced dose gradient. Instead of having a margin applied throughout the treatment, as would be done for conventional external beam radiotherapy which would irradiate additional NT on every fraction, a procedure could be defined that corrects only treatments that would

have moved out of tolerance and have added up to a relevant systematic error because the movement was always in the same direction; i.e. an “individually customizable margin” so to say.

For such a procedure a higher number of fractions is required so that a pattern can be established. Therefore five fractions would be preferable to three fractions. The initial set-up is done as normal. At the end of each treatment or every time the treatment is interrupted a post CBCT is done and the position recorded. Then the results of the post CBCT are evaluated for total shift out of these three fractions and the remaining two fractions are used to “correct” any systematic position deviation by a corrective treatment displacement in the opposite direction so that the accidental displacement and the deliberate displacement in the opposite direction cancel out, as seen in Figure 3.8. To avoid errors of correction in the wrong direction such a procedure should be automated as is the pre-treatment correction [174].

Slow drift seems to be the dominant cause of displacement [165, 166] of a patient. The position of the reflector is internally measured in X, Y and Z directions individually by the HDMM, but not displayed on the system. Then the total vector is calculated and displayed. The reason for not displaying the full data is that the displacement of the nose tip due to potential head rotation does not necessarily represent the displacement of the target. However, detailed information about direction and speed of the reflector movement might (but does not have to) correlate with the movement of the target and might be useful to differentiate between random or systematic displacement. Final confirmation would be needed from a post CBCT.

Any displacement would still cause extra NT irradiation. However, with this method treatment could be planned without margin, thus sparing NT and at the same time still providing a strategy to cover intrafraction uncertainties of up to 2 mm by a deliberate corrective displacement in the opposite direction. With this method only that part of the NT is irradiated that was irradiated due to intrafraction displacement (one to three fractions) and the opposing part for the corrective fractions rather than the entire surrounding NT for five treatments. This could reduce the NT volume irradiated with a high dose

significantly and would only increase GI if a correction is needed. As seen in Figure 3.6 B) even with a displacement of 4 mm the GI is still below 3.0.

The technique may also allow relaxing the threshold of the HDMM for patients who struggle to keep still or allow treating patients where the reflector cannot be placed on a convenient point to be tracked during the whole procedure.

3.4.4 eXtend

Without a CBCT system the exact position of the patient cannot be verified with an eXtend system. In the previous work, some suggestions have been made of how to minimize a margin based on the knowledge of the target position in relation to the centre of rotation mouthpiece [1]. In addition to that, a higher number of fractions could further reduce the effect of positional uncertainties. If the displacement is systematic the total effect is similar to a single fraction. Any random displacement in additional fractions reduces the deviation of the 50% isodose and improves coverage and $D_{(min)}$.

3.4.5 Limitations of this study

The study has been conducted for lesions with volumes of 10.72 cm^3 or larger. The assumption was that the volume is near spherical and that TV and PIV are similar in size. A spherical volume is typical for a metastasis but not necessarily so for a meningioma. Small lesions will be investigated separately because in those cases PIV is bigger than TV and the simplifications made for the margin estimations cannot be applied.

In this study the aim was to find characteristic patterns in how set-up errors influence the total dose. For that reason, displacements have been chosen to cover shift (systematic error), spread (worst case of random error with opposing displacements) and selected combinations of them. Real set-up errors will typically be something in between the selected cases. A five fraction treatment is unlikely to have all the displacements in different directions as simulated in this work. It is more realistic that some of the fractions are

displaced in the same or similar directions and with different magnitude. The result of a real five fraction treatment might be similar to the $3F_{\pm XZ}$ simulation or even to the $3F_{XYZ}$ scheme with a significant systematic contribution.

The effect of cancellation depends on the dose gradient. This work shows the potential effects and strategies for displacements of up to 2 mm for multi-shot plans. However, in a multi shot plan the situation is more complex than shown in Figure 3.8. The gradient is not always smooth as for the single shot used for the illustration of the principle. Therefore the effect is likely dependent on the planning style. This work demonstrates that the principle works for multi-shot plans. However, it is likely that the gradient should be smooth and shots should not be placed on or even outside the target in order to improve conformity. A good GI as described by Paddick and Lippitz (2006) [69] should be achieved. Furthermore, no investigations have been made here for the effect for plans with other prescribed isodose levels such as 70% or 80%.

The possibility to “correct” an underdosage in the target and the respective overdosage in the NT on the opposite side seems to have potential for the future. It should be noted that the calculations in this work are based on physical dose. The BED effects are not necessarily the same. Physical dose cannot be easily converted into BED because the effects for small volumes and high dose levels are not well researched [171, 172]. Furthermore dose rate has an impact too [175].

Using the last part (last few fractions) of the treatment course to correct a systematic error characterised during the first part requires an exact recording of the intrafraction movement and post fraction positions. Careful quality assurance for such a technique would be essential. The total displacement (averaged from post treatment CBCT values) of the first three fractions would have to be measured and evaluated automatically. To avoid correction in the wrong direction the “correction coordinate” would need to be evaluated automatically; ideally together with an automatic sumPlan calculation including the effect of the measured displacements for each fraction plus the calculated dose distribution for the planned corrective treatment fraction about to be delivered next. This could be implemented similarly to the pre-treatment correction [174]. Icon™ has the tools (CBCT, marker tracking with X, Y and Z

coordinate information, HDMM) to realise this potential development and for the overall workflow to be further developed.

3.5 Conclusion

Prescribing the treatment dose to the 50% isodose minimizes the effect of random error on coverage.

In order to characterise the random distribution, SRS fractionation schemes with higher fraction numbers are preferable in terms of coverage. More fractions allow the quantification of potential systematic errors and the potential to develop the GK Icon workflows to correct systematic error for up to 2 mm displacement.

Any applied margins do not only increase the irradiated NT but also irradiate it with higher than the prescribed dose.

BED is not well investigated or characterised in a steep dose gradient situation and for high doses. BED effects are likely to change the effects of coverage and especially on the GI in one or the other direction.

Chapter 4:
Dose to brainstem due to positional uncertainty

The work in this chapter will form the basis of a paper to be submitted for publication.

4.1 Background and Introduction

4.1.1 Fractionated SRS and uncertainties

Treating the whole target volume is essential to avoid recurrence. However, it is equally essential to protect organs at risk that are vital for survival. One of the most important and critical organs is brainstem (BS) and this is used here as an example of OAR effects. The BS connects the brain to the rest of the body. It controls the flow of messages. It also controls many vital body functions such as breathing, sleeping, heart rate, or blood pressure. Each function is located in a specific region within the BS. For that reason, the function of a damaged part of the BS cannot be substituted by another part as is possible in a parallel organ like the lung or kidney where a certain percentage of the volume may be spared, but the location is not critical. Hence no percentage of volume can be irradiated safely over the tolerance dose for BS.

A “tolerance dose” is defined in relation to the treatment. When the disease treated is not life threatening the tolerance dose is lower compared to the treatment of a malignant and life threatening disease. Tolerance dose is a value that balances the risk in relation to the benefit. Or in other words: keeping the dose below the tolerance dose does not guarantee that the patient will not suffer from side effects.

Tissue damage is a function of dose and volume. In single-fraction SRS necrotic brain tissue can be observed at dose levels of 12 Gy [13, 113, 140, 176-182]. As a general rule of thumb, the tolerance dose for brainstem is

therefore 12 Gy for a BS volume of maximal 10mm^3. “Rule of thumb” because there are two exceptions. One is with the treatment of the trigeminal nerve. In cases where the trigeminal is hypersensitive, the nerve can be "blocked". There are various options to do this, such as drugs, surgery, injections, and others. Radiosurgery is only one possible method. In order to numb the nerve, a high point dose of 70-90 Gy has to be applied where the nerve passes through the skull bone [84, 85] right next to the BS. However, the volume is an important factor, and the trigeminal treatment is done with a single small 4 mm shot [183]. The accepted tolerance dose for BS in this situation varies from a maximum of 10 mm^3 with 12 Gy and no more than 1 mm^3 with 15 Gy [86, 184] up to the 50% isodose touching the BS. In our hospital, 80 Gy and the 40% isodose touching the BS was used at the time this work was carried out. As an aside: comparing the contouring of different clinicians shows differences which may reach a millimetre or even more, which would influence the dose to the BS without affecting the reported numbers.

The other exception for a higher BS dose is when the tumour itself would cause severe side effects and possibly death, for example, when the tumour is completely embedded in the BS. In this situation, the exact location of the tumour (BS function in that place), tumour doubling rate, and other factors have to be assessed on a case to case basis for the radiation oncologist to decide the optimum balance. Especially in such situations where the safe dose for the BS has to be exceeded, it is much more important to keep the dose as low as possible while not compromising the target.

4.1.2 Effect of uncertainties on nearby tissue

In the previous work [1] potential uncertainty of eXtend, the GK relocatable repositioning system, was evaluated. On eXtend a vacuum assisted mouthpiece is used to ensure the correct position of the patient’s head. A change in the level of the vacuum is assumed to be due to a patient movement and pauses the treatment. Generally, the pause would be triggered for a target movement of less than 1 mm but potential movements of up to 2 mm were observed.

The most recent GK model, the Icon system, uses a different approach for set up and intrafraction surveillance. An individually moulded cushion and a thermoplastic mask is used for the initial set up. The correct position is verified against a stereotactic reference planning cone beam CT (planning CBCT). Displacement and rotation are then corrected before treatment commences. During the treatment the correct position is surveyed with a tracking system based on a reflector placed on the nose tip. Its position is compared to the reflectors on the rigid reference system of the Icon mask adapter. A tolerance, typically 1 mm, can be set in the high definition motion manager (HDMM) which would stop the treatment if it is exceeded and the position corrected with an additional CBCT. Wright et al [185] measured the reliability of the reflector of the nose tip by introducing a known error and using a phantom head. They found good agreement between induced reflector displacement and reflector indication on the HDMM within 0.15 mm. Based on the phantom measurement they found in most cases that the intracranial anatomy is displaced 43% (mean) less than the nose tip but can be displaced more than the nose tip and may reach 2 mm or more depending on the lesion location. The HDMM system internally measures translation in X, Y and Z directions, calculates a total vector and displays the total magnitude of it but not the direction.

Chung et al [39] evaluated the inter- and intrafraction motion of four patients in the mask system treated clinically on a Clinac for 28 sessions in total. As in the phantom experiment of Wright et al, Chung too found that the displacement of the nose tip reflector may be different to that of the target. For the target they found the mean displacement during treatment (difference between pre and post CBCT) was 0.27 mm. The largest intrafraction variation of the target was 3.63 mm. On the other side the maximum intrafraction motion of the nose tip indicated by the reflector was 3.16 mm while the CBCT for the nose tip reflector indicated a movement of 3.71mm or 0.55 mm more than the HDMM system detected. The potential uncertainties based on four patients and a HDMM action level of 1 mm would be about 1.5 mm.

In the previous work [2] the dose gradient was found to decrease with increasing displacement. This means the physical dose inside the target decreases but remains above the prescribed dose while the dose outside the

target in NT and OAR increases. However, with fractionation the dose per fraction in the OAR is reduced to levels below 7.5 Gy and benefits from the repair effect.

This chapter evaluates the effects of uncertainties on OAR dose in terms of BED outside the target using the brainstem as an example. Lesions in or near the BS are of particular interest. Any tumour growth damaging the BS may lead to the death of the patient, but the same could happen with too large a volume of the BS irradiated excessively, for example due to an added margin or a reduced dose gradient. Strategies to minimise underdosage due to set up error without the necessity of adding a margin would be of significant benefit.

4.1.3 Physical dose and biological effective dose

So far GK SRS has typically been delivered in a single fraction with a clearly defined dose, prescribed to the ~50% isodose line. Treatment with hypo-fractionation should keep the BED at the prescribed isodose level the same (or higher) than that for the single fraction treatment. Cell death depends on fraction dose, the total dose, the overall time in which the dose is delivered and the cell type [154, 171]. Up to about 6-8 Gy per fraction the relationship between physical dose and BED is described by the linear quadratic (LQ) model [186, 187]. The model is widely used in fractionated radiation therapy for fraction doses in the range 1.8-5 Gy and occasionally up to 8 Gy. For these lower doses some of the damage to the DNA can be repaired between fractions. These repair mechanisms work better for NT than for tumour tissue hence the advantage for NT with fractionation. The higher the dose the higher the damage and the less effective the repair. The LQ-model is a continuously upward bending curve describing the higher damage for higher doses. However, for higher doses above around 6-8 Gy, depending on the cell type, the damage to the DNA is so high that no repair is possible and the formula overestimates the BED and so, for example, cannot be applied to doses used in single fraction SRS. There has been considerable experience with single fractions where a single high dose is delivered but there is limited data in the

range between 6 - 8 Gy per fraction and the higher SRS doses [139, 171, 188, 189]. In the higher dose region, where the LQ model overestimates the dose effect, BED has a linear relation to the physical dose and the multi target model, which assumes a minimum number of hits is required to destroy the DNA, predicts the outcome better [115].

Park et al [131] suggested a universal survival curve (USC) that combines the two models, tweaking the parameters from (historic) in vitro survival studies, covering a range of potential values, such that the two parts of the curve, the low dose range for fractionated RT where the LQ model is used and the high dose range from single fraction SRS where the multi target model is applied, transition seamlessly into each other [131]. More recently, this approach, to combine LQ model and multi target model, has become more popular with the option of in-silico experiments [190].

In order to add the correct BED in the case of a displacement and for comparison with a single fraction treatment the conversion of physical dose to BED for higher doses is needed. This work will investigate the BED outside the target in the BS with and without positional displacement

4.2 Material and methods

4.2.1 Calculation of BED

For the theoretical study in this work the split formula from Park et al. [131] was used. In this formula equation 1 describes the conversion of physical dose to BED in the lower dose region up to the transition dose using the LQ model while equation 2 describes the conversion for the higher dose range using the multi target model. The parameters have been selected to ensure that both parts of the curve match.

$$BED = D\left(1 + \frac{d}{\frac{\alpha}{\beta}}\right)$$ equation 1 for $d \leq D_T$

$$BED = \frac{1}{\alpha D_0}\left(D - nD_q\right)$$ equation 2 for $d \geq D_T$

n	number of fractions
d	fraction dose [Gy]
D	Total dose (n*d) [Gy]
α/β	dose at which the linear and quadratic components of cell killing are equal [Gy]
α	parameter of initial slope of cell survival curve [Gy^{-1}]
D_0	Parameter of the slope of the multi target curve [Gy]; slope is 1/ D_0
D_q	x-intersection of multi target curve [Gy]
D_T	Dose at which the LQ model transitions to the multi target model

The BS is outside the target therefore the physical dose to the BS is below the prescribed physical dose which, for fractionated delivery, is less than 8 Gy and therefore covered by the commonly used LQ part of the split formula. However, the physical dose to the target is ideally above 20 Gy but can be lower if compromises are required due to size (more NT irradiated with higher doses) or OAR such as BS nearby, doses can be reduced to 18 Gy or even 16 Gy. In order to choose the steepness of the linear part of the high dose curve other reference points from the literature were used to fit the curve. Millar et al [175] evaluated the BED for a GK treatment of a patient with a meningioma and calculated the BED for 12, 13 and 14 Gy dependent on the dose rate which was indicated by the number of shots. The steeper the linear part of the curve the higher the effect of fractionation. For that reason the lower end of the range was chosen as reference to optimise the curve parameters. The BED values for 12 Gy, 13 Gy and 14 Gy physical dose were 45.5 Gy, 52.2 Gy and 58 Gy, respectively. Furthermore, this work compares the effect of fractionation compared to a single fraction for the same plan, so the doserate would be the same for all treatments.

This investigation focused on the potential effect of the gradient in the low dose volume outside the tumour. Of particular interest is what effect one fraction

out of three or five fractions displaced towards the BS could have on the total BED to the BS, increasing the BED in the BS for that one treatment while the other fractions are displaced in different directions.

4.2.2 Target selection

For this investigation nine patients were selected. Seven had medium sized targets (range 611-4840 mm^3) in close proximity (2) to, overlapping with (2), or embedded (5) in the brainstem as can be seen in Figure 4.1. In addition to that, two extreme situations were added with a small target (15.3 mm^3) in the brainstem and a large target (14570 mm^3) approximately 5 mm dorsal to the brainstem.

The targets are shown in Figure 4.1 where the lesions and their position in relation to the brainstem are shown for seven patients in transverse slices including the plan. Figure 4.2 shows an extreme situation with a lesion inside the brainstem leaving only a small rim of brainstem and Figure 4.3 shows a large lesion in close proximity to the brainstem so that high doses reach inside the brainstem.

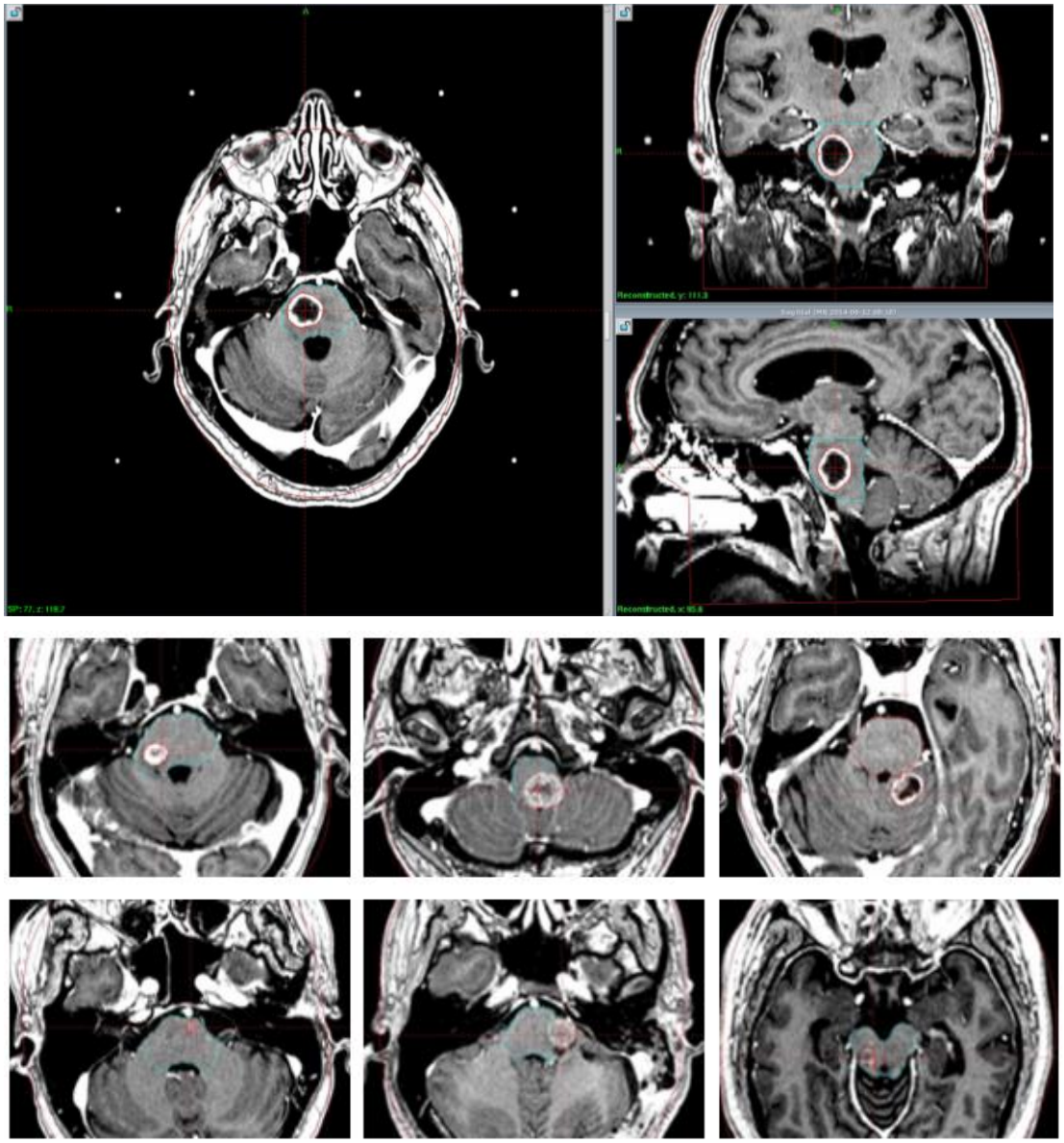

Figure 4.1: *Overview of the general location of the medium sized lesions and transverse slice of the BS and the lesion for seven patients evaluated in this study.*

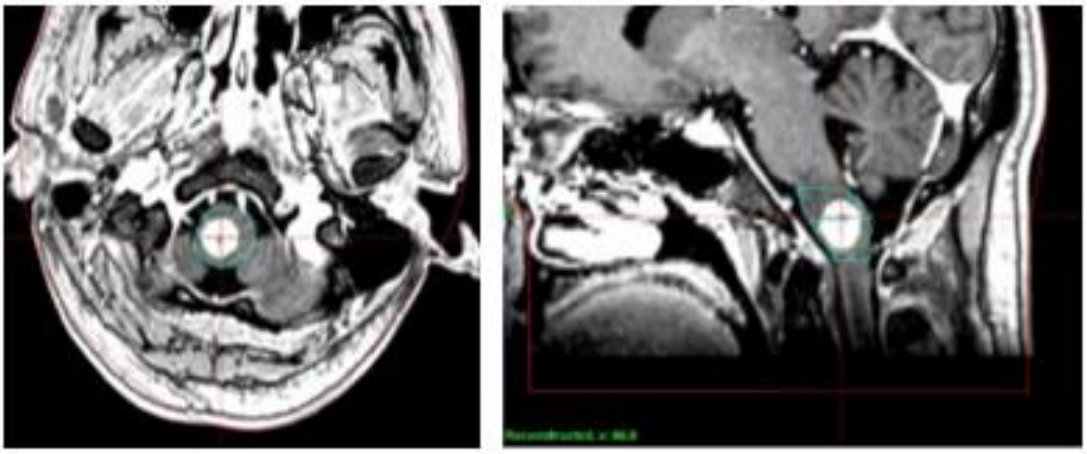

Figure 4.2: *: transverse and sagittal slice of a lesion in the brainstem. The lesion is an extreme location completely embedded in the BS leaving only a small rim of BS.*

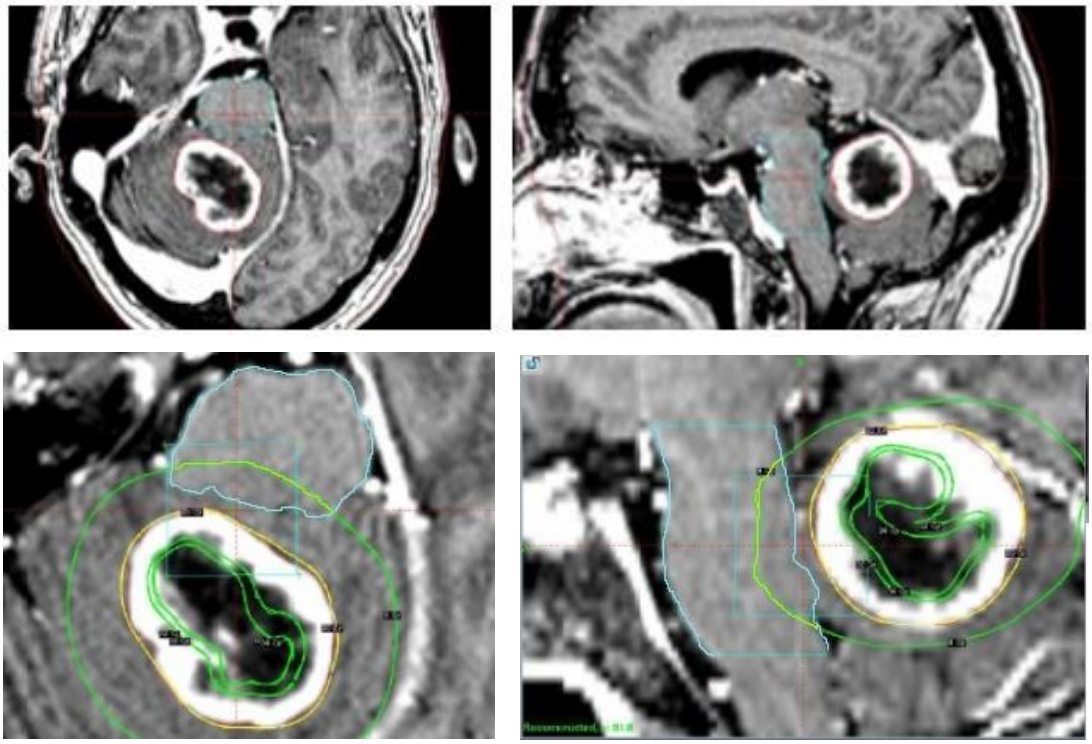

Figure 4.3: *A large lesion at approximately 5 mm distance to the brainstem was selected. Due to the size of the target the BED gradient is less steep and the 9Gy isodose (BED 48.5 Gy, depending on the prescribed dose) reaches far into the brainstem (outer green line in lower zoomed images).*

4.2.3 Planning

For each case, target and brainstem were contoured. A reference plan using GammaPlan Software® (GP, Version 10.2.0, Elekta AB, Stockholm, Sweden) was created. No special optimisation (no blocking of sectors) to reduce the dose to the BS was made other than a tight conformation to the target because the contact area was too large to avoid it. The physical dose was prescribed to a nominal 50% of the maximum physical dose. Then the 3D dose distribution (resolution 0.5 mm) and the contours of target and BS were exported as DICOM RT files and further processed with in-house software based on Matlab and Excel where it was converted to BED for further processing and evaluation.

4.2.4 Simulated displacement

As in the previous work [2] three and five fractions have been simulated. The displacement was in +X (lateral) for the first fraction, +Y (ventro/dorsal) for the second fraction, and +Z (cranio/caudal) for the third fraction for the simulation of Plan $3F_{XYZ}$. Accordingly the displacements for the Plan $3F_{\pm XZ}$ were in +X for the first, -X for the second and in +Z direction for the third fraction. The five fraction plans represent an extreme spread scenario with symmetric opposing displacements in +X for the first fraction and -X direction for the second fraction. The displacement in Y direction (+Y for the third and -Y for the fourth fraction) was also symmetrical. The fifth fraction was simulated in +Z direction ($5F_{\pm X\pm YZ}$). All plans have been calculated for displacements of 0.0 mm, 0.5 mm, 1.0 mm, 1.5 mm and 2.0 mm. A predefined set of displacements have been used to evaluate extreme situations. This approach allows to define a range of reference situations that cover typical clinical displacement values, but go further to consider trends. With three or five fractions there is no averaging out of the total dose distribution. For real patients the actual measured displacements can then be compared with these reference situations for an indication of likely effects to aid in decisions about further treatment fractions. A pure systematic shift with all fractions displaced in the

same direction was not included in this evaluation since it is basically only a displacement of the ideal curve as demonstrated with the physical dose in the previous work [2].

The displacement schemes were chosen to be zero (single fraction, three fractions and five fractions), pseudo-random (displacements in opposing directions in order to keep the resulting systematic error low but have a large “spread”), and a combination of the two where a systematic displacement and a random displacement is simulated. The systematic shift is always towards the BS to simulate the worst case for the OAR.

4.2.5 Creating a SumPlan for multiple fractions

For each fraction the BED distribution was shifted according to the above described displacements and added to the total BED of each voxel. In addition to the volume of the BS irradiated, it is also important that on each slice at least a part of the BS receives a BED well below tolerance BED since the BS is predominantly a serial organ. A profile through a critical diameter was also evaluated for the effect of the total BED. Of interest was the BED change due to positional displacement in the low dose area, i.e. up to the prescribed BED. The prescribed physical dose levels are 1 x 18 Gy for a single fraction, 3 x 7.5 Gy = 22.5 Gy and 5 x 5.5 Gy = 27.5 Gy for the fractionated schemes and the respective BED doses are 1 x 78.5 Gy, 3 x 25.5 Gy = 76.5 Gy and 5 x 15.6 Gy = 78 Gy. A more detailed description can be found in the previous work dealing with effects of similar geometric uncertainties on the target volume doses in fractionated GK treatments [2].

For the single plan and fractionated plans with no displacement the dose was calculated in physical dose and BED. For the plans with displacements only BED was calculated.

4.2.6 Parameters evaluated from the simulation:

Dose profiles orthogonal to the target surface were evaluated in terms of physical dose and BED for three different fraction schemes (1, 3, and 5 fractions) and three different scenarios of set-up errors ($3F_{XYZ}$, $3F_{\pm XZ}$ and $5F_{\pm X\pm YZ}$) with displacements of 0.5 mm, 1.0 mm 1.5 mm and 2.0 mm. In addition the DVH of the BS dose was evaluated.

4.3 Results

4.3.1 Calculation of BED chosen parameter

The conversion formula was split into two parts at the transition dose D_T of 7 Gy, taken as a mid-value between 6 and 8 Gy to which the LQ model is valid. For the lower part α/β was set to 3 for the brainstem [139, 140].

The parameters for the high dose range were adapted from Park et al [131] and modified to fit the low dose part of the curve and to go through the points reported by Millar et al [175] in the high dose region. The parameters were 0.18 Gy^{-1} for α, 1.1 Gy for D_0 and 2.45 Gy for D_q. The resulting curve is shown in Figure 4.4.

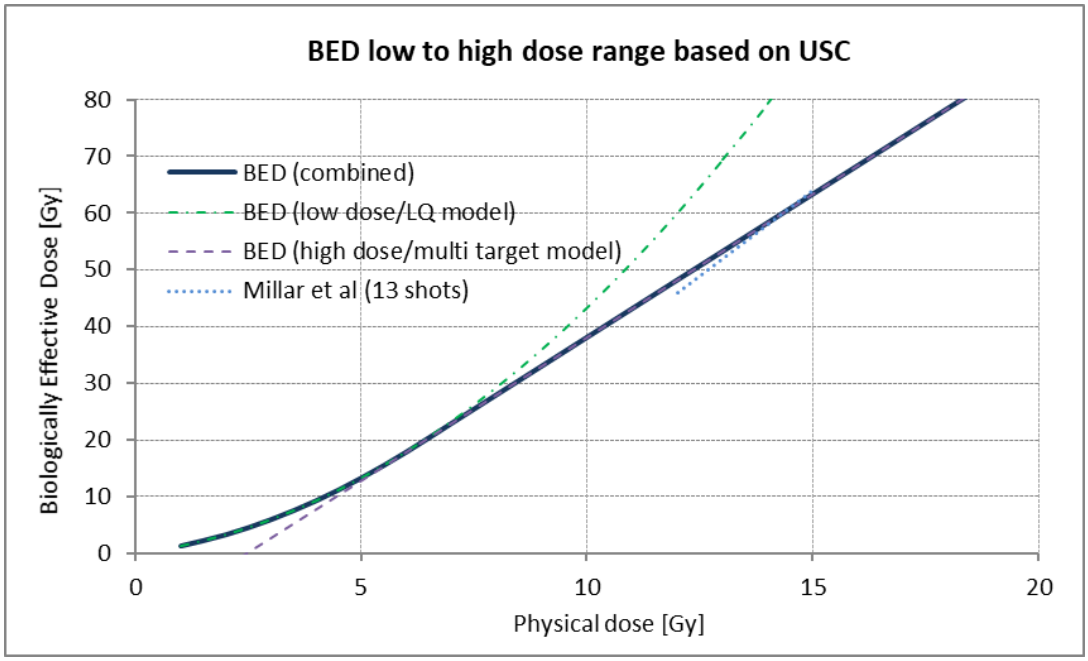

Figure 4.4: *BED is plotted as a function of physical dose where BED calculation for low and high physical dose uses the combined universal survival curve (USC) based on Park et al [131]. For doses below 7 Gy the LQ model was used to convert the physical dose into BED (green dashed/dotted line). For high physical doses a linear curve is used (thin purple dashed line partly overlaying the combined curve). Additional points in the high physical dose range (blue dotted line) have been derived from the work of Millar et al. [175]) The combined curve is used for comparison of the plans.*

Based on this conversion curve (Figure 4.4) the BED for fractionated treatment was calculated. Table 4.1 lists the physical dose and the appropriate BED for the reference (prescription) doses, maximum doses and the respective physical doses to 1 x 12 Gy in a single fraction treatment, a frequently used measure of BS toxicity and necrosis. The percentage changes are shown relative to the single fraction regime.

Table 4.1. *Physical dose and the corresponding BED with single fraction as reference (Ref)*

Fract. Scheme	Physical dose / BED	1x18Gy	3x7.5Gy	5x5.5Gy
	BED	1x78.5Gy	3x25.5Gy	5x15.6Gy
Total prescribed dose				
	Phys dose (Change [%])	18Gy (0%, Ref)	22.5Gy (+25%)	27.5Gy (+53%)
	BED (Change [%])	78.5Gy (0%, Ref)	76.5Gy (-2.5%)	77.9Gy (-0.8%)
Total max dose				
	Phys dose (Change [%])	36Gy (0%, Ref)	45Gy (+25%)	55Gy (+53%)
	BED (Change [%])	170Gy (0%, Ref)	191Gy (+12.8%)	217Gy (+27.6%)
Equiv of 1x12Gy Physical Dose				
	Phys dose (Change [%])	12Gy (0%, Ref)	15Gy (+25%)	18.3Gy (+53%)
	BED (Change [%])	48.5Gy (0%, Ref)	39.9Gy (-17.7%)	40.7Gy (-16.1%)

4.3.2 Fractionation versus single fraction (BED)

Fractionation increases the BED inside the target while it is reduced outside and this steeper dose gradient (BED gradient) allows a better protection of the BS (Figure 4.5, target as seen in Figure 4.7). The position of the 48.5 Gy BED (1 x 12 Gy physical dose) isodose for the hypo-fractionated treatment is shifted by 0.45 mm towards the target thus reducing the BED to the BS compared to the single fraction SRS. These results are valid for the selected fractionation schemes and may vary if other fraction numbers and doses are used.

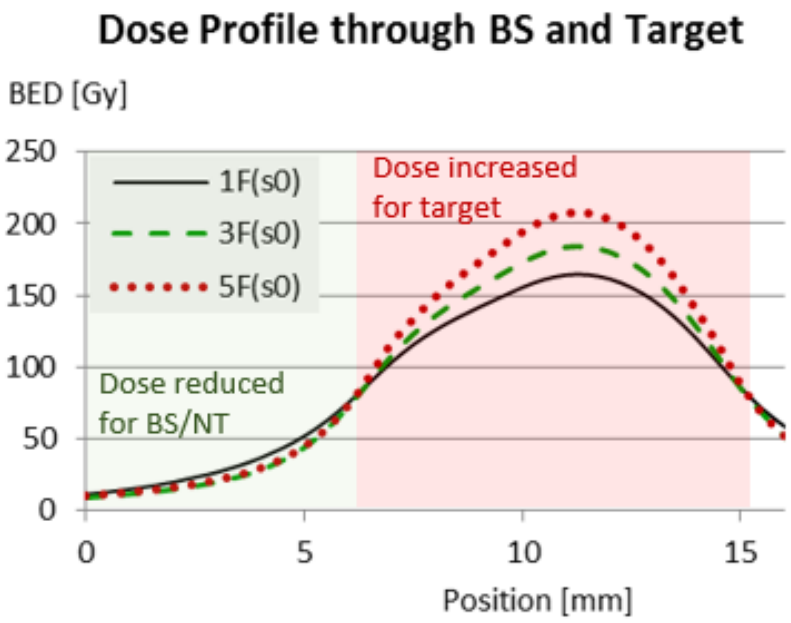

Figure 4.5: *Profile of the BED for single fraction (1F), three (3F) and five fractions (5F), each with no displacement (s0). BED is the same for all three schemes at the level of the prescribed isodose. With increasing number of fractions the gradient increases.*

The DVH of the BED for the same three fractionation schemes show the same effect as the profiles. The BED to the BS is lower for the fractionated treatments than for the single fraction treatment (Figure 4.6, target as seen inFigure 4.7). The BED in the target was omitted in the DVH because the parameters to calculate BED are specific to each cell type and likely differ for the tumour cells compared to the BS cells.

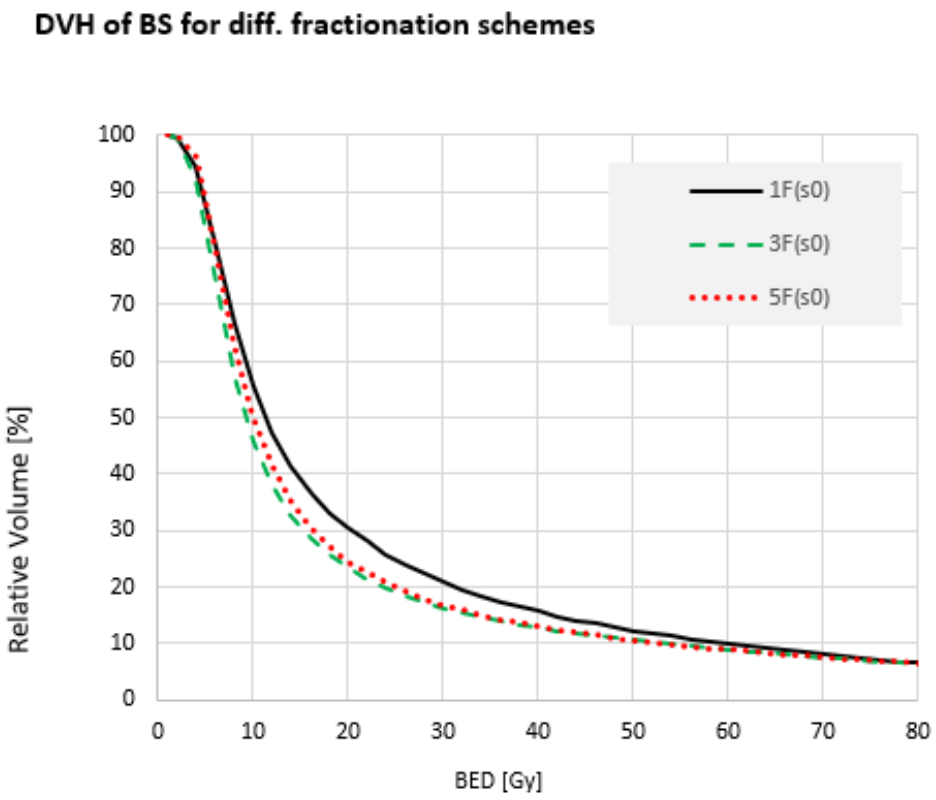

Figure 4.6: *The DVH of the BED to the BS (BED below 80 Gy) for different fractionation schemes without displacement (s0) shows a lower dose to the BS for fractionated treatment (3F, 5F) than for the single fraction treatment (1F).*

4.3.3 Introducing positional uncertainties

Applying a displacement of 2 mm for the $3F_{XYZ}$ plan (combination of spread and shift) the BED to the BS increases. Considering the profile, in Figure 4.7 the example of a medium sized target embedded in the BS, the effect of pushing the treatment towards the BS increases the BED at the target line by 9.8 Gy (standard deviation (SD) 4.6 Gy). However, only about 0.4 mm (SD 0.1 mm) of the BS receives this increased BED when one fraction is displaced by 2.0 mm towards the BS and the other two fractions are displaced in ventral and dorsal directions by 2.0 mm (Figure 4.7, top left).

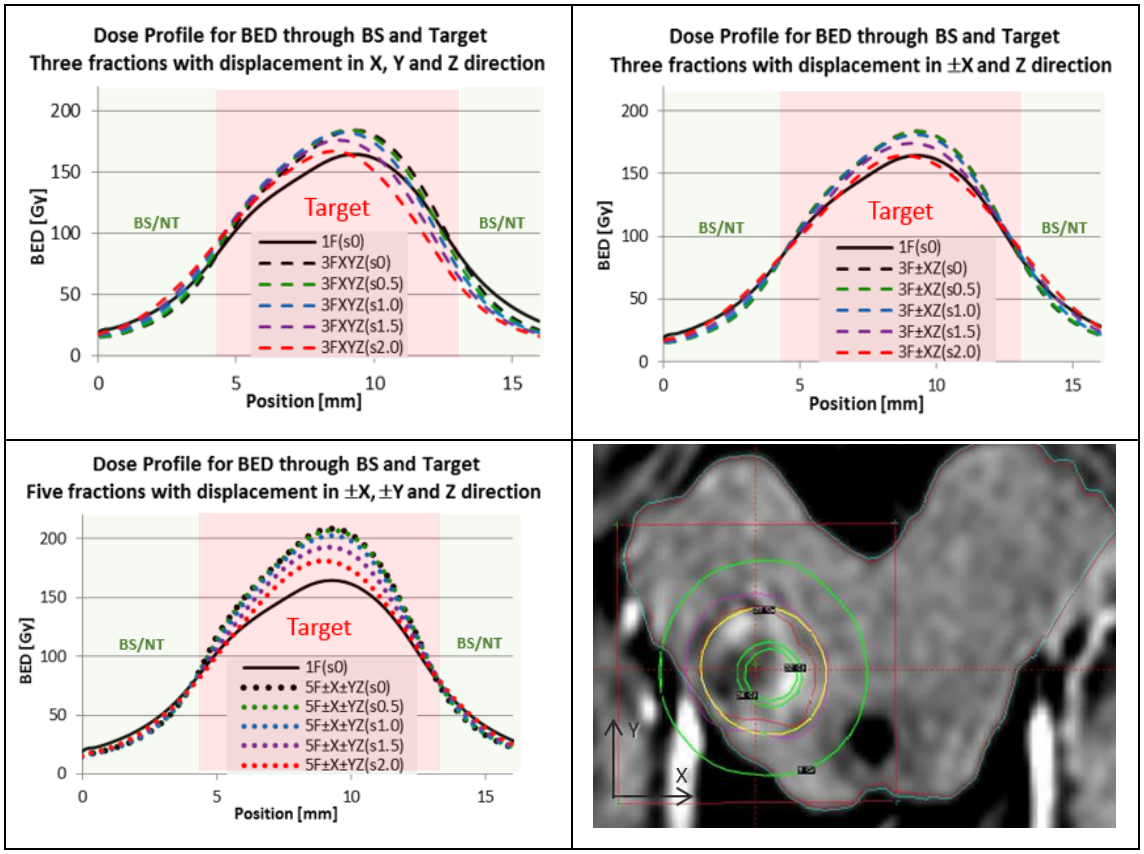

Figure 4.7: *Profile through the centre of the lesion embedded in the BS. The displacement for the three fraction plan was in X (lateral, fraction one), Y (ventro-dorsal, fraction two) and Z direction (cranio-caudal, fraction three). A systematic shift is visible with an underdosage (BED) of the target on the right side and a small overdosage (BED) of the BS on the left side. However, the overdosage (BED) is only observed in a range of less than 0.5 mm ($3F_{XYZ}$, top left). For the other two schemes where the displacement is predominantly in opposing directions ($3F_{\pm XZ}$, top right and $5F_{\pm X\pm YZ}$, bottom left) no displacement of the overall or total BED from all three or five fractions respectively can be seen. The displacement in opposing directions results in a lower BED_{max} and a reduced BED gradient.*

When the displacement component is predominantly symmetric (spread) with two displacements in opposing directions ($3F_{\pm XZ}$ as seen in Figure 4.7 top right and $5F_{\pm X\pm YZ}$ as seen in Figure 4.7 bottom left) then the main effect is a slight increase of BED to the BS. With increasing displacement per fraction the BED to the BS is increased until it reaches the BED of the single fraction plan with about 1.5 mm displacement per fraction. No significant volume of the BS receives a BED higher than the prescribed dose, or in other words the dose increase due to one displacement towards the BS is not critical if another displacement is in the opposite direction. This is unlike the situation of a conventional treatment with homogeneous dose distribution.

The effect of the BED reduction due to the hypo-fractionation is also visible in the DVH of the BS. However, the effect of increased/reduced BED to the BS due to the shift component is almost undetectable because of the lack of positional information in a DVH and the large volume of the brainstem compared to the target volume.

In Figure 4.8 top right the DVH of the BS with the target close to but not embedded in the BS shows the increase of BED to the BS when $3F_{XYZ}$ displacement is recalculated. However, despite the increase the BED is still generally below the BED to the BS from a single fraction. The BS volume receiving 48 Gy BED (1x12 Gy equivalent) is smaller for a displacement of 0.5 and 1.0 mm than for the single fraction while the volume of the $3F_{XYZ}$ plan with a displacement of 1.5 and 2.0 mm is slightly larger than that of a single fraction treatment.

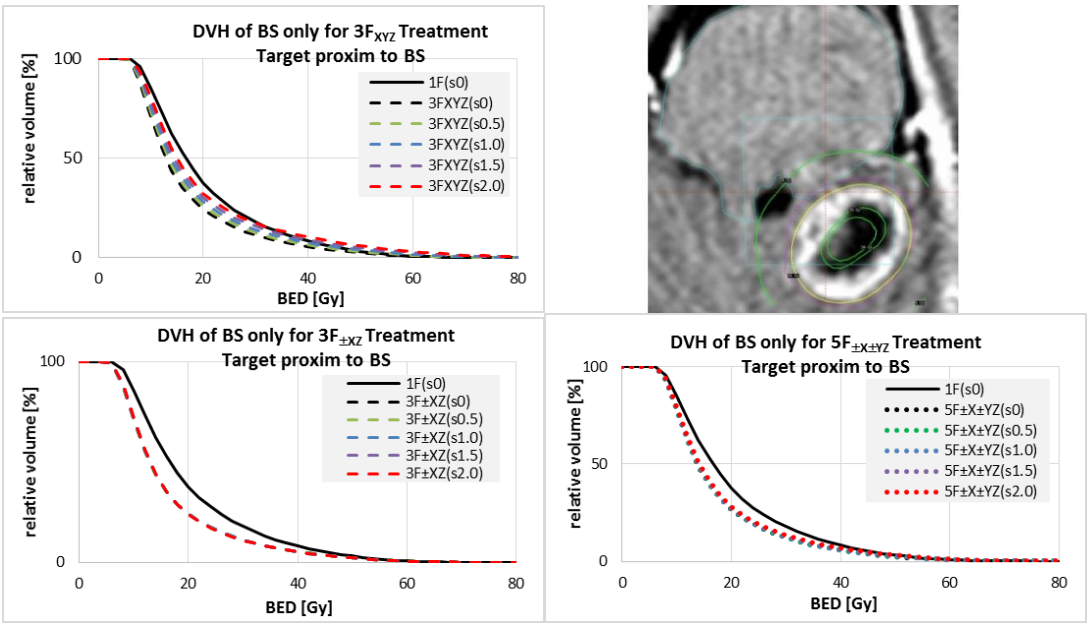

Figure 4.8: *DVH based on BED of the BS only. The target is close to the BS and the displacement was simulated towards the BS. The DVH of the three fraction plan with a shift (systematic) element shows an increase of BED dose to the BS but still below the BED for a single fraction. For the other two treatments there is no significant change observable in the DVH of the BS.*

For the plans simulated with spread (Figure 4.8 bottom left for $3F_{\pm XZ}$ and Figure 4.8 bottom right for $5F_{\pm X\pm YZ}$) the BED to the BS for fractionated treatments remains below that of the single fraction treatment.

4.3.4 Comparison of small volume to large volume

With increasing spread the BED gradient becomes less steep. For small volumes this may lead to a dose reduction inside the target. Figure 4.9 top shows the decline of the BED dose gradient for a large volume where the BED in the centre remains constant but the border areas are reduced to almost the BED of the single fraction. For small volumes (Figure 4.9 bottom) the flat top area is not reached in the initial plan due to the small size. With increasing spread in the fractionated treatments the BED to the target is reduced and becomes, in this example, below the BED from a single fraction treatment when the fractionated treatments have a displacement of 2 mm.

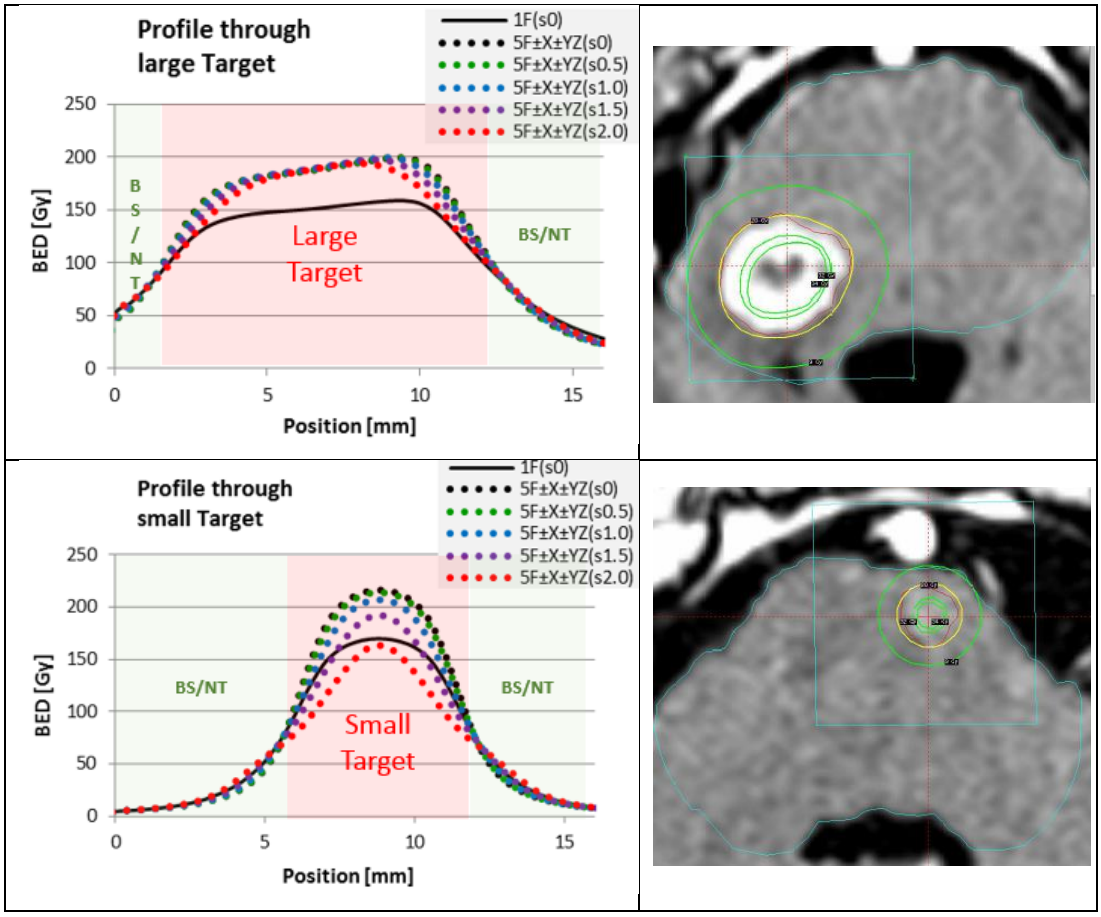

Figure 4.9: *Profile through a medium/large target (top) and a small target (bottom) shows the reduction in BED gradient with increasing spread.*

4.4 Discussion

Radiation therapy with conventional fractionation uses the advantage of the better repair for NT compared to tumour cells. A higher α/β for tumour cells than for NT is a particular advantage in regions where the two types of cells are mixed. With single fraction SRS another advantage is present. Solid tumour cells often suffer from low oxygenation and are therefore more resistant to irradiation. With the high single dose the damage is so great that all cells are killed. Moving to hypo-fractionation mixes the two effects. Depending on planning strategies, cell parameters and fractionation schemes, to mention just the most important factors, the tumour is still treated with a high fraction dose where the multi-target model is dominant. However, in the border region the two effects are mixed or transitioning from one into the other, whereas in traditional SRS the dose effect of the multi target model was

relevant to a few millimetres beyond the target volume. In fractionated treatments the LQ model needs to be applied which reduces the BED adjacent to the target where tumour cells could potentially be infiltrating into the BS or other NT.

While the general behaviour of the BED usually follows the results presented in this work, it is essential to emphasize that the details may differ depending on cell type and other parameters. The most challenging problem is that the parameters for the conversion from physical dose to BED are cell type dependent. This means that an individual BED distribution should be calculated for each cell type present. As a result either the BED distribution might contain steps and sudden changes in direction/steepness at positions where the cell type changes or an individual BED isodose plan for each cell type should be calculated.

Parameters for conversion factors are known from in-vitro experiments for the LQ model of the most important NT types. For other cell types the values have to be estimated or ideally evaluated.

Even when the conversion parameters are well known the conversion to BED also depends on the dose rate, so respectively on the plan characteristics such as source strength, shot size, plan efficiency and shot placement [175, 191]. In this work the principal changes in BED between single fraction and hypo-fractionated have been evaluated and discussed. The exact values of BED may differ and need to be evaluated individually case by case. With the option of in-silico experiments research has started in the direction of such cell type specific BED calculation with combined models [190, 192-194].

With the move to hypo-fractionation the prescribed (physical) dose, at the 50% or similar isodose, moves closer to the transition (physical) dose between the two conversion models, resulting in a BED increase inside the target where the physical dose is higher and a BED reduction outside the target where it is lower. This is equivalent to a steeper BED gradient across the two areas.

With the steeper BED gradient, in the displacement scenarios modelled the BED to the BS increases only in a very small region near the target. However,

any shift rapidly results in an under dosage (BED) of the target as compared to a single fraction plan without displacement. The effect of a pure systematic shift, albeit with physical dose, has been modelled in previous work [2]. The mask system allows more movement of the patient head then the fixed frame would. Chung et al 2014 [39] measured the potential displacement in the Icon mask on a Clinac system at up to 3 mm. A Clinac system is not fully comparable with the Icon system. With clinical use on the Icon a reflector is placed on the nose tip and the position is measured using infrared cameras to detect patient movement. A HDMM threshold can be defined, usually 1 mm, at which the treatment is paused. Chung et al found good agreement between the marker as detected by the HDMM system and the CBCT but measured up to 0.5 mm differences in some cases meaning the treatment might only be stopped at a nose displacement of 1.5 mm. Wright et al 2017 [185] evaluated the displacement of the target in relation to the nose tip marker for eleven patients. No patient case showed a target displacement greater than the marker displacement. However, in the phantom study part of their work, 16 of the 161 displacement simulations showed a potential intracranial displacement of the target that exceeded the displacement in the nose tip marker. The most severe case was 1.2 mm more than the marker meaning more than 2 mm target displacement is possible depending on the lesion location, when the HDMM threshold is set at 1mm. These results are highly dependent on the origin of rotation.

In the plans considered for this work the 48 Gy (BED) isodose is always about 0.5mm closer to the target for hypo-fractionated treatments than for the single fraction treatment, meaning that in areas with BED below that value (when the physical dose prescribed is 1x18 Gy to the 50% isodose line) the fractionated treatments have a smaller volume with increased BED than a single fraction treatment. However, it also means that the BED reduction to the target on the opposite side is bigger than that of a single fraction with the same displacement and an underdosage might lead to a recurrence. Adding a margin would increase the volume of the BS with high dose. In previous work [2] the physical dose was shown to change minimally at the 50% isodose level

when displacements are in opposite directions. In this work the same effect can be observed when the dose is calculated in BED. As seen previously, a spread results mainly in a reduction of the BED gradient. Since the HDMM is set to a certain level, usually 1.0 mm, to pause the treatment and since the position of the target may have moved even more than that, repeating the CBCT could quantify the true magnitude and direction of the target movement. The displacement could then be corrected and the treatment re-started.

In this experiment the treatments were simulated to be in one place for the whole treatment meaning the simulation assumed a displaced treatment start. In a clinical treatment all initial displacements are corrected before the treatment starts. For a displacement occurring during treatment it is not clear whether it was displaced immediately after the start or just shortly before the HDMM paused the treatment. As can be seen in the $5F_{\pm X\pm YZ}$ and $3F_{\pm XZ}$ SumPlans displacements of even 2 mm do not significantly increase the total BED as long as the displacement is random and in different directions. When the displacements are in a similar direction, such as in the series of the $3F_{XYZ}$ plans, the BED to the BS at that side increases. Since the profiles suggest an underdosage of the target on the opposite side a margin might be considered. However a margin would further increase the dose to the BS, which would work against the advantage of GK treatment to minimize dose to OAR and normal tissues in the usual no margin approach. It may be possible instead to consider quantifying systematic displacements in earlier fractions to consider corrections in later fractions, but this requires further work and careful evaluation and to be considered within the framework of the specific workflows used.

4.5 Conclusion

Fractionation reduces the BED to the BS by increasing the steepness of the BED dose gradient compared to a single fraction treatment, which in turn will increase the safety margin towards OAR. This is especially the case for doses below 7 Gy. In this simulation the BED of the prescribed dose at the 50% isodose level was kept constant for all fractionation schemes. Positional

uncertainties in fractionated treatments then reduce the BED gradient, but it remains steeper than the BED curve from a single fraction treatment. Random displacements in near opposing directions cancel each other out meaning a single displacement towards the BS does not result in an increased BED_{max} in the BS if another fraction is displaced in the opposite direction.

Chapter 5:
Evaluation of the options for a correction instead of a margin.

The work in this chapter will form the basis of a paper to be submitted for publication.

5.1 Background and Introduction

5.1.1 Fractionated SRS and uncertainties

To treat a solid tumour successfully with stereotactic radiosurgery (SRS) it is important to ensure that all tumour cells receive a minimum dose which depends on the cell type. It is equally important to avoid toxicity of normal tissue, especially to organs at risk (OAR) such as the brainstem (BS). Until recently Gamma Knife treatments have been single fraction treatments, with a fixed used to minimize set up uncertainties. This single fraction is treated with a high dose that limits the treatable targets in size and location (proximity to an OAR) [3]. Hypo-fractionated SRS (hfSRS) can reduce the toxicity of OAR because the biologically effective dose (BED) to the OAR is reduced [152] but fractionation requires a relocatable positioning system that introduces positional uncertainties [36, 195-197]. Positional uncertainties may reduce the dose to the tumour and at the same time increase the dose to the OAR.

5.1.2 Avoiding underdosage of the target

For fractionated treatment a mask system is applied which allows repositioning within a few millimetre. Before the treatment starts a cone beam CT (CBCT) is acquired to evaluate the exact position of the tumour and correct any detected displacement before irradiation is started. However, Chung et al [39] found that the patient and with them the target may move up to 3.6mm inside

the mask between start and end of a single treatment session. To avoid large movements during irradiation GK Icon has a high definition motion management (HDMM) system, which measures the position of a reflector placed on the nose tip to estimate the patient's movement. Although the movement of the nose tip is not necessarily identical with that of the target it may be assumed that in general the target moves less than the reflector. Wright et al [185] evaluated the displacement of the reflector and the target in eleven patients and found in all cases that the target movement was less than the reflector movement. A more systematic evaluation of 16 potential locations evaluated in a phantom showed that a target displacement of up to 1.2 mm larger than the movement of the reflector placed on the nose tip is possible. This means a theoretical target displacement of 2.0 mm is possible at the trigger level of 1.0 mm.

A displacement may result in an underdosage of the target and lead to a recurrence. To avoid underdosage in conventional radiation therapy a margin is applied.

5.1.3 Avoiding overdosage on BS and OAR

Normal tissues that surround tumours in the brain are mostly brain tissue and often very important and sensitive organs like optic nerve, chiasm or BS. Due to the steep dose gradient any displacement would lead to an increase in dose to the OAR. Even worse, due to the steep dose gradient and because the dose is prescribed to the 50% isodose a displacement would not just increase the volume of the OAR receiving the prescribed dose but the dose in the OAR would also be higher than the prescribed dose. Adding a margin to avoid underdosage of the tumour would increase the problem. Margins should therefore be avoided or minimized in GK SRS.

5.1.4 Differences between GK-SRS and conventional fractionated external beam RT

The concept of adding margins to avoid underdosage originates from conventional radiation therapy (RT). For this type of treatment, a low fraction-dose is used for a high number of fractions, the prescribed dose and the maximum dose are similar with the aim of a homogeneous dose distribution and a D(max) of less than or equal to 107% [108] of the prescribed dose. Under these conditions any displacements, random or systematic, lead to a reduction of the volume receiving the prescribed dose. In conventional RT larger movements are observed (patient and organ movement) and in addition to that a degree of cell infiltration into the NT area is assumed. For these reasons it is necessary to irradiate mixed cell tissues consisting of NT and tumour cells. Each cell type has a different dose that will kill the cell. Usually the toxic dose to the tumour is slightly lower than that for a NT cell. Achieving a homogeneous dose distribution in the target volume maximises the therapy effect with best tumour control and low (tolerable) NT damage. This difference in toxic dose for NT cells and tumour cells allows the use of a margin to cover all tumour cells without exceeding toxic dose for NT cells at the same time.

This condition does not exist in brain SRS. The brain as an organ usually does not move like lung or bowel. Tumours treated with SRS are considered to be solid without mixing with normal tissue several millimetres away from the tumour and last but not least, most organs adjacent to a brain tumour are highly sensitive and benefit from a low dose which can be achieved by a steep dose gradient.

With the skull attached G-Frame is screwed directly to the skull bone and then mounted to the GK-treatment couch, accuracy was well below a millimetre and the impact of uncertainty of low concern. Therefore, and because it was a single fraction, there were no investigations made in how displacements affect the total dose. The dose gradient above the prescribed dose and the dose inhomogeneity might behave differently than for conventional RT. Furthermore, with only five or less fractions no statistical averaging is happening. However, re-positioning systems for (hypo-)fractionated treatments introduces greater positional uncertainty.

5.1.5 Alternative method: Correction of displaced treatment.

Investigating the effect of positional uncertainties to the total dose distribution (biologically effective dose (BED)) showed that a random error (two displacements in opposing direction had almost no effect on the volume of the prescribed dose or the target coverage for a displacement of up to 1.5 to 2.0 mm (depending on the plan characteristics [2]). This means, no margin is required to compensate for underdosage due to random error. However, a systematic error (or a shift) would cause an underdosage in the target and an overdosage in the NT or OAR next to the target. A margin certainly would cover the underdosed area but would further increase the volume and the dose to the OAR which has a relatively larger impact due to the small volumes compared to conventional RT. For a small volume of 0.3cm^3 or 1 cm diameter, a margin of 1 mm increases the volume receiving target dose by 73%. Since opposing displacements cancel each other out due to the dose gradient and the prescribed dose to 50% [2] and as seen in chapter four prepared to publish, it might be possible to actively correct a displacement. This chapter tests the hypothesis that displacements from the first three fractions can be corrected in the remaining two fractions.

A displacement should be the exception. Applying a margin and increasing toxicity without justification and need, if there is any safe and proven alternative, is open to debate around radiation protection and ethical issues. In our previous work [1, 2] random error was shown to have little effect on the dose distribution. On close consideration, it turned out that two treatments displaced in opposite directions result in a loss of gradient but almost no change in coverage when prescribed to the 50% isodose. In this work, the feasibility is evaluated of defining a treatment strategy that allows to correct a potential displacement after it has occurred.

5.2 Material and methods

The procedure is a modification from the previous work as presented in chapter 4 and [2]. A single patient was selected with a medium sized tumour (9 mm diameter) embedded in the Brainstem (BS). The original GP plan was used to simulate the fractionated treatment with induced uncertainties simulated and added in-silico using GP, Excell and Matlab. Lesion, location and plan are shown in Figure 5.1.

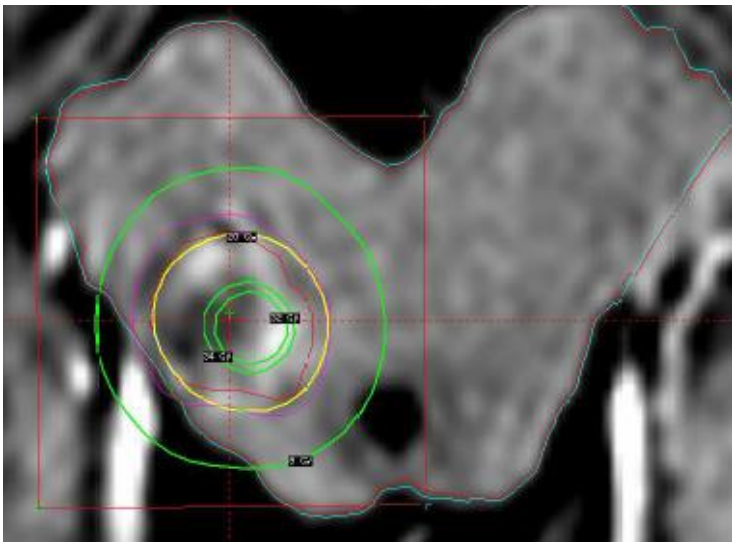

Figure 5.1: *Transversal slice of the BS and the lesion of the target chosen for this study. The lesion is 9 mm in diameter and embedded in the brainstem.*

As treatment, a five-fraction-scheme was chosen where the first three fractions have been assumed to be “treated” and observed only i.e. the displacement was only recorded but “not corrected”. Then the mean displacement of all three treatments was evaluated and a correction in the opposite direction was made for the remaining two fractions. For comparison, the SumPlan of the last two fractions were also calculated without correction and the SumPlan calculated. All doses were processed as BED. The dose of 5.5 Gy (physical dose) was prescribed to the 50% isodose line.

5.2.1 Displacement

The displacement was assumed to be due to a combination of systematic error and random error. As systematic error 0 mm, 0.5 mm, 1.0 mm, 1.5 mm and 2 mm were chosen. All systematic displacements were in the X direction. For each systematic error value, ten treatments of five fractions with weighted random error have been simulated. The weighted random error assumed that no or small deviations are more likely than large ones and used a Gaussian distribution.

For each fraction, the magnitude of the displacement was defined by multiplying the maximum displacement of 2 mm by a value between zero and one received from a random number generator. The direction of the displacement was similarly defined. The simulated directions were +X, -X, +Y, -Y, +Z, and -Z. The range between zero and one was divided into six sections. Each direction was assigned to a section. This value, with the according direction, was then added to the systematic displacement.

For each treatment the total dose of each voxel was calculated as the sum of the BED of all five fractions with, and without correction.

5.2.2 Evaluation

For the evaluation, the total dose (BED) for each treatment series was calculated without correction for all five treatments and with correction where three treatments have been observed and evaluated for displacement and the remaining two treatments have been “displaced” in the opposite direction to correct for the first three treatments’ systematic displacement. For the corrected fractions the calculated error as defined by the random number generator was included in the correction, meaning that theoretically the displacement could be up to 2 mm larger or smaller than calculated.

A profile was drawn through the centre of the target in the lateral direction, the direction with the systematic error hence the most visual effect and in ventro/dorsal direction where random error dominates. In addition, the DVH

for the whole volume as well as the DVH for the target and for the BS was calculated.

Of special interest are the volume underdosed inside the target and the volume outside the target, especially in the BS, with a dose increase.

For this work BED was calculated with parameters for brain cells only. In truth, the tumour cells and brain tissue would have to be calculated independently. In this work this simplification is reasonable as only the principle of a correction approach is explored.

5.3 Results

5.3.1 Profiles

The profiles in the lateral direction (shift direction) are shown in Figure 5.2 (random error only), Figure 5.3 (random error and 1 mm systematic shift) and Figure 5.4 (random error and 2 mm systematic shift). On the top of each pair the five fractions without corrections are shown and on the bottom of each pair the same displacements but corrected for the last two fractions. For the corrected series with the systematic introduced shift of 0.0mm a slightly larger variation in the 10 plans is visible (due to random shift). However, it is barely noticeable. When the shift is 1.0 mm a large part of the target/profile is underdosed. This underdosage disappears completely when the last two fractions are used to correct the first three fractions. Note, 1.0mm is the threshold on which the treatment is interrupted. For a shift of 2.0 mm the correction starts to fail. The steep dose gradient on the left side of the profile cannot be compensated for by the lower dose of the corrected two treatments. However, it was still possible to correct the underdosage on the right side of the profile.

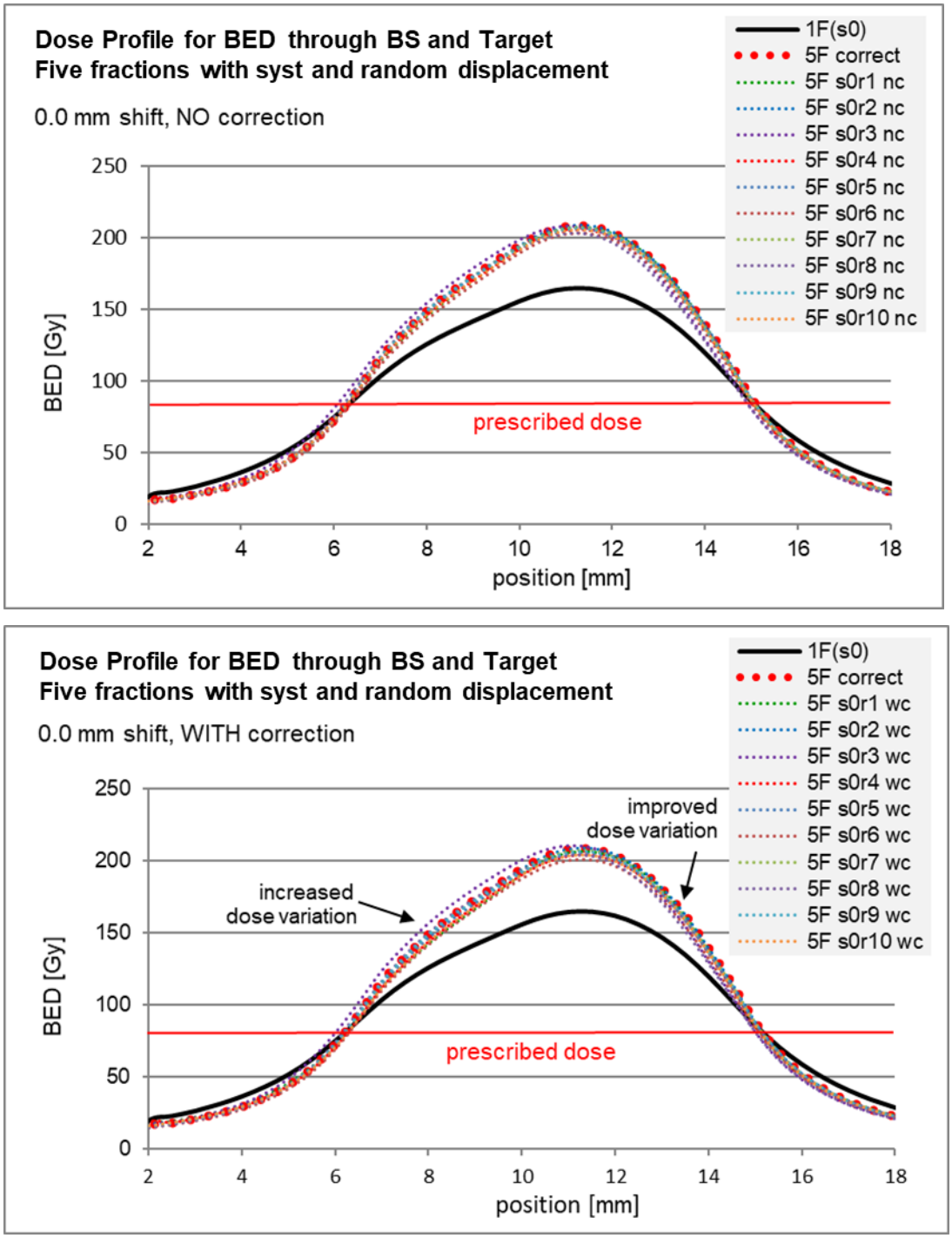

Figure 5.2: *An existing plan for a single fraction (black profile dose in BED) was used to simulate a fractionated treatment with uncertainties. Ten courses with applied uncertainty were simulated and the total dose calculated (dotted profiles). All uncertainties were random in this series.* ***1mm systematic displacement*** *was added.*

Top image: *all fractions have been applied with the displacement as calculated from the random generator. The introduced uncertainties result in small deviations from the ideal, calculated distribution.*

Bottom image. *Here the first three fractions have been analysed for the mean displacement, and this evaluated displacement was "corrected" in the last two fractions. This "correction" resulted in an increased dose variation among the fractionated courses.*

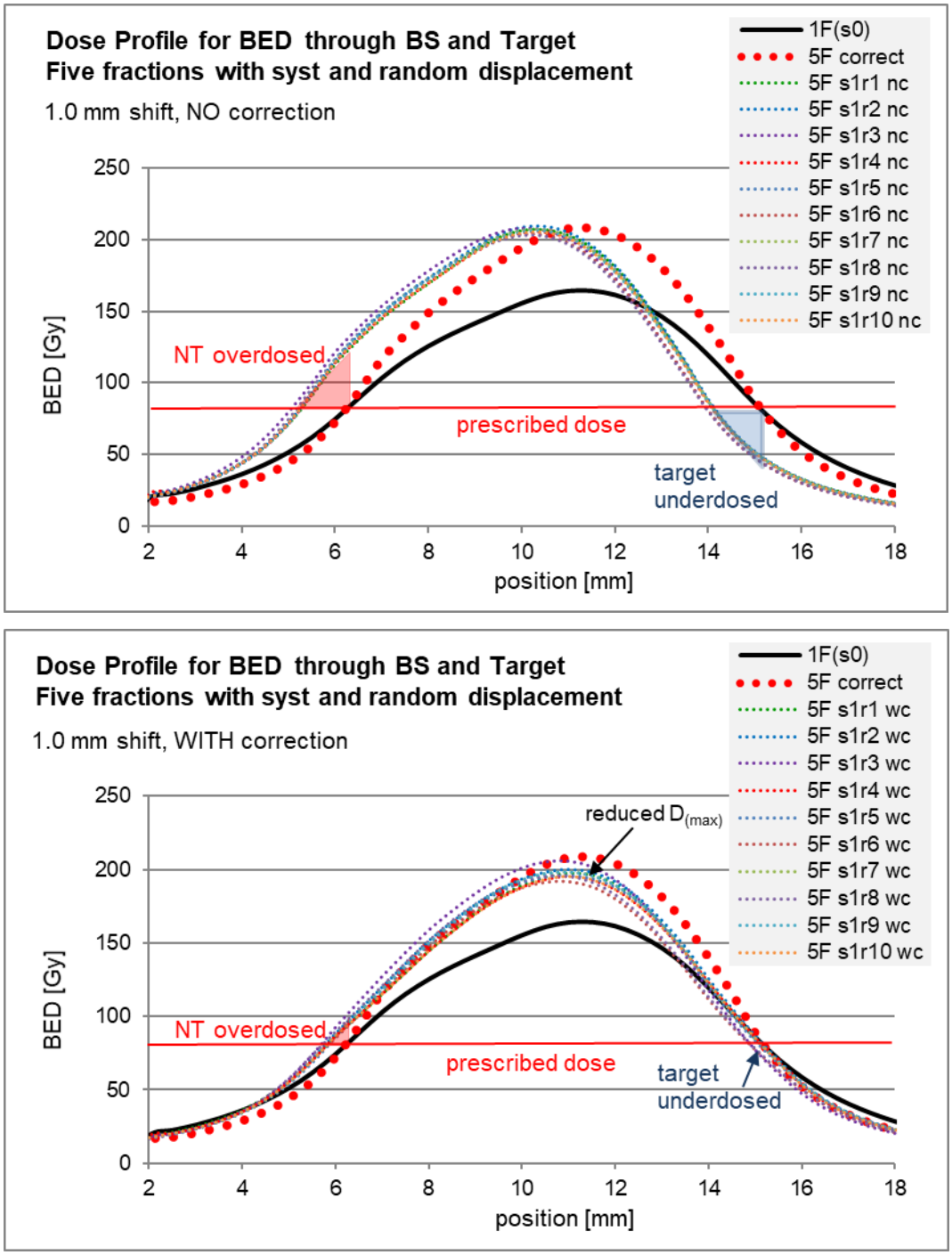

Figure 5.3: *An existing plan for a single fraction (black profile dose in BED) was used to simulate a fractionated treatment with uncertainties. Ten courses with applied uncertainty were simulated and the total dose calculated (dotted profiles). All uncertainties were random in this series.* ***1mm systematic displacement*** *was added to each fraction.*

Top image: *all fractions have been applied with the displacement as calculated from the random generator. The profile shows a clear under dosage of the target on the right side of the profile (blue triangle) and an increase in dose in BS on the left side (red triangle).*

Bottom image. *Here the first three fractions have been analysed for the mean displacement, and this evaluated displacement was "corrected" in the last two fractions. This correction increased the dose to the target (right side) and reduced the dose to the BS to near planned dose.*

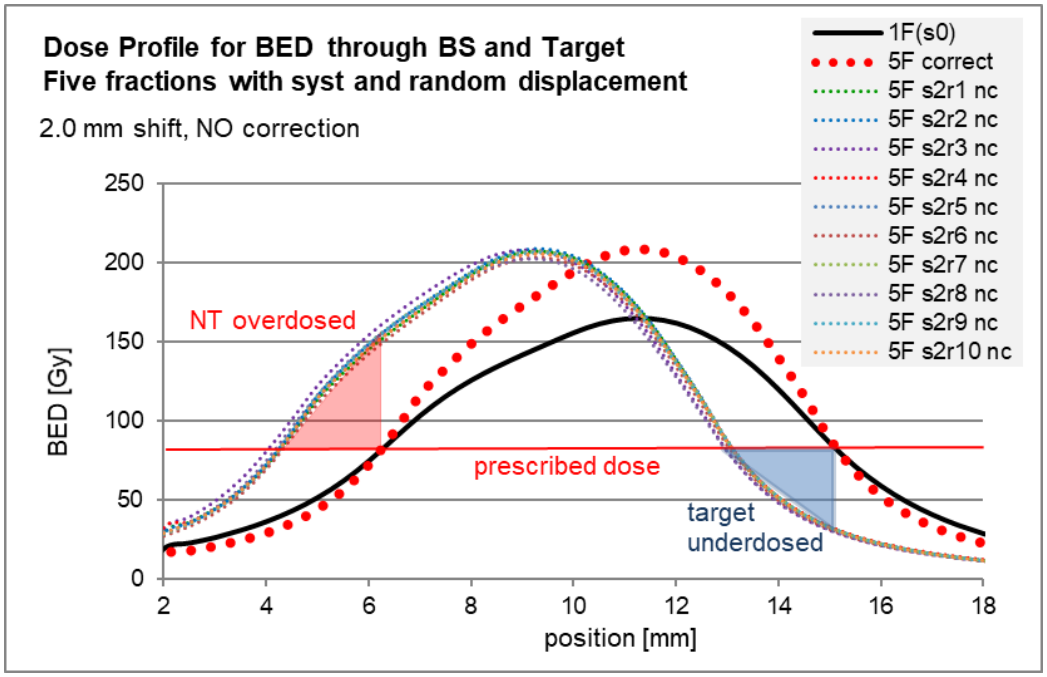

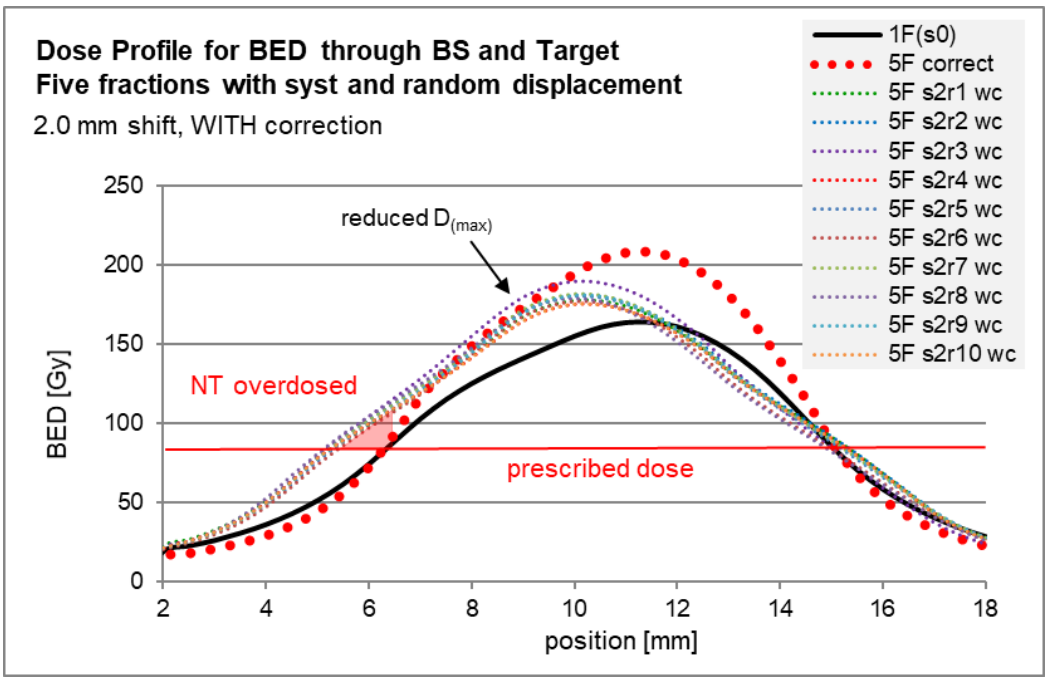

Figure 5.4: *An existing plan for a single fraction (black profile dose in BED) was used to simulate a fractionated treatment with uncertainties. Ten courses with applied uncertainty were simulated and the total dose calculated (dotted profiles). All uncertainties were random in this series.* ***2mm systematic displacement*** *was added to each fraction.*

Top image: *all fractions have been applied with the displacement as calculated from the random generator. The profile shows a clear under dosage of the target on the right side of the profile (blue triangle) and an increase in dose in the BS on the left side (red triangle).*

Bottom image. *Here the first three fractions have been analysed for the mean displacement, and this evaluated displacement was "corrected" in the last two fractions. In this case, the under dosage of the target was corrected, and increased dose to the BS was reduced. The dose profile has significantly widened because the displacement exceeds the shot gradient. It is still a significant improvement.*

5.3.2 Dose Volume Histogram of the Target

The DVH of the dose to the target is shown in Figure 5.5 with random error only, in Figure 5.6 with 1 mm systematic shift and random error and in Figure 5.7 with 2 mm systematic shift in addition to the random error. The top curve for each is without correction while the bottom curve is with correction.

In Figure 5.5 the increase of BED due to fractionation is visible (top curve, red area between the single fraction curve and the fractionated curves). Introducing a correction (bottom curves) increases the variation of the dose distributions for the ten simulated plans. The dose range is slightly increased between courses, and in one series a small reduction in coverage is visible.

When a systematic displacement is introduced, 1 mm in Figure 5.6 and 2 mm in Figure 5.7, then 15% and 30% of the target respectively of it is underdosed. When the last two fractions are used to correct the displacement of the first three fractions the underdosing almost disappears. The 2 mm shift is too large to be fully compensated. The displacement goes beyond the dose gradient. However, the underdosed volume is still significantly reduced. This is at the expense of the high dose area inside the target which is slightly reduced (but still above the BED of a single fraction).

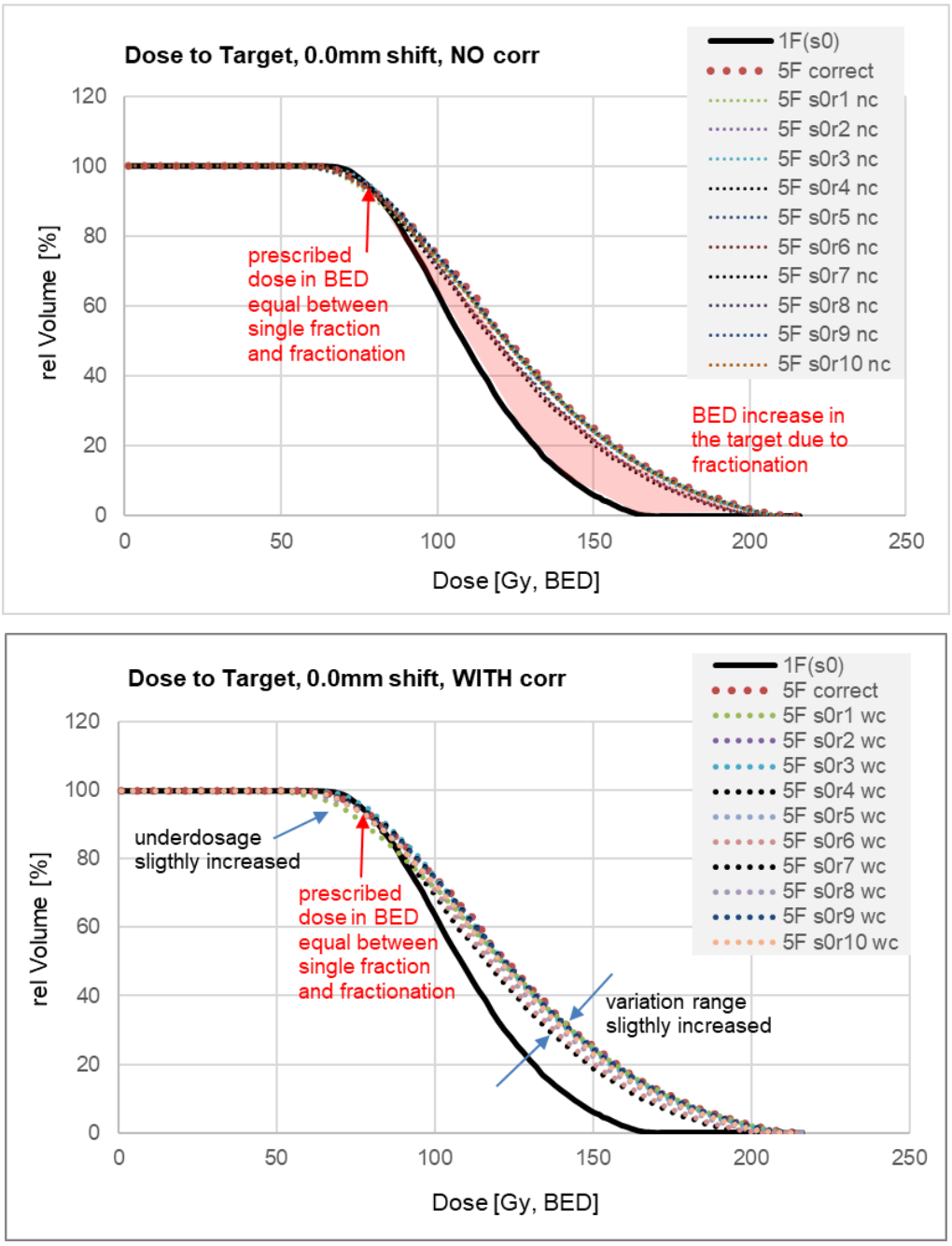

Figure 5.5: *An existing plan for a single fraction (black DVH in BED) was used to simulate a fractionated treatment with uncertainties. Ten courses with applied uncertainty were simulated and the total dose calculated (dotted DVH). All uncertainties were random in this series.* ***0mm systematic displacement*** *was added to each fraction.*

Top image: *all fractions have been applied with the displacement as calculated from the random generator. The DVH shows small variations in the total dose. The red area visualizes the gain in BED due to fractionation.*

Bottom image. *Here the first three fractions have been analysed for the mean displacement, and this evaluated displacement was "corrected" in the last two fractions. Because there was no systematic component in the displacement the total dose of the different simulations are more than without correction. The BED gained inside the target is reduced and some parts of the target are slightly underdosed.*

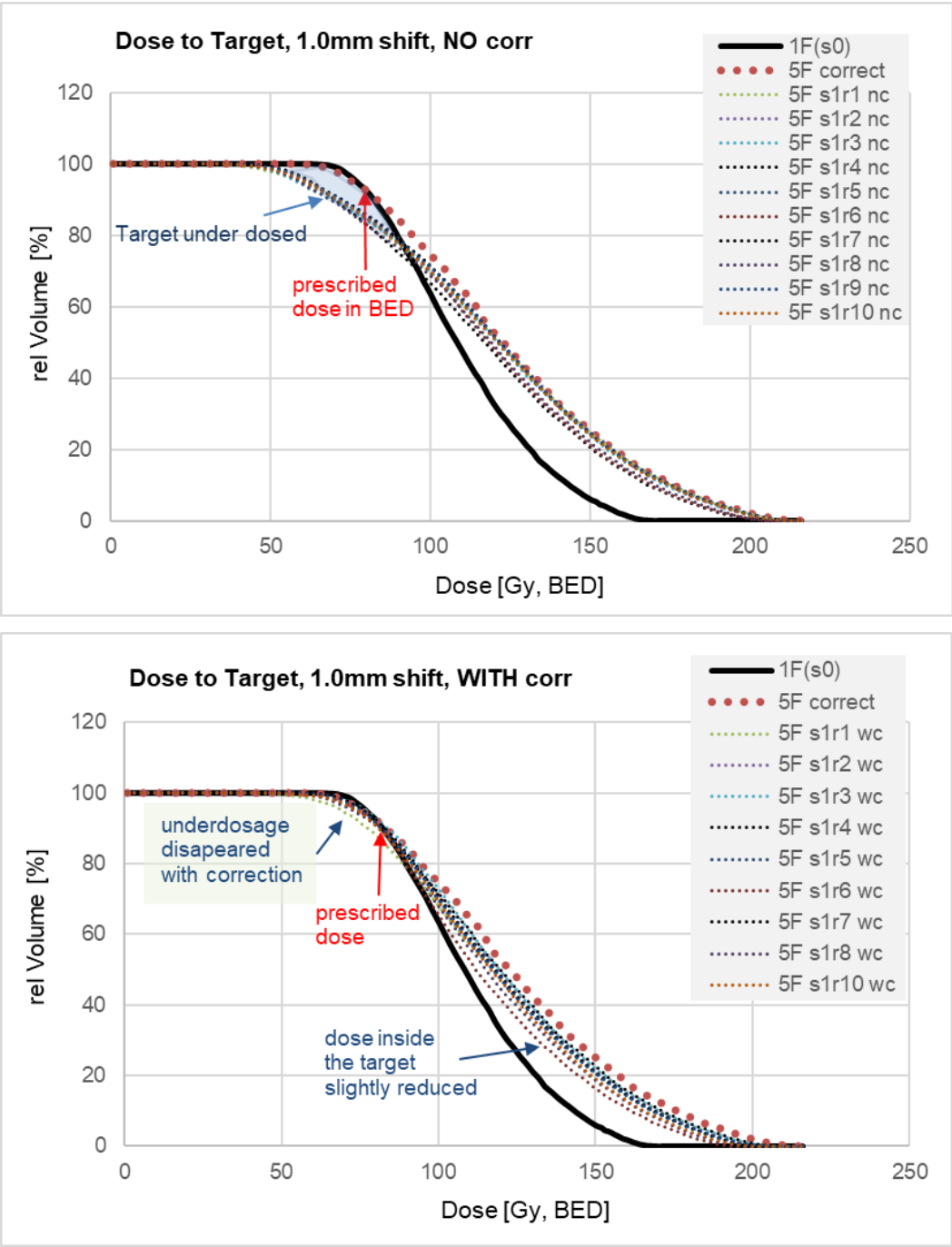

Figure 5.6: *An existing plan for a single fraction (black DVH in BED) was used to simulate a fractionated treatment with uncertainties. Ten courses with applied uncertainty were simulated and the total dose calculated (dotted DVH). All uncertainties were random in this series.* ***1mm systematic displacement*** *was added to each fraction.*

Top image: *all fractions have been applied with the displacement as calculated from the random generator. The DVH shows small variations in the total dose. With 1 mm systematic displacement, the target is underdosed in some areas (blue area).*

Bottom image. *Here the first three fractions have been analysed for the mean displacement, and this evaluated displacement was "corrected" in the last two fractions. The under dosage in the target is almost completely corrected at the cost of a slight reduction of the BED inside the target.*

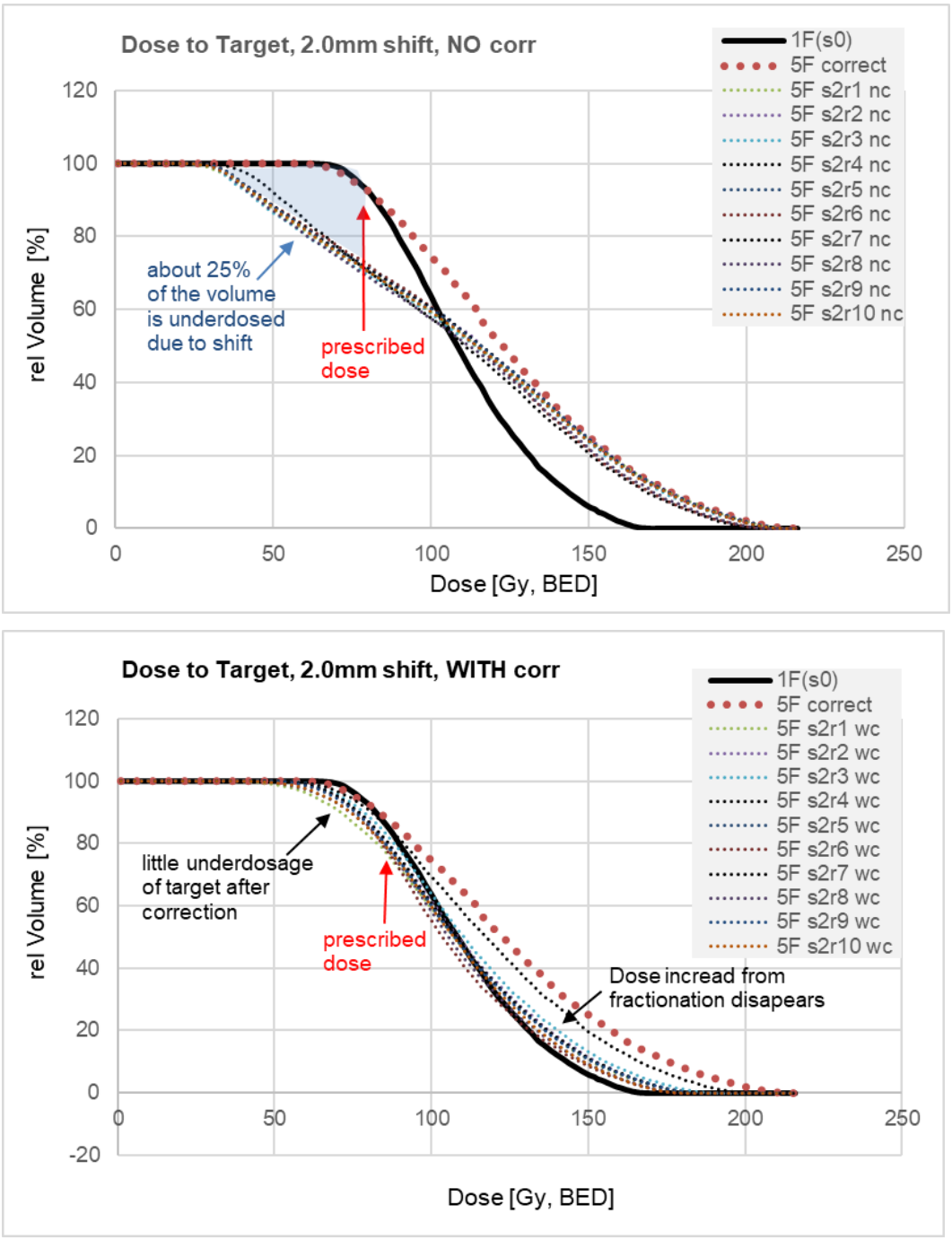

Figure 5.7: *An existing plan for a single fraction (black DVH in BED) was used to simulate a fractionated treatment with uncertainties. Ten courses with applied uncertainty were simulated and the total dose calculated (dotted DVH). All uncertainties were random in this series.* ***2mm systematic displacement*** *was added to each fraction.*

Top image: *all fractions have been applied with the displacement as calculated from the random generator. The DVH shows that about 30% of the target is underdosed (blue area). The little "bump" in the DVH at 50% is a sign that the displacement is larger than the penumbra width.*

Bottom image. *Here the first three fractions have been analysed for the mean displacement, and this evaluated displacement was "corrected" in the last two fractions. Most of the under dosage is eliminated. The dose gain due to fractionation is almost completely lost. BED is still equal to that of a single fraction.*

5.3.3 Dose Volume Histogram of the brainstem

Figure 5.8 to Figure 5.10 show the difference between no correction (top of the pair) and with correction for the last two fractions (bottom of the pair). Figure 5.8 is calculated with random error only. No systematic error was introduced. In this situation, the correction did not introduce an increase in BS dose. Figure 5.9 shows the same configuration, but with 1 mm systematic error added to the random error. In the top image without correction, an increase in dose to the BS can be seen. This increased dose is reduced with correction. Figure 5.10 with 2 mm systematic simulated error shows this effect and the potential of the correction very clearly. **Error! Reference source not found.** Note, for SRS the limit for the BS is often 12 Gy to not more than 10 mm^3. This is is only a tiny part of the total BS volume. Compensating a displacement reduced the dose to the BS almost to the planned value.

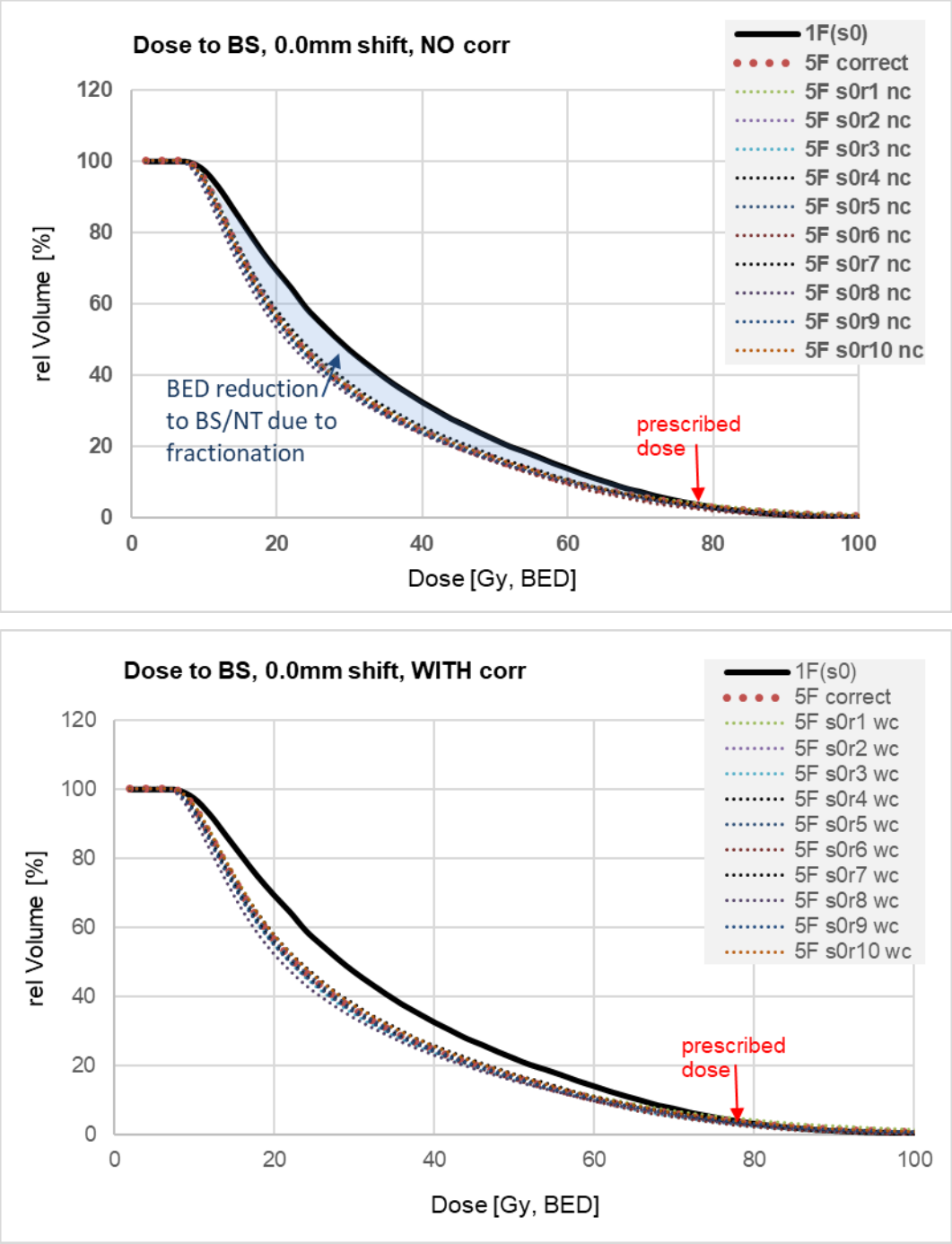

Figure 5.8: *An existing plan for a single fraction (black DVH in BED) was used to simulate a fractionated treatment with uncertainties. Ten courses with applied uncertainty were simulated and the total dose calculated (dotted DVH). All uncertainties were random in this series.* ***0mm systematic displacement*** *was added to each fraction.*

Top image: *all fractions have been applied with the displacement as calculated from the random generator. The DVH shows small variations in the total dose. The blue area visualizes the reduction in BED to the BS due to fractionation.*

Bottom image. *Here the first three fractions have been analysed for the mean displacement, and this evaluated displacement was "corrected" in the last two fractions. Almost no change is visible in the DVH of the BS.*

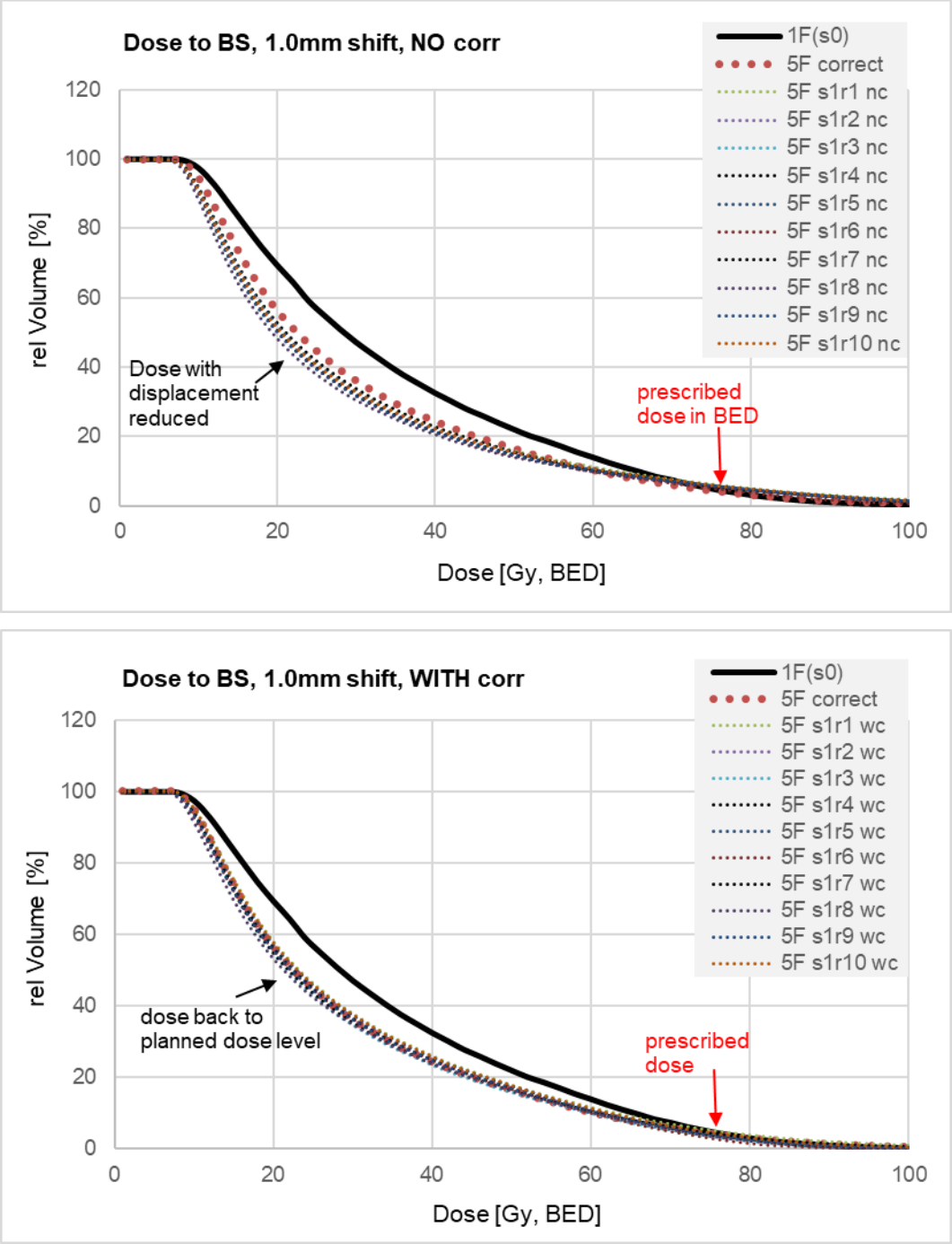

Figure 5.9: *An existing plan for a single fraction (black DVH in BED) was used to simulate a fractionated treatment with uncertainties. Ten courses with applied uncertainty were simulated and the total dose calculated (dotted DVH). All uncertainties were random in this series.* ***1mm systematic displacement*** *was added to each fraction.*

Top image: *all fractions have been applied with the displacement as calculated from the random generator. The DVH shows a further reduction in the low dose region of the BS. However, in the high dose region a dose increase is visible (due to the small target compared to the total BS volume this is difficult to spot).*

Bottom image. *Here the first three fractions have been analysed for the mean displacement, and this evaluated displacement was "corrected" in the last two fractions. The 1 mm, systematic displacement in the first three fractions, was almost completely corrected with the*

last two fractions.

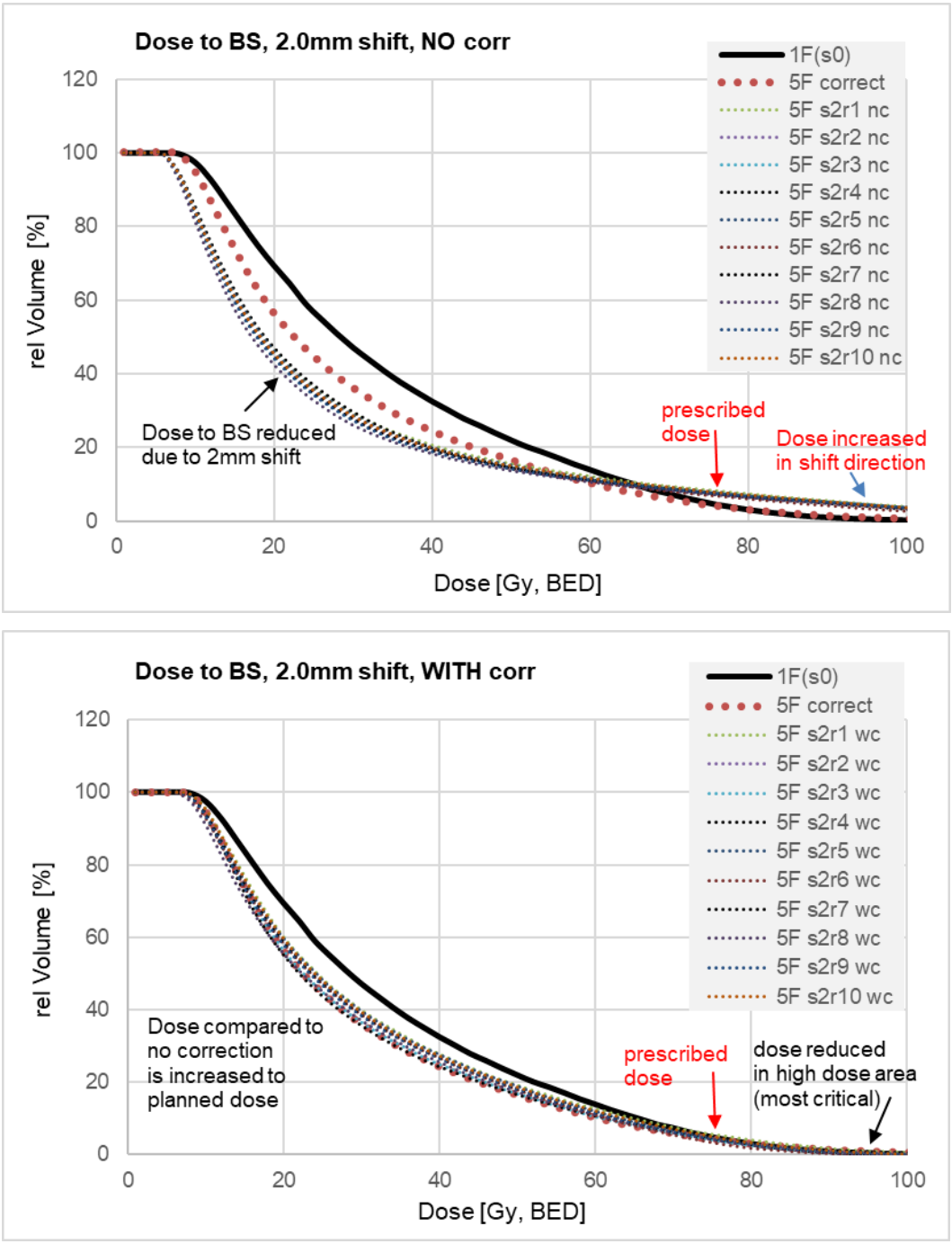

Figure 5.10: *An existing plan for a single fraction (black DVH in BED) was used to simulate a fractionated treatment with uncertainties. Ten courses with applied uncertainty were simulated and the total dose calculated (dotted DVH). All uncertainties were random in this series.* ***2mm systematic displacement*** *was added to each fraction.*

Top image: *all fractions have been applied with the displacement as calculated from the random generator. The DVH shows a further reduction in the low dose region of the BS. With a systematic displacement of 2 mm the dose increase in the BS is clearly visible in the DVH.*

Bottom image. *Here the first three fractions have been analysed for the mean displacement, and this evaluated displacement was "corrected" in the last two fractions. The 2 mm, systematic*

displacement in the first three fractions, was almost completely corrected with the last two fractions.

5.4 Discussion

SRS is a high precision treatment. With a region as delicate as the brain dose to NT (brain, BS, optic nerve, chiasm …) should be kept as low as possible.

In usual practice no margin is used with GK Icon. Instead a CBCT scan is performed pre-treatment and a continuous surveillance of the patient with the reflector on the nose tip as part of the HDMM is used. Generally, the treatment is interrupted at a displacement of the reflector of 1mm. This means that the treatment will have started correctly but has “moved” out of the treatment limits. The impact of such a displacement is different than the one simulated in this work. However, from previous work and this work it is known that displacements in random/opposite direction have a minimal influence on the total dose distribution. Therefore, if the treatment is interrupted and the target appears to move randomly no correction is required. However, if the displacement is each time in the same direction action might be considered since even a small displacement of 1.0mm may make a significant impact as the profiles and DVHs show.

Real displacements cannot be directly compared to the simulated displacements in this work. Every treatment is started with no error after the CBCT. When the treatment is interrupted some movement must have happened between the beginning of the treatment and the interruption at 1 mm displacement of the nose tip. In this case it might be possible to link the reflector movement to the target movement. This should be done for each patient individually because each patient behaves differently, and the target location is at a different place in relation to the reflector. This would be challenging.

An alternative could be to add a margin. However, when calculating the required margin the compensation effect should be considered. A margin should be chosen to be smaller than the expected displacement.

A third method might be a margin for the last two sessions. This method is a mix of margin and compensation technique. The first three treatments are observed. If there is no problem no margin is added. All OAR and NT are optimally protected. However, if, in a very rare case the patient moves in the same direction for each treatment fraction the underdosed part of the target might be corrected by adding a margin around the whole target. This way the target is adequately treated, but the NT receives an increased dose. However, this increase in dose is only received when needed and not prophylactically for all patients.

The method to correct a displaced treatment works because the dose distribution inside the target is inhomogeneous and much higher than the prescribed dose. The potential range of correction depends on the steepness of the dose gradient. With greater steepness (small lesions) a smaller displacement can be corrected. It also depends on the difference between prescribed dose and dose inside the target reducing the potential correction range with higher prescribed isodose level. In this work the dose is prescribed to the 50% isodose which resulted in almost 2mm correction range. If the dose would be prescribed to 70% the correction range would be reduced [2].

5.5 Conclusion

It is possible in principle to correct a displacement of the first three treatments in the last two treatments with minimal risk (remaining random error, lack of options to distinguish between systematic and random error). However, since treatments begin with no displacement the challenge is to find a way to correct a dynamic change during treatment. Further investigations to link the reflector position with the target may lead to a novel technique to handle positional uncertainties. Meanwhile the findings can be used to define a reduced margin. Patients who move randomly do not need a margin for the PTV to ensure coverage.

Chapter 6:
Summary and future work

The work presented in this thesis was motivated by the development and availability of a new version of Gamma Knife (GK) that, in addition to the traditional single fraction stereotactic radiosurgery (SRS) allows for fractionated treatment, the Gamma Knife Perfexion with the eXtend relocatable patient positioning system. The option of fractionating GK SRS was introduced to increase the range of brain lesions treatable, by reducing the biologically effective dose (BED) outside the target, since the dose level there can be in the range of the LQ model, while the dose to the target is still in the multi target model applicable region. In this thesis three questions were asked. A fourth question then arose from the results of the work done.

1. What is the positional accuracy of the system?
2. What is the effect of positional displacement on dose to the target?
3. What is the dose to an organ at risk (OAR) when positional displacement occurs?
4. Based on the results from answering questions two and three: Can a correction strategy be developed in order to reduce dose to normal tissue (NT) and OAR?

6.1 What is the accuracy of the system?

When this work was started the eXtend system was only recently in use. It used a dental mould to position the patient's head and a vacuum surveillance system to monitor potential significant patient positional changes. However, it had the disadvantage that there was no direct method to verify the actual positional uncertainty other than with the relocation check tool (RCT) prior to treatment. A displacement even as low as one millimetre may have a significant impact on a small target hence it was important to quantify the displacement in order to develop a strategy to cope with it.

This work (Chapter 2) showed that the trigger level pauses the treatment at small displacements of about 0.5 mm. However, the main problem is due to

possible rotation which might scale up the displacement for the tumour depending on its position to potentially 2.0 mm. This work was published in the Journal of Radiosurgery & SBRT in 2016 as a full paper [1].

For the further work, this value of up to 2 mm was taken as the potential displacement that should be considered to have to be dealt with, even if on rare occasions.

Elekta later introduced a new system, the Icon, during the course of this research. The dental mould has been replaced by a mask system and the vacuum surveillance is replaced by a nose tip reflector. In addition an integral cone beam CT (CBCT) imager can measure the exact displacement of the target. Other groups have investigated this and found that the likely displacement is small, but 2 mm and even more are possible. Thus, the 2 mm used for the following work is still valid and relevant.

The work in Chapter 2 quantifies the potential uncertainties and begins to consider their dosimetric impact and so provides data to support and evaluate clinical practice and decisions for fractionated GK treatments.

6.2 What effect does a displacement have on dose distribution for the target?

The next step (Chapter 2) was to evaluate the wider dosimetric effect of a displacement; sub questions have been the impact for three fraction and for five fraction treatments. Would a lower number of fractions be better because there are fewer occasions where a displacement could occur? Or would a higher number of fractions be better to average out any random uncertainties? In addition, what is the impact of a systematic error (each fraction in the same or similar direction) compared to a random error (for each displacement being in different directions, including in near opposite directions)?

As expected a systematic displacement for all fractions has a similar effect as a displacement in a single fraction. The dose distribution is simply shifted.

However, the result for the “random” displacement was unexpected. In fractionated conventional external beam conformal therapy, with a homogeneous dose distribution inside the target, a random displacement results in an underdosage of the target. Hence, a margin around the target prevents the target from being underdosed. This is not the case for GK plans. Due to the dose inhomogeneity where the dose inside the target is up to twice as high as the prescribed dose (when typically prescribing to about the 50% isodose) an underdosage due to displacement in one direction is almost perfectly compensated by a displacement in the near opposite direction. This means a higher fraction number is more favourable because random displacements are more likely to compensate each other in this way. This work was published as a full paper in 2017 in the Journal of Radiosurgery & SRBT [2].

6.3 What effects do displacements have on OAR?

Fractionated SRS changes not only the dose (BED) to the target but also the dose to the OAR. This is evaluated in Chapter 4. Due to the lower fraction dose, as compared to single fraction SRS, the BED to the OAR is reduced and the OAR better protected. Displacement towards the OAR results in an increased dose. Unlike in conventional linac-based multi-fraction conformal RT, this dose increase is not limited by the prescribed dose. With conventional conformal RT the dose maximum is close to the prescribed dose and the dose distribution over the target volume is relatively homogeneous and thus small displacements still limit the dose to the OAR to about the prescribed dose even if a displacement moved the OAR completely into the high dose region. In GK SRS the dose inside the target is twice as high as the prescribed dose (since prescribed dose is commonly close to 50%) thus if a displacement is towards the OAR, the dose can increase relatively rapidly to the OAR in a potentially harmful way. This effect is increased by the greater damage from higher fraction doses due to the multi target effect.

For a random displacement the BED in the OAR increased slightly but never reached the BED dose in the OAR from a single fraction SRS. A systematic displacement results either in an underdosage or an over dosage depending on the direction. This work is being submitted for publication.

The work in Chapters 3 and 4 together suggested a possible novel approach to handling systematic displacements that was proposed and (in silico) feasibility tested in Chapter 5.

6.4 A proposal and theoretical testing of a correction strategy for systematic displacements

An under dosage to the tumour, e.g. from a systematic displacement, may lead to a recurrence. In conventional RT this is taken into account by adding a margin. As shown in the OAR section, a margin in GK SRS would increase the dose to the OAR beyond the therapeutic window. A margin would do similar damage in all directions as a displacement in one direction does. So a margin could prevent an underdosage but could produce significant damage and therefore destroy the advantage of SRS which is a precise treatment where the prescribed dose matches the tumour outline with the best possible precision.

In the evaluation of the effects of displacement for target and OAR displacements in opposite directions were shown largely to cancel each other out for GK SRS. Minimal changes occur in the reduced doses inside the target and in the increased doses to the NT around the target due to the reduction of the steepness of the dose at the target border. The prescribed dose itself remains constant. If this finding can be used as the basis of correcting a systematic displacement no margin would be required and no compromise in precision would be needed.

In this first evaluation of the feasibility of a correction approach (Chapter 5), the task was simplified by assuming the treatment would be delivered without patient movement during the treatment. In reality the treatment starts without any displacement (other than imaging uncertainty) but during treatment the

patient moves. With tracking technologies movements of a few millimetres can be corrected as soon as they are identified.

To do this though, requires estimating the magnitude of any systematic displacement and in addition considering how subsequent random uncertainties might affect a correction. Unfortunately the direction and magnitude of any random displacement cannot be predicted by definition. If it is in the same direction as the correction movement it might worsen the situation. If it is in the opposite direction it might cancel out the correction.

Testing the proposed correction strategy with a series of simulated displacements showed that a correction is feasible and improved the overall dose to the tumour with minimal influence of the dose to the OAR and NT. However the test setup assumed that the displacement was present during the whole fractionation and did not change during the treatment. The real situation is more complex. With the Icon a CBCT is made prior to the treatment. Any displacement is a result of a motion of the patient during treatment. In the simulation the whole dose distribution was displaced. In a treatment the different shots would be displaced and each shot slightly differently to the others. In reality, the treated dose distribution does not match the planned one. A simple correction of a displacement that occurs in the middle of the treatment is therefore overcorrecting the displacement. However, this strategy is a completely novel suggestion that may allow the possibility to treat without margins, even for potential displacements of up to 2 mm. This work is being submitted for publication to demonstrate the principle and feasibility, whilst recognising that this needs further development and testing before any clinical use.

6.5 What can be applied in clinical practice from this work?

From the measurements of the trigger level of eXtend [1] and from the work of other groups [39, 99, 185] it is known that the potential displacement is small but may reach up to 2 mm. With Icon, a CBCT measures the rotation and displacement of the patient/tumour and corrects it before the treatment starts.

When the reflector on the nose tip moves more than a millimetre (level may be set differently) the treatment stops and a CBCT can evaluate the exact displacement of the target. An active correction as described in chapter 5 is not yet clinically applicable. More research is needed on how best to apply this approach in clinical practice where, after the initial correction before treatment starts, any displacement only applies to a part of the treatment. However, the knowledge of the effects of displacements from the simulated situations for targets (Chapter 3) and OAR (Chapter 4) can be used to judge the impact of the displacement and help with clinical evaluation and decisions. Some patients move frequently. The results of this project can indicate patients for whom this might be a problem and those for whom it is no problem. If this movement is in a different direction each time then the dosimetric consequences are small. With a CBCT the patients with systematic displacement can be identified and a possible correction in the form of a margin can be considered, or a correction strategy, once further developed and tested for clinical applicability and safety, might be used. When the CBCT finds displacement in different directions no action is required.

6.6 Future work

This work is the first of its kind. The assumptions/simplifications are relatively basic and can be further refined and the range of situations tested can be extended. With eXtend it is possible that the displacement is present right from the beginning of the treatment. If the trigger level is activated, the displacement to be dealt with would be a combination of static/systematic (from the beginning of each fraction and in the same direction) and dynamic (arising during treatment in various directions) displacement/movement. Even this scenario is not identical in clinical practice with the assumptions applied in the simulation .

Today the Icon system is becoming more widely used. Treatment with the Icon starts without any displacement (except uncertainty of the imaging system). However, with a mask system small movements, i.e. dynamic positional displacements, in the order of millimetres are possible during

irradiation. The impact of movement on dose distribution for a system that delivers the dose shot by shot is not yet investigated. One problem is that so far not even characteristics of the possible types of movement are investigated. There might be sudden step-wise movements or smooth, continuous drift movements, or combinations.

The evaluation in this work considered static displacements and led to a proposal of a correction after part of the treatment. Ideally a displacement should be measured immediately and corrected before it has an impact. A CBCT can only be made when the irradiation is stopped. However, the reflector on the nose tip is monitored continuously. Because the position of the target varies from patient to patient and the reflector cannot distinguish between a rotation and a shift it is not possible to correlate the reflector movement to the tumour movement. However, it might be that for each patient (or at least most) having a five-fraction treatment, a correlation could be established after the first three treatments (using the CBCT after each treatment pause). If such a correlation could be established a correction movement might be developed for the remaining two fractions. If this could be realised a near perfect treatment, across all five fractions taken together, could be achievable.

It frequently happens that patients move out of the tolerance zone during irradiation. A possible practical application for at least 5 fraction treatments would be to observe the first three fractions and evaluate in which direction the patient moves. If each time there is a different direction, there is no need for action according to the results from chapters three and four. If the movement is always in the same direction, the result may be an underdose of the target volume. A simplified “correction” strategy could be evaluated. Instead of a margin for the whole treatment the first three fractions could be observed and if a displacement occurs a margin of the according size could be applied for the remaining two fractions. The aim would be to evaluate if this would have the same effect for the underdosed area as a correction and also the effect of a margin for the opposite area. So a strategy could be developed that is only applied if the patient moves always in the same direction. Patients who do not

move or move in different directions do not need correction. In a next step, the effect on dose distribution due to movement (dynamic) could be evaluated (marker tracking) and a possible dynamic correction movement could be calculated for the last two sessions. This would be possible if the marker can be correlated with the patient's movement. Such a correlation would be different for each patient because each patient has their own movement pattern.

6.7 Some comments on the future for radiation therapy and for technology advances

Radiation therapy is almost 125 years old. After the groundbreaking discovery of x-rays, there was a continuous development to improve techniques by the invention and technical and clinical development of linear accelerators, MLC, IMRT, VMAT, SBRT, etc. Greater understanding of the biology behind the therapy led to safer applications and novel fractionations and combinations with other modalities. Personalised medicine is attempting greater precision per individual patient.

Significant research is currently being carried out in novel areas with potential for further combination with the 'traditional' treatment modalities, for example in immunotherapy and in gene therapy. The results are promising but cannot yet be widely applied to larger groups of patients. Such therapies add to the approach to individually adjust treatment for a specific patient. In the past, it has been shown that a therapy that alleviates some symptoms is not necessarily better in terms of survival than no treatment. Long-term results and results from large studies are still missing for immunotherapy and gene therapy, including still for safe application which needs still further research. Even if those issues are solved, it is likely that new types of therapy will be used as an integral part of wider combined treatment methods, along with other treatments rather than replacing all previous therapies.

Radiotherapy technology continues to advance, e.g. via automation, image guidance moving to MRI-guidance (MR-linacs), adaptive therapy, motion management systems, etc. Linac radiotherapy has significantly improved, and with onboard imaging, it can reach submillimeter accuracy similar to the Gamma-Knife. Is it likely that the Gamma Knife will be replaced by linac technology? In general, probably not by conventionally designed linacs. Even though these can treat arcs, they still do not provide the steep dose gradient achieved by the GK, especially for small lesions. The dose distribution from a linac is more homogenous than that of a GK and whilst a homogenous dose distribution is vital for a mixed cell volume, it is not for a solid tumour containing only targeted cancer cells. Other advantages of the GK over a linac include

the compact design and built-in radiation protection, meaning that only a small room with little extra room shielding is required. This makes GK a relatively simple, high precision treatment unit dedicated to brain lesions.

Recently Mackie (the inventor of the Tomotherapy system, see Chapter 1) and Adler (the inventor of the Cyberknife system, see Chapter 1) together have developed a new treatment device called ZAP-X. It consists of a Linac tube mounted on a gyroscope. The gyroscope looks like a helmet similar to the GK system (Figure 6.1). The patient is moved on a couch into the gyroscope system similar to the GK set up. Unlike GK, the patient area is shielded too, so no external shielding is required at all. This system has some similar characteristics to GK, plus it has the advantage that it contains no radioactive sources. Handling, managing and changing these in the GK is expensive and an additional risk factor. The ZAP-X treated its first patient in Dec 2018. It could prove to be a close competitor to the GK and especially as it arises from developers, in Mackie and Adler, who have successfully designed and marketed other novel radiotherapy devices. Commercial competition, timing and market and clinical acceptability can determine the success or failure of novel designs. For example, the Mitsubishi Vero (reference), a gimbaled-head system with significant treatment degrees of freedom for dynamic adaptive treatment was viewed as technologically revolutionary, but was discontinued for commercial reasons after only 25 systems were installed. The evolution, acceptability and success of such systems can only be judged after some time.

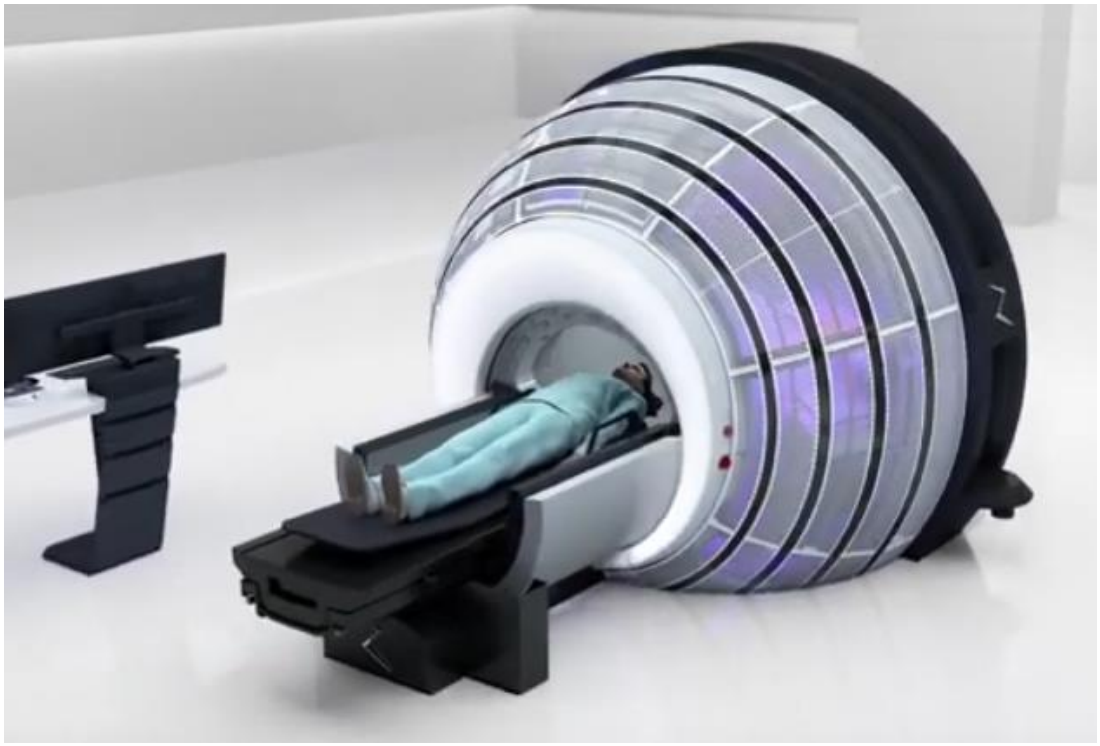

Figure 6.1: *The new Zap-X unit developed by Mackie (inventor of the tomotherapy) and Adler (inventor of the Cyberknife). The system has similar characteristics to the GK but with a linear accelerator tube mounted on a gyroscopic mechanism instead of distributed radioactive sources. It contains built in imaging. The shielding requirements are almost nil because the patient is shielded while treated. A video is available with the folloing link: https://zapsurgical.com/*

6.8 Concluding remarks

Finally, in overall summary, the work presented here has considered the relatively recently introduced Gamma Knife systems designed to enable routine fractionated radiosurgery. It has evaluated likely positional uncertainties and simulated the dosimetric impacts of these for targets and organs at risk for GK hypofractionated treatments of small lesions in the brain, where treatment is typically limited by doses and effects on critical normal tissues such as brainstem. Simulated dose distributions were systematically studied for target lesions and nearby organs at risk in realistic clinical situations across a range of potentially likely systematic and random displacement scenarios. The findings provide novel information that can inform and optimise clinical strategies and decisions for the application of fractionated GK treatments for brain lesions and lead to suggestions of future work to develop this further and for its clinical application. In addition to evaluating and characterising the effects, when the dose is prescribed to the 50% isodose, as is often the case for GK treatments, a novel way to deal with positional uncertainties has been proposed for fractionated treatments of at least 5 fractions. This novel correction strategy was feasibility tested showing it could reduce the toxicity of NT and OAR adjacent to the tumour and has potential to be further developed and clinically tested to deal with uncertainties without using margins. The complete work forms the basis of a systematic approach to considering positional uncertainties in fractionated GK use and presents ways in which it can be extended and taken forward, enabling support of wider clinical use of these treatment approaches.

Reference

1. Reiner, B., et al., *Quantifying the trigger level of the vacuum surveillance system of the Gamma-Knife eXtend™ positioning system and evaluating the potential impact on dose delivery.* Journal of Radiosurgery & SBRT, 2016. **4**(1): p. 31-42.
2. Reiner, B., et al., *Quantifying the effects of positional uncertainties and estimating margins for Gamma-Knife® fractionated radiosurgery of large brain metastases.* Journal of Radiosurgery & SBRT 2017. **4**(4): p. 275-287.
3. Lippitz, B., et al., *Stereotactic radiosurgery in the treatment of brain metastases: The current evidence.* Cancer Treatment Reviews, 2013. **40**(1): p. 48-59.
4. Andrews, D.W., et al., *Whole brain radiation therapy with or without stereotactic radiosurgery boost for patients with one to three brain metastases: phase III results of the RTOG 9508 randomised trial.* The Lancet, 2004. **363**(9422): p. 1665.
5. UK, C.r. *Brain, other CNS and intracranial tumours Key Facts*. 2014-2016 30/09/19 [cited 2019 15 Sept.]; Available from: http://www.cancerresearchuk.org/cancer-info/cancerstats/keyfacts/brain-cancer/.
6. Baumert, B.G., et al., *Fractionated stereotactic radiotherapy boost after post-operative radiotherapy in patients with high-grade gliomas.* Radiotherapy and Oncology, 2003. **67**(2): p. 183-190.
7. Andrews, D.W., et al., *Whole brain radiation therapy with or without stereotactic radiosurgery boost for patients with one to three brain metastases: phase III results of the RTOG 9508 randomised trial.* The Lancet, 2004. **363**(9422): p. 1665-1672.
8. Choi, C.Y.H., et al., *Stereotactic Radiosurgery of the Postoperative Resection Cavity for Brain Metastases: Prospective Evaluation of Target Margin on Tumor Control.* International Journal of Radiation Oncology*Biology*Physics, 2012. **84**(2): p. 336-342.
9. Asher, A.L., et al., *A New Treatment Paradigm: Neoadjuvant Radiosurgery Before Surgical Resection of Brain Metastases With Analysis of Local Tumor Recurrence.* International Journal of Radiation Oncology*Biology*Physics, 2014. **88**(4): p. 899-906.
10. U. M. Lütolf and U. Ulmer, *clinical practice.* University Hospital Zurich, Switzerland, 1995-2000. **personal communication**.
11. Balducci, M., et al., *Radiosurgery or Fractionated Stereotactic Radiotherapy plus Whole-brain Radioherapy in Brain Oligometastases: A Long-term Analysis.* Anticancer Res, 2015. **35**(5): p. 3055-9.
12. Barani, I.J. and D.A. Larson, *Radiation therapy of glioblastoma.* Cancer Treat Res, 2015. **163**: p. 49-73.
13. Chang, E.L., et al., *Neurocognition in patients with brain metastases treated with radiosurgery or radiosurgery plus whole-brain irradiation: a*

randomised controlled trial. The Lancet Oncology, 2009. **10**(11): p. 1037-1044.

14. Choi, C.Y.H., et al., *What Is the Optimal Treatment of Large Brain Metastases? An Argument for a Multidisciplinary Approach.* Int J Radiat Oncol Biol Phys, 2012. **84**(3): p. 688-693.
15. Ernst-Stecken, A., et al., *Phase II trial of hypofractionated stereotactic radiotherapy for brain metastases: Results and toxicity.* Radiother. Oncol., 2006. **81**(1): p. 18-24.
16. Mehta, M.P., et al., *The American Society for Therapeutic Radiology and Oncology (ASTRO) evidence-based review of the role of radiosurgery for brain metastases.* Int J Radiat Oncol Biol Phys, 2005. **63**(1): p. 37-46.
17. Patchell, R.A., et al., *Postoperative radiotherapy in the treatment of single metastases to the brain: a randomized trial.* Jama, 1998. **280**(17): p. 1485-9.
18. Patchell, R.A., *The management of brain metastases.* Cancer Treat Rev, 2003. **29**(6): p. 533-40.
19. Skeie, B.S., et al., *Gamma Knife Surgery versus Reoperation for Recurrent Glioblastoma Multiforme.* World Neurosurgery, 2012. **78**(6): p. 658-669.
20. Hughes, R.T., et al., *Initial SRS for Patients With 5 to 15 Brain Metastases: Results of a Multi-Institutional Experience.* International Journal of Radiation Oncology*Biology*Physics, 2019. **104**(5): p. 1091-1098.
21. Dirven, L., et al., *Impact of Radiation Target Volume on Health-Related Quality of Life in Patients With Low-Grade Glioma in the 2-Year Period Post Treatment: A Secondary Analysis of the EORTC 22033-26033.* International Journal of Radiation Oncology*Biology*Physics, 2019. **104**(1): p. 90-100.
22. Fan, X.-W., et al., *Simultaneously avoiding the hippocampus and hypothalamic-pituitary axis during whole brain radiotherapy: A planning study.* Medical Dosimetry, 2019. **44**(2): p. 130-135.
23. Andreas, J.J.M. and V. Kundapur, *Hippocampus Avoidance Whole-brain Radiation Therapy: A Practical Intensity-modulated Radiation Therapy Planning and Delivery Approach to RTOG 0933.* Journal of Medical Imaging and Radiation Sciences, 2015. **46**(1): p. 78-84.
24. Ghia, A., et al., *Distribution of Brain Metastases in Relation to the Hippocampus: Implications for Neurocognitive Functional Preservation.* International Journal of Radiation Oncology*Biology*Physics, 2007. **68**(4): p. 971-977.
25. Leksell, L., *The stereotactic method and radiosurgery of the brain.* Acta Chir Scand, 1951(102): p. 316-319.
26. Leksell, L., *Stereotaxis and radiosurgery: An operative system.* Thomas Publishers, 1971.

27. Bjartmarz, H. and S. Rehncrona, *Comparison of Accuracy and Precision between Frame-Based and Frameless Stereotactic Navigation for Deep Brain Stimulation Electrode Implantation.* Stereotactic and Functional Neurosurgery, 2007. **85**(5): p. 235-242.

28. Treuer, H., et al., *Impact of target point deviations on control and complication probabilities in stereotactic radiosurgery of AVMs and metastases.* Radiother Oncol, 2006. **81**(1): p. 25-32.

29. Novotny Jr, J., et al., *Quality control of the stereotactic radiosurgery procedure with the polymer-gel dosimetry.* Radiother. Oncol., 2002. **63**(2): p. 223-230.

30. Cho, Y., et al., *Evaluating Stress-related Uncertainties in Stereotactic Frame-based Localization for Gamma Knife Radiosurgery.* Int J Radiat Oncol Biol Phys, 2009. **75**(3, Supplement): p. S691-S692.

31. Theodorou, K., C. Kappas, and C. Tsokas, *A new non-invasive and relocatable immobilization frame for fractionated stereotactic radiotherapy.* Radiotherapy and Oncology, 1998. **47**(3): p. 313-317.

32. Bova, F.J., et al., *The university of Florida frameless high-precision stereotactic radiotherapy system.* International Journal of Radiation Oncology*Biology*Physics, 1997. **38**(4): p. 875-882.

33. Kooy, H.M., et al., *Adaptation and verification of the relocatable gill-thomas-cosman frame in stereotactic radiotherapy.* International Journal of Radiation Oncology*Biology*Physics, 1994. **30**(3): p. 685-691.

34. Takahashi, T., et al., *Measurement of repositioning accuracy during fractionated stereotactic radiotherapy for intracranial tumors using noninvasive fixation of BrainLAB radiotherapy equipment.* International Journal of Radiation Oncology*Biology*Physics, 2006. **66**(4, Supplement): p. S67-S70.

35. Das, S., et al., *Geometric Uncertainties in High Precision Radiotherapy for Brain Tumors: A Prospective Study.* Int J Radiat Oncol Biol Phys, 2011. **78**(3, Supplement): p. S686.

36. Baumert, B.G., et al., *Repositioning accuracy of fractionated stereotactic irradiation: assessment of isocentre alignment for different dental fixations by using sequential CT scanning.* Radiother. Oncol., 2005. **74**(1): p. 61-66.

37. Bednarz, G., et al., *Report on a randomized trial comparing two forms of immobilization of the head for fractionated stereotactic radiotherapy.* Medical Physics, 2009. **36**(1): p. 12-17.

38. Boda-Heggemann, J., et al., *Repositioning accuracy of two different mask systems—3D revisited: Comparison using true 3D/3D matching with cone-beam CT.* Int J Radiat Oncol Biol Phys, 2006. **66**(5): p. 1568-1575.

39. Chung, C., et al., *Clinical Evaluation of a Novel Thermoplastic Mask System With Intrafraction Motion Monitoring Using IR Tracking and*

Cone Beam CT for Gamma Knife Radiosurgery. Int J Radiat Oncol Biol Phys, 2014. **90**(1, Supplement): p. S848.

40. Clark, B.G., T. Teke, and K. Otto, *Penumbra evaluation of the varian millennium and BrainLAB M3 multileaf collimators.* International Journal of Radiation Oncology*Biology*Physics, 2006. **66**(4, Supplement): p. S71-S75.
41. Cosgrove, V.P., et al., *Commissioning of a micro multi-leaf collimator and planning system for stereotactic radiosurgery.* Radiother. Oncol,, 1999. **50**(3): p. 325-335.
42. Almeida, T.V.R., et al., *Positioning deviations in frameless and frame-based intracranial stereotactic radiosurgery.* Radiation Physics and Chemistry, 2019: p. 108363.
43. Mackie, T.R., et al., *Image guidance for precise conformal radiotherapy.* International Journal of Radiation Oncology*Biology*Physics, 2003. **56**(1): p. 89-105.
44. Han, C., et al., *Dosimetric comparisons of helical tomotherapy treatment plans and step-and-shoot intensity-modulated radiosurgery treatment plans in intracranial stereotactic radiosurgery.* Int J Radiat Oncol Biol Phys, 2006. **65**(2): p. 608-616.
45. Yu, C. and D. Shepard, *Treatment planning for stereotactic radiosurgery with photon beams.* Technol Cancer Res Treat., 2003. **2**(2): p. 93-104.
46. Adler, J.D., et al., *Visual field preservation after multisession cyberknife radiosurgery for perioptic lesions.* Neurosurgery, 2008. **62**(Suppl 2): p. 733-43.
47. Andrews, D.W., et al., *A review of 3 current radiosurgery systems.* Surgical Neurology, 2006. **66**(6): p. 559-564.
48. Gibbs, I.C., et al., *Dosimetric quality assurance analysis of cyberknife extracranial radiosurgery of the spine.* International Journal of Radiation Oncology*Biology*Physics, 2001. **51**(3, Supplement 1): p. 252.
49. Ma, L., et al., *A dosimetric comparison of fan-beam intensity modulated radiotherapy with gamma knife stereotactic radiosurgery for treating intermediate intracranial lesions.* Int J Radiat Oncol Biol Phys, 1999. **45**(5): p. 1325-1330.
50. Gevaert, T., et al., *Dosimetric comparison of different treatment modalities for stereotactic radiosurgery of arteriovenous malformations and acoustic neuromas.* Radiotherapy and Oncology, 2013. **106**(2): p. 192-197.
51. Kim, H., et al., *Tumor volume threshold for achieving improved conformity in VMAT and Gamma Knife stereotactic radiosurgery for vestibular schwannoma.* Radiotherapy and Oncology, 2015. **115**(2): p. 229-234.

52. Verellen, D., et al., *Assessment of the uncertainties in dose delivery of a commercial system for linac-based stereotactic radiosurgery.* Int J Radiat Oncol Biol Phys, 1999. **44**(2): p. 421-433.

53. Seravalli, E., et al., *A comprehensive evaluation of treatment accuracy, including end-to-end tests and clinical data, applied to intracranial stereotactic radiotherapy.* Radiotherapy and Oncology, 2015. **116**(1): p. 131-138.

54. Kestin, L., et al., *Dose-response relationship with clinical outcome for lung stereotactic body radiotherapy (SBRT) delivered via online image guidance.* Radiother Oncol, 2014. **110**(3): p. 499-504.

55. Koshy, M., et al., *Increasing radiation therapy dose is associated with improved survival in patients undergoing stereotactic body radiation therapy for stage I non-small-cell lung cancer.* Int J Radiat Oncol Biol Phys, 2015. **91**(2): p. 344-50.

56. Li, Q., et al., *Stereotactic ablative radiotherapy (SABR) using 70 Gy in 10 fractions for non-small cell lung cancer: exploration of clinical indications.* Radiother Oncol, 2014. **112**(2): p. 256-61.

57. Martin, A. and A. Gaya, *Stereotactic Body Radiotherapy: A Review.* Clinical Oncology, 2010. **22**(3): p. 157-172.

58. Nelson, J.W., et al., *Stereotactic Body Radiotherapy for Lesions of the Spine and Paraspinal Regions.* Int J Radiat Oncol Biol Phys, 2009. **73**(5): p. 1369-1375.

59. Song, C.W., et al., *Radiobiological basis of SBRT and SRS.* Int J Clin Oncol, 2014. **19**(4): p. 570-8.

60. Soldà, F., et al., *Stereotactic radiotherapy (SABR) for the treatment of primary non-small cell lung cancer; Systematic review and comparison with a surgical cohort.* Radiotherapy and Oncology, 2013. **109**(1): p. 1-7.

61. Lee, W.-Y., et al., *Outcomes and cost-effectiveness of gamma knife radiosurgery and whole brain radiotherapy for multiple metastatic brain tumors.* Journal of Clinical Neuroscience, 2009. **16**(5): p. 630-634.

62. Simonová, G., et al., *Fractionated stereotactic radiotherapy with the Leksell Gamma Knife: feasibility study.* Radiother. Oncol., 1995. **37**(2): p. 108-116.

63. Paddick, I., *A simple scoring ratio to index the conformity of radiosurgical treatment plans.* J Neurosurg, 2000. **93**(supplement 3): p. 219-222.

64. Riet, A.v.t., et al., *A conformation number to quantify the degree of conformality in brachytherapy and external beam irradiation: Application to the prostate.* Int J Radiat Oncol Biol Phys, 1997. **37**(3): p. 731-736.

65. Lomax, N.J. and S.G. Scheib, *Quantifying the degree of conformity in radiosurgery treatment planning.* Int J Radiat Oncol Biol Phys, 2003. **55**(5): p. 1409-1419.

66. Feuvret, L., et al., *Conformity index: A review.* Int J Radiat Oncol Biol Phys, 2006. **64**(2): p. 333-342.

67. Shaw, E., et al., *Radiation Therapy Oncology Group: radiosurgery quality assurance guidelines.* Int J Radiat Oncol Biol Phys, 1993. **27**(5): p. 1231-9.

68. Knöös, T., I. Kristensen, and P. Nilsson, *Volumetric and dosimetric evaluation of radiation treatment plans: radiation conformity index.* International Journal of Radiation Oncology*Biology*Physics, 1998. **42**(5): p. 1169-1176.

69. Paddick, I. and B. Lippitz, *A simple dose gradient measurement tool to complement the conformity index.* J Neurosurg, 2006. **105 Suppl**: p. 194-201.

70. Massager, N., et al., *Dosimetric and Clinical Analysis of Spatial Distribution of the Radiation Dose in Gamma Knife Radiosurgery for Vestibular Schwannoma.* Int J Radiat Oncol Biol Phys, 2011. **81**(4): p. e511-e518.

71. Balagamwala, E.H., et al., *The Importance of the Conformality, Heterogeneity, and Gradient Indices in Evaluating Gamma Knife Radiosurgery Treatment Plans for Intracranial Meningiomas.* Int J Radiat Oncol Biol Phys, 2012. **83**(5): p. 1406-1413.

72. Reiner, B., et al., *In Regard to Balagamwala et al.* Int J Radiat Oncol Biol Phys, 2013. **85**(5): p. 1154-1155.

73. Shehata, M.K., et al., *Stereotatic radiosurgery of 468 brain metastases < or =2 cm: implications for SRS dose and whole brain radiation therapy.* Int J Radiat Oncol Biol Phys, 2004. **59**(1): p. 87-93.

74. Hazard, L.J., R.L. Jensen, and D.C. Shrieve, *Role of stereotactic radiosurgery in the treatment of brain metastases.* Am J Clin Oncol, 2005. **28**(4): p. 403-10.

75. Hasegawa, T., et al., *Long-term outcomes of Gamma Knife surgery for cavernous sinus meningioma.* J Neurosurg, 2007. **107**(4): p. 745-51.

76. Liscak, R., et al., *Gamma knife radiosurgery of meningiomas in the cavernous sinus region.* Acta Neurochir (Wien), 1999. **141**(5): p. 473-80.

77. Pollock, B.E. and S.L. Stafford, *Results of stereotactic radiosurgery for patients with imaging defined cavernous sinus meningiomas.* Int J Radiat Oncol Biol Phys, 2005. **62**(5): p. 1427-31.

78. Kondziolka, D., et al., *Stereotactic radiosurgery for convexity meningiomas.* J Neurosurg, 2009. **111**(3): p. 458-63.

79. Ganz, J.C., W.A. Reda, and K. Abdelkarim, *Gamma Knife surgery of large meningiomas: early response to treatment.* Acta Neurochir (Wien), 2009. **151**(1): p. 1-8.

80. Flannery, T.J., et al., *Long-term control of petroclival meningiomas through radiosurgery.* J Neurosurg, 2010. **112**(5): p. 957-64.

81. Flickinger, J.C., et al., *Evolution in technique for vestibular schwannoma radiosurgery and effect on outcome.* Int J Radiat Oncol Biol Phys, 1996. **36**(2): p. 275-280.

82. Niranjan, A., et al., *Dose reduction improves hearing preservation rates after intracanalicular acoustic tumor radiosurgery.* Neurosurgery, 1999. **45**(4): p. 753-62; discussion 762-5.

83. Regis, J., et al., *Radiosurgery: operative technique, pitfalls and tips.* Prog Neurol Surg, 2008. **21**: p. 54-64.

84. Rogers, C.L., et al., *Gamma knife radiosurgery for trigeminal neuralgia: the initial experience of The Barrow Neurological Institute.* Int J Radiat Oncol Biol Phys, 2000. **47**(4): p. 1013-9.

85. Kondziolka, D., et al., *Gamma Knife stereotactic radiosurgery for idiopathic trigeminal neuralgia.* J Neurosurg, 2010. **112**(4): p. 758-65.

86. Flickinger, J.C., et al., *Does increased nerve length within the treatment volume improve trigeminal neuralgia radiosurgery? a prospective double-blind, randomized study.* Int J Radiat Oncol Biol Phys, 2001. **51**(2): p. 449-454.

87. Jeremy, G., *Gamma Knife Neurosurgery.* SpringerWienNewYork, 2011: p. 321-322.

88. Yamamoto, Y., et al., *Interim report on the radiosurgical treatment of cerebral arteriovenous malformations. The influence of size, dose, time, and technical factors on obliteration rate.* J Neurosurg, 1995. **83**(5): p. 832-7.

89. Hasegawa, T., et al., *Long-term results after stereotactic radiosurgery for patients with cavernous malformations.* Neurosurgery, 2002. **50**(6): p. 1190-7; discussion 1197-8.

90. Izawa, M., et al., *Long-term complications after gamma knife surgery for arteriovenous malformations.* J Neurosurg, 2005. **102 Suppl**: p. 34-7.

91. Spatola, G., et al., *Results of Gamma Knife anterior capsulotomy for refractory obsessive-compulsive disorder: results in a series of 10 consecutive patients.* J Neurosurg, 2018: p. 1-8.

92. Ma, L., et al., *Whole-procedural Radiological Accuracy for Delivering Multi-session Gamma Knife Radiosurgery With a Relocatable Frame System.* Technology in Cancer Research and Treatment, 2013.

93. Bhatnagar, J.P., et al., *First year experience with newly developed Leksell Gamma Knife Perfexion.* J Med Phys, 2009. **34**(3): p. 141-8.

94. Ruschin, M., et al., *Investigation of intracranial peripheral dose arising from the treatment of large lesions with Leksell GammaKnife Perfexion.* Medical Physics, 2009. **36**(6): p. 2069-2073.

95. Sayer, F.T., et al., *Initial Experience with the eXtend System: A Relocatable Frame System for Multiple-Session Gamma Knife Radiosurgery.* World Neurosurgery, 2011. **75**(5-6): p. 665-672.

96. Lindquist, C. and I. Paddick, *The Leksell Gamma Knife Perfexion and comparisons with its predecessors.* Neurosurgery, 2007. **61**(3 Suppl): p. 130-40; discussion 140-1.

97. Jaffray, D.A., et al., *Flat-panel cone-beam computed tomography for image-guided radiation therapy.* International Journal of Radiation Oncology*Biology*Physics, 2002. **53**(5): p. 1337-1349.

98. Lutz, W., K. Winston, and N. Maleki, *A system for stereotactic radiosurgery with a linear accelerator.* Int J Radiat Oncol Biol Phys, 1988. **14**(2): p. 373-81.

99. Ruschin, M., et al., *Performance of a Novel Repositioning Head Frame for Gamma Knife Perfexion and Image-Guided Linac-Based Intracranial Stereotactic Radiotherapy.* Int J Radiat Oncol Biol Phys, 2010. **78**(1): p. 306-313.

100. Reiner, B., G. Wright, and P. Bownes, *Commissioning of the Extend™ system for Gamma Knife®*, in *IPEM*. 2011: London.

101. van Herk, M., et al., *The probability of correct target dosage: dose-population histograms for deriving treatment margins in radiotherapy.* Int J Radiat Oncol Biol Phys, 2000. **47**(4): p. 1121-1135.

102. McKenzie, A., M. van Herk, and B. Mijnheer, *Margins for geometric uncertainty around organs at risk in radiotherapy.* Radiother. Oncol., 2002. **62**(3): p. 299-307.

103. van Herk, M., P. Remeijer, and J.V. Lebesque, *Inclusion of geometric uncertainties in treatment plan evaluation.* Int J Radiat Oncol Biol Phys, 2002. **52**(5): p. 1407-1422.

104. Stroom, J.C., et al., *Inclusion of geometrical uncertainties in radiotherapy treatment planning by means of coverage probability.* International Journal of Radiation Oncology*Biology*Physics, 1999. **43**(4): p. 905-919.

105. Stroom, J.C. and B.J.M. Heijmen, *Geometrical uncertainties, radiotherapy planning margins, and the ICRU-62 report.* Radiotherapy and Oncology, 2002. **64**(1): p. 75-83.

106. Bethesda, M., *ICRU Report 50. Prescribing, Recording, and Reporting Photon Beam Therapy. .* International Commission on Radiation Units and Measurements, 1993.

107. Bethesda, M., *ICRU Report 62. Prescribing, Recording, and Reporting Photon Beam Therapy (Supplement to ICRU Report 50).* International Commission on Radiation Units and Measurements, , 1999.

108. *ICRU Report 29. Dose Specification for Reporting External Beam Therapy with Photons and Electrons.* 1978.

109. Measurements, I.I.C.o.R.U.a., *Prescribing, recording, and reporting photon-beam intensity-modulated radiation therapy (IMRT). ICRU Report 83.* J ICRU, 2010. **10**: p. 1-106.

110. Torrens, M., et al., *THE STANDARDISATION OF TERMINOLOGY IN RADIOSURGERY: Report from the Standardization Committee of the*

International Leksell Gamma Knife Society (DRAFT DOCUMENT [3.3] FOR CIRCULATION TO LGKS MEMBERS), 2012.

111. Torrens, M., et al., *Standardization of terminology in stereotactic radiosurgery: Report from the Standardization Committee of the International Leksell Gamma Knife Society: special topic.* J Neurosurg., 2014. **Suppl 121**: p. 2-15.

112. Regine, W.F., et al., *Neurocognitive outcome in brain metastases patients treated with accelerated-fractionation vs. accelerated-hyperfractionated radiotherapy: an analysis from Radiation Therapy Oncology Group Study 91-04.* Int J Radiat Oncol Biol Phys, 2001. **51**(3): p. 711-717.

113. Korytko, T., et al., *12 Gy gamma knife radiosurgical volume is a predictor for radiation necrosis in non-AVM intracranial tumors.* Int J Radiat Oncol Biol Phys, 2006. **64**(2): p. 419-424.

114. Lyman, J.T., *Complication Probability as Assessed from Dose-Volume Histograms.* Radiation Research, 1985. **104**(2): p. S13-S19.

115. Burman, C., et al., *Fitting of normal tissue tolerance data to an analytic function* Int J Radiat Oncol Biol Phys, 1991. **21**(1): p. 123-135.

116. Bentzen, S.M., et al., *Quantitative Analyses of Normal Tissue Effects in the Clinic (QUANTEC): An Introduction to the Scientific Issues.* Int J Radiat Oncol Biol Phys, 2010. **76**(3, Supplement 1): p. S3-S9.

117. Lyman, J.T., *Normal tissue complication probabilities: Variable dose per fraction.* Int J Radiat Oncol Biol Phys, 1992. **22**(2): p. 247-250.

118. Emami, B., et al., *Tolerance of normal tissue to therapeutic irradiation.* Int J Radiat Oncol Biol Phys, 1991. **21**(1): p. 109-122.

119. Spring, E. and P. Holmberg, *Evaluation of experimental irradiation fractionation with the single-hit, multi-target model.* Acta Radiol Ther Phys Biol, 1968. **7**(4): p. 297-306.

120. Elkind, M. and G. Whitmore, *The radiobiology of cultured mammalian cells.* Gordon & Breach, 1967. **New York**.

121. Lea, D.E., R.B. Haines, and E. Bretscher, *The bactericidal action of X-rays, neutrons and radioactive radiations.* J Hyg (Lond), 1941. **41**(1): p. 1-16.

122. Lea, D.E. and C.A. Coulson, *The distribution of the numbers of mutants in bacterial populations.* J Genet, 1949. **49**(3): p. 264-85.

123. Nomiya, T., *Discussions on target theory: past and present.* J Radiat Res, 2013. **54**(6): p. 1161-3.

124. Brenner, D.J., *The Linear-Quadratic Model Is an Appropriate Methodology for Determining Isoeffective Doses at Large Doses Per Fraction.* Seminars in Radiation Oncology, 2008. **18**(4): p. 234-239.

125. Kirkpatrick, J.P., J.J. Meyer, and L.B. Marks, *The Linear-Quadratic Model Is Inappropriate to Model High Dose per Fraction Effects in Radiosurgery.* Seminars in Radiation Oncology, 2008. **18**(4): p. 240-243.

126. Courdi, A., *High doses per fraction and the linear-quadratic model.* Radiother. Oncol., 2010. **94**(1): p. 121-122.

127. Hoban, P.W., L.C. Jones, and B.G. Clark, *Modeling late effects in hypofractionated stereotactic radiotherapy.* Int J Radiat Oncol Biol Phys, 1999. **43**(1): p. 199-210.

128. Iwata, H., et al., *Estimation of Errors Associated With Use of Linear-Quadratic Formalism for Evaluation of Biologic Equivalence Between Single and Hypofractionated Radiation Doses: An In Vitro Study.* Int J Radiat Oncol Biol Phys, 2009. **75**(2): p. 482-488.

129. Carlson, D.J., et al., *Hypofractionation Results in Reduced Tumor Cell Kill Compared to Conventional Fractionation for Tumors With Regions of Hypoxia.* Int J Radiat Oncol Biol Phys, 2011. **79**(4): p. 1188-1195.

130. Jones, B., et al., *Biological equivalent dose assessment of the consequences of hypofractionated radiotherapy.* Int J Radiat Oncol Biol Phys, 2000. **47**(5): p. 1379-1384.

131. Park, C., et al., *Universal Survival Curve and Single Fraction Equivalent Dose: Useful Tools in Understanding Potency of Ablative Radiotherapy.* Int J Radiat Oncol Biol Phys, 2008. **70**(3): p. 847-852.

132. Clark, B.G., et al., *The integral biologically effective dose to predict brain stem toxicity of hypofractionated stereotactic radiotherapy.* Int J Radiat Oncol Biol Phys, 1998. **40**(3): p. 667-675.

133. Kong, C., et al., *A new index comparable to BED for evaluating the biological efficacy of hypofractionated radiotherapy schemes on early stage non-small cell lung cancer: Analysis of data from the literature.* Lung Cancer, 2014. **84**(1): p. 7-12.

134. Voyant, C., et al., *Biological effects and equivalent doses in radiotherapy: A software solution.* Reports of Practical Oncology & Radiotherapy, 2014. **19**(1): p. 47-55.

135. Fleming, C., et al., *A Method for the Prediction of Late Organ-at-Risk Toxicity After Radiotherapy of the Prostate Using Equivalent Uniform Dose.* International Journal of Radiation Oncology*Biology*Physics, 2011. **80**(2): p. 608-613.

136. Liu, F., et al., *Modeling Regional Sensitivity of Radiation Pneumonitis using Multi-institutional EUD Atlases from Phase I Dose Escalation Protocols for Non-small Cell Lung Cancer.* Int J Radiat Oncol Biol Phys, 2010. **78**(3, Supplement 1): p. S46-S46.

137. Bentzen, S.M., et al., *Biomarkers and Surrogate Endpoints for Normal-Tissue Effects of Radiation Therapy: The Importance of Dose-Volume Effects.* Int J Radiat Oncol Biol Phys, 2010. **76**(3, Supplement 1): p. S145-S150.

138. Marks, L.B., R.K. Ten Haken, and M.K. Martel, *Guest Editor's Introduction to QUANTEC: A Users Guide.* Int J Radiat Oncol Biol Phys, 2010. **76**(3, Supplement 1): p. S1-S2.

139. Lawrence, Y.R., et al., *Radiation Dose-Volume Effects in the Brain.* Int J Radiat Oncol Biol Phys, 2010. **76**(3, Supplement 1): p. S20-S27.

140. Mayo, C., E. Yorke, and T.E. Merchant, *Radiation Associated Brainstem Injury.* Int J Radiat Oncol Biol Phys, 2010. **76**(3, Supplement 1): p. S36-S41.

141. Zaider, M. and H.I. Amols, *A little to a lot or a lot to a little: is NTCP always minimized in multiport therapy?* Int J Radiat Oncol Biol Phys, 1998. **41**(4): p. 945-950.

142. Peng, L., et al., *Updated risk models demonstrate low risk of symptomatic radionecrosis following stereotactic radiosurgery for brain metastases.* Surg Neurol Int, 2019. **10**: p. 32.

143. Laura Licon, A., et al., *A quantitative measure for radiation treatment plan quality.* J buon, 2018. **23**(5): p. 1460-1466.

144. Beaton, L., et al., *Cardiac death after breast radiotherapy and the QUANTEC cardiac guidelines.* Clin Transl Radiat Oncol, 2019. **19**: p. 39-45.

145. Yen, C.-P. and L. Steiner, *Gamma Knife Surgery for Brainstem Arteriovenous Malformations.* World Neurosurgery, 2011. **76**(1–2): p. 87-95.

146. Jung, E.W., et al., *Gamma Knife radiosurgery in the management of brainstem metastases.* Clinical Neurology and Neurosurgery, 2013. **115**(10): p. 2023-2028.

147. Ma, L., et al., *Apparatus dependence of normal brain tissue dose in stereotactic radiosurgery for multiple brain metastases.* Journal of Neurosurgery, 2011. **114**(6): p. 1580-1584.

148. Park, S.-H., et al., *Gamma knife radiosurgery for multiple brain metastases from lung cancer.* Journal of Clinical Neuroscience, 2009. **16**(5): p. 626-629.

149. Gevaert, T., et al., *Dosimetric comparison of different treatment modalities for stereotactic radiosurgery of arteriovenous malformations and acoustic neuromas.* Radiother. Oncol., 2013. **106**(0): p. 192-197.

150. Al-Shamy, G. and R. Sawaya, *Management of brain metastases: the indispensable role of surgery.* J Neurooncol, 2009. **92**((3)): p. 275-82.

151. Feuvret, L., et al., *Stereotactic radiotherapy for large solitary brain metastases.* Cancer/Radiothérapie, 2014. **18**(2): p. 97-106.

152. Märtens, B., et al., *Hypofractionated stereotactic radiotherapy of limited brain metastases: a single-centre individualized treatment approach.* BMC Cancer., 2012. **12**.

153. Mehta, M., et al., *A cost-effectiveness and cost-utility analysis of radiosurgery vs. resection for single-brain metastases.* Int J Radiat Oncol Biol Phys, 1997. **39**(2): p. 445-454.

154. Yuan, J., et al., *Hypofractionation Regimens for Stereotactic Radiotherapy for Large Brain Tumors.* Int J Radiat Oncol Biol Phys, 2008. **72**(2): p. 390-397.

155. Ganz, J.C., et al., *Protection of the anterior visual pathways during gamma knife treatment of meningiomas.* British Journal of Neurosurgery, 2010. **24**(3): p. 233-243.

156. Kim, Y.-J., et al., *Single-Dose Versus Fractionated Stereotactic Radiotherapy for Brain Metastases.* Int J Radiat Oncol Biol Phys, 2011. **81**(2): p. 483-489.

157. Tuniz, F., et al., *Multisession cyberknife stereotactic radiosurgery of large, benign cranial base tumors: preliminary study.* Neurosurgery, 2009. **65**(5): p. 898-907.

158. Schlesinger, D., et al., *Interfraction and intrafraction performance of the Gamma Knife Extend system for patient positioning and immobilization.* J Neurosurg. , 2012. **117**(Suppl:): p. 217-24.

159. Ma, L., et al., *Impact of Millimeter-Level Margins on Peripheral Normal Brain Sparing for Gamma Knife Radiosurgery.* Int J Radiat Oncol Biol Phys, 2014. **89**(1): p. 206-213.

160. Devriendt, D., et al., *Five-fraction Gamma Knife radiosurgery using the Extend relocatable system for benign neoplasms close to optic pathways.* Practical Radiation Oncology, 2015(0).

161. Goh, A.S.C., et al., *Benign Orbital Apex Tumors Treated with Multisession Gamma Knife Radiosurgery.* Ophthalmology, 2013. **120**(3): p. 635-641.

162. Kim, M.-S., et al., *Gamma knife radiosurgery for orbital tumors.* Clinical Neurology and Neurosurgery, 2008. **110**(10): p. 1003-1007.

163. Nguyen, J.H., et al., *Multisession Gamma Knife Radiosurgery: A Preliminary Experience with a Noninvasive, Relocatable Frame.* World Neurosurgery, 2014. **82**(6): p. 1256-1263.

164. Gevaert, T., et al., *Setup Accuracy of the Novalis ExacTrac 6DOF System for Frameless Radiosurgery.* International Journal of Radiation Oncology*Biology*Physics, 2012. **82**(5): p. 1627-1635.

165. Murphy, M.J., *Intrafraction Geometric Uncertainties in Frameless Image-Guided Radiosurgery.* Int J Radiat Oncol Biol Phys, 2009. **73**(5): p. 1364-1368.

166. Murphy, M.J., et al., *Patterns of patient movement during frameless image-guided radiosurgery.* Int J Radiat Oncol Biol Phys, 2003. **55**(5): p. 1400-1408.

167. Masi, L., et al., *Cone Beam CT Image Guidance for Intracranial Stereotactic Treatments: Comparison With a Frame Guided Set-Up.* Int J Radiat Oncol Biol Phys, 2008. **71**(3): p. 926-933.

168. Wangerid, T., et al., *Implication of using MRI co-registered with CT in Leksell Gamma Knife® dose planning for patients with vestibular schwannoma.* Clinical Neurology and Neurosurgery, 2015. **138**: p. 10-15.

169. Shaw, E., et al., *Single dose radiosurgical treatment of recurrent previously irradiated primary brain tumors and brain metastases: final*

report of RTOG protocol 90-05. Int J Radiat Oncol Biol Phys, 2000. **47**(2): p. 291-8.

170. Lee, C.C., et al., *Large intracranial metastatic tumors treated by Gamma Knife surgery: outcomes and prognostic factors.* J Neurosurg, 2014. **120**(1): p. 52-9.

171. Marks, L.B., et al., *Use of Normal Tissue Complication Probability Models in the Clinic.* Int J Radiat Oncol Biol Phys, 2010. **76**(3, Supplement 1): p. S10-S19.

172. Mayo, C., et al., *Radiation Dose-Volume Effects of Optic Nerves and Chiasm.* Int J Radiat Oncol Biol Phys, 2010. **76**(3, Supplement 1): p. S28-S35.

173. Choi, C.Y.H., et al., *Stereotactic Radiosurgery of the Postoperative Resection Cavity for Brain Metastases: Prospective Evaluation of Target Margin on Tumor Control.* Int J Radiat Oncol Biol Phys, 2012. **84**(2): p. 336-342.

174. Meyer, J., et al., *Positioning accuracy of cone-beam computed tomography in combination with a HexaPOD robot treatment table.* Int J Radiat Oncol Biol Phys, 2007. **67**(4): p. 1220-1228.

175. Millar, W.T., et al., *The role of the concept of biologically effective dose (BED) in treatment planning in radiosurgery.* Physica Medica, 2015. **31**(6): p. 627-633.

176. Flickinger, J.C., et al., *A multi-institutional analysis of complication outcomes after arteriovenous malformation radiosurgery.* Int J Radiat Oncol Biol Phys, 1999. **44**(1): p. 67-74.

177. Flickinger, J.C., et al., *Development of a model to predict permanent symptomatic postradiosurgery injury for arteriovenous malformation patients.* Int J Radiat Oncol Biol Phys, 2000. **46**(5): p. 1143-1148.

178. Chin, L., L. Ma, and S. DiBiase, *Radiation necrosis following gamma knife surgery: a case-controlled comparison of treatment parameters and long-term clinical follow up.* J Neurosurg., 2001. **94**(6): p. 899-904.

179. Blonigen, B.J., et al., *Irradiated Volume as a Predictor of Brain Radionecrosis After Linear Accelerator Stereotactic Radiosurgery.* Int J Radiat Oncol Biol Phys, 2010. **77**(4): p. 996-1001.

180. Broemme, J., et al., *Adjuvant therapy after resection of brain metastases. Frameless image-guided LINAC-based radiosurgery and stereotactic hypofractionated radiotherapy.* Strahlenther Onkol, 2013. **189**(9): p. 765-70.

181. Davidson, L., et al., *Delayed toxicity from gamma knife radiosurgery to lesions in and adjacent to the brainstem.* Journal of Clinical Neuroscience, 2009. **16**(9): p. 1139-1147.

182. Johnson, M.D., et al., *Analysis of Risk Factors for Development of Radiation Necrosis Following Gamma Knife Radiosurgery for Brain Metastases.* International Journal of Radiation Oncology*Biology*Physics, 2013. **87**(2, Supplement): p. S279-S280.

183. Kondziolka, D., et al., *Histological effects of trigeminal nerve radiosurgery in a primate model: implications for trigeminal neuralgia radiosurgery.* Neurosurgery, 2000. **46**(4): p. 971-6; discussion 976-7.

184. Sheehan, J., et al., *Gamma knife surgery for trigeminal schwannoma.* J Neurosurg, 2007. **106**(5): p. 839-45.

185. Wright, G., et al., *Validity of the use of nose tip motion as a surrogate for intracranial motion in mask-fixated frameless Gamma Knife® Icon™ therapy.* Journal of Radiosurgery & SBRT 2017. **4**(4): p. 289-301.

186. Fowler, J.F., *The linear-quadratic formula and progress in fractionated radiotherapy.* Br J Radiol, 1989. **62**(740): p. 679-694.

187. Thames, H.D., et al., *Time-dose factors in radiotherapy: a review of the human data.* Radiother. Oncol., 1990. **19**(3): p. 219-235.

188. Bostrom, J.P., et al., *Risk-adapted single or fractionated stereotactic high-precision radiotherapy in a pooled series of nonfunctioning pituitary adenomas: high local control and low toxicity.* Strahlenther Onkol, 2014. **190**(12): p. 1095-103.

189. Kuperman, V.Y., *Effect of radiation protraction on BED in the case of large fraction dose.* Med Phys, 2013. **40**(8): p. 081716.

190. Zhao, L., et al., *A generalized target theory and its applications.* Scientific Reports, 2015. **5**: p. 14568.

191. Wright, G., et al., *Quantifying and improving the efficiency of Gamma Knife treatment plans for brain metastases: results of a 1-year audit.* J Neurosurg, 2014. **121 Suppl**: p. 44-50.

192. McMahon, S.J., *The linear quadratic model: usage, interpretation and challenges.* Physics in Medicine & Biology, 2018. **64**(1): p. 01TR01.

193. Wang, J., et al., *A Generalized Linear-Quadratic Model for Radiosurgery, Stereotactic Body Radiation Therapy, and High-Dose Rate Brachytherapy.* Science translational medicine, 2010. **2**: p. 39ra48.

194. Crispin-Ortuzar, M., et al., *A radiobiological model of radiotherapy response and its correlation with prognostic imaging variables.* Physics in Medicine and Biology, 2017. **62**(7): p. 2658-2674.

195. Williams, J.A., *Fractionated stereotactic radiotherapy (FSR) for acoustic neuromas.* Int J Radiat Oncol Biol Phys, 2000. **48**(3, Supplement 1): p. 253-254.

196. Sweeney, R., et al., *A simple and non-invasive vacuum mouthpiece-based head fixation system for high precision radiotherapy.* Strahlenther Onkol. , 2001. **177**(1): p. 43-7.

197. van Santvoort, J., R. Wiggenraad, and P. Bos, *Positioning Accuracy in Stereotactic Radiotherapy Using a Mask System With Added Vacuum Mouth Piece and Stereoscopic X-Ray Positioning.* Int J Radiat Oncol Biol Phys, 2008. **72**(1): p. 261-267.